Implications of Environmental and Landscape Change for Population Connectivity and the Persistence of Aridland Amphibians

Meryl Mims

A dissertation
submitted in partial fulfillment of the
requirements for the degree of

Doctor of Philosophy

University of Washington
2015

Reading Committee:
Julian Olden, Chair
Lorenz Hauser
Adam Leaché

Program Authorized to Offer Degree:
School of Aquatic and Fishery Sciences

University of Washington

Abstract

Implications of Environmental and Landscape Change for Population Connectivity and the Persistence of Aridland Amphibians

Meryl Mims

Chair of the Supervisory Committee:
Julian Olden, Associate Professor
School of Aquatic and Fishery Sciences

The study of how population structure and persistence are shaped by attributes of species and the environment is a central scientific pursuit in ecology and conservation. In this dissertation, I explore four themes central to this pursuit. First, I examined the extent to which species' ecological strategies – their life histories, biology, and behavior – predict patterns and drivers of population connectivity. This research represents a critical step in evaluating the potential of multi-taxa inference in landscape genetics. I examined a suite of hypothesized relationships between genetic connectivity and landscape connectivity for three desert anuran species and found a positive relationship between population differentiation and water dependency, e.g. longer larval development periods and site fidelity for reliable water sources. I also found that aquatic connectivity is important across all species, particularly when considered with

topography (slope). Second, I built upon the work of my first chapter and proposed more general traits-based frameworks to enhance the utility of landscape genetics in multispecies conservation. I proposed guiding principles for the formal development, testing, and generalization of traits-based frameworks to advance the utility, efficiency, and effectiveness of genetic inference in contemporary ecology and conservation. Third, I employed population genetic techniques to examine the population structure, diversity, and connectivity of *Hyla wrightorum*, an anuran native to the southwestern United States and Mexico. *Hyla wrightorum* exists as a Distinct Population Segment (DPS) in the Huachuca Mountains and Canelo Hills of southeastern Arizona, USA. Due to concerns about declining observations of the species within the DPS, its small geographic and isolated extent within the Huachuca Mountains and Canelo Hills, and presumably small population sizes, the DPS is currently a candidate for federal protection under the Endangered Species Act. I found evidence of larger than expected effective population sizes, significant genetic differentiation between populations, and an isolation-by-distance pattern among populations. These results suggest that the DPS may be less vulnerable to extirpation than previously expected, but some small effective population sizes and the limited geographic extent of the DPS justify current concern for the persistence of this DPS. Finally, I used a spatially-explicit individual based model to simulate the response of the Arizona Treefrog (*Hyla wrightorum*) to reductions in breeding habitat availability in an isolated portion of its range. I found that reductions in breeding habitat resulted in population declines, with the greatest population declines for *H. wrightorum* associated with both a reduction in breeding habitat availability and recruitment failure. Reduced breeding habitat also resulted in increased synchrony and decreased variability through time, which likely indicates a transition from a metapopulation to isolated populations. Taken together, the four chapters of this dissertation

advance the use of landscape and population genetics in multispecies conservation, and they will contribute directly to the conservation of dryland aquatic species.

Contents

Chapter 1: Ecological strategies predict associations between aquatic and genetic connectivity for dryland amphibians

Authors: M.C. Mims, I.C. Phillipsen, D.A. Lytle, E.E. Hartfield Kirk, J.D. Olden

Published in *Ecology*, 2015, 96:1371-1382.

1A. Abstract

The study of how population genetic structure is shaped by attributes of the environment is a central scientific pursuit in ecology and conservation. But limited resources may prohibit landscape genetics studies for many threatened species, particularly given the pace of current environmental change. Understanding the extent to which species' ecological strategies – their life histories, biology, and behavior – predict patterns and drivers of population connectivity is a critical step in evaluating the potential of multi-taxa inference in landscape genetics. We present results of a landscape genetic study of three dryland amphibians: the canyon treefrog (*Hyla arenicolor*), red-spotted toad (*Anaxyrus punctatus*), and Mexican spadefoot (*Spea multiplicata*). These species characterize a range of ecological strategies – driven primarily by different water dependencies – enabling amphibian survival in arid and semi-arid environments. We examined a suite of hypothesized relationships between genetic connectivity and landscape connectivity across species. We found a positive relationship between population differentiation and water dependency, e.g. longer larval development periods and site fidelity for reliable water sources. We also found that aquatic connectivity is important for all species, particularly when considered

with topography (slope). The effect of spatial scale varied by species, with canyon treefrogs and Mexican spadefoots characterized by relatively consistent results at different scales in contrast to the stark differences in results for red-spotted toads at different scales. Using ecological information to predict relationships between genetic and landscape connectivity is a promising approach for multi-taxa inference and may help inform conservation efforts where single-species genetic studies are not possible.

1B. Key words

Landscape genetics, anurans, life histories, dryland ecology, traits

1C. Introduction

Mounting concern for the survival of species in human-modified environments has strengthened interest in how species biology and landscape heterogeneity interact to structure populations. Population genetic structure is a fundamental consideration in applied conservation (Allendorf and Luikart 2007), which has led to greater research emphasis on integrating population genetics with emerging spatial methodologies to elucidate the landscape genetics of species (Manel et al. 2003). Substantial progress has been made in the last decade toward quantifying associations between landscape features and genetic connectivity of single species, and interest in explicitly testing for generalizations across multiple species is increasing (Manel and Holderegger 2013). Multispecies inference may be a promising way to identify emerging patterns of landscape influence on population connectivity across taxa and to reveal transferable relationships according to biological attributes such as dispersal ability (Richardson 2012) and life history (Bradbury et al. 2008, Hughes et al. 2013). Ecological strategies – the life history, biology, and

behavior of a species – may provide a means to generalize associations between genetic connectivity and structural connectivity (i.e., the physical linkages between habitat patches via a landscape feature such as riparian networks or ridgelines: Taylor et al. 1993), or what is commonly considered "landscape connectivity". The potential for generalized, multi-taxa relationships between genetic and landscape connectivity is important in light of limited management resources or logistical complications that render single species studies unfeasible for many species of conservation concern.

Aquatic habitat supports a range of obligate aquatic species; some species require perennial water for the duration of their life cycle, whereas others require water for only a short period to fulfill a portion of their life cycle. The water requirements, dispersal abilities, and other traits of aquatic species coupled with the distribution (spatial and temporal) of aquatic habitat may be major factors that influence the population structure of a diverse array of species including plants (Imbert and Lefèvre 2003, Nilsson et al. 2010), insects (Hughes et al. 2013, Robertson et al. 2014), fishes (Hughes et al. 2013), amphibians (Richardson 2012), and birds (Kingsford et al. 2004, Cadena et al. 2011). In arid and semi-arid (hereafter "dryland") environments characterized by sparse, sometimes unpredictable, and often temporary aquatic habitat, the link between aquatic species ecology and aquatic habitat on the landscape in driving population structure may be more pronounced due to the arid terrestrial matrix between aquatic habitats (Finn et al. 2007, Phillipsen and Lytle 2013). Conversely, the need to reach temporally and spatially variable aquatic habitat may decouple the link between the aquatic habitat and population genetic structure for aquatic species with high dispersal ability (Chan and Zamudio 2009, Cadena et al. 2011).

Quantifying genetic connectivity among populations of aquatic animals – and determining how this is influenced by landscape factors such as hydrology – is critical for conservation planning now and in the future. Worldwide threats to water security for society and freshwater diversity require efficient and effective conservation planning (Vörösmarty et al. 2010). In recent decades, amphibians have declined globally as a result of major threats including habitat loss, disease, and non-native species (Stuart et al. 2004, Sodhi et al. 2008). These ubiquitous challenges for amphibians worldwide are also true of anurans (frogs and toads) in dryland environments. In the American Southwest, habitat loss is an ongoing challenge as limited perennial water is often appropriated for human use, and groundwater pumping results in continued reduction in surface water availability (Marshall et al. 2010, Jaeger et al. 2014). Current demand for and conflict over these resources foreshadows increasing demand and decreasing availability as climate change increases aridity in the region (Seager et al. 2007).

Anurans native to this region utilize a variety of life history and behavioral strategies to survive in a harsh, arid landscape. Some species are specialists that live in either perennial or ephemeral freshwater habitats, and others occupy niches intermediate to these two extremes. If these anurans have dispersal limitations that correspond with their habitat requirements, the patterns of population structure among these species may be as diverse as their ecological strategies related to water use.

In this study, we examine the relationship between genetic and structural connectivity for three dryland anurans common to the American Southwest: the canyon treefrog (*Hyla arenicolor*), the red-spotted toad (*Anaxyrus punctatus*), and the Mexican spadefoot (*Spea multiplicata*). These species represent a range of water dependencies typical of dryland anurans and thus provide a unique opportunity to investigate whether ecological strategies – in this case

defined by water requirements – can be used to generalize the associations between genetic and structural connectivity. Although canyon treefrogs have unique behavioral adaptations thought to minimize evaporative water loss, adults require frequent (possibly daily) access to water (Snyder and Hammerson 1993). The larval period is estimated to range between 6 and 11 weeks (Zweifel 1961, Stebbins 2003). Red-spotted toads are common near intermittent and ephemeral water sources in the Mojave and Sonoran deserts. They show evidence of some site fidelity, returning to similar stream sections and even burrows when displaced (Weintraub 1974). The larval period of red-spotted toads is estimated to last between 4 and 8 weeks (Tevis 1966, Brennan and Holycross 2006). Mexican spadefoots are ephemeral specialists that breed in temporary pools and ponds filled by summer monsoon thunderstorms. Vibrations from rainfall and/or thunder are thought to signal emergence of spadefoot toads that aestivate in burrows deep underground and emerge to breed in ephemeral pools (Dimmitt and Ruibal 1980). The larval period of Mexican spadefoots ranges between 2 to 4 weeks (Buchholz and Hayes 2000).

Our primary objective was to test whether water dependency – a defining element of aquatic species' ecological strategies – provides a means to generalize the likely mechanisms, and hence patterns, of anuran population structure. First, we hypothesized that genetic population connectivity was inversely related to water requirements, the primary driver of species ecology in an environment in which desiccation risk is a considerable threat for aquatic species (Table 1.1). We also expected that water availability explained a greater degree of population genetic structure (Fig. 1.1C) as species-specific water requirements increased. Land cover, topography, and geographic distance were expected to have heterogeneous effects across species. We predicted that terrestrial resistance (canopy cover and urban land use) would be most important for canyon treefrogs (Fig. 1.1B), the species with the highest desiccation risk for which

permeability of the matrix between breeding sites may drive genetic connectivity. We also expected that topographic resistance (slope) would limit gene flow for red-spotted toads and Mexican spadefoots, whereas canyon treefrogs are adept climbers and may disperse more easily across complex topography (Fig. 1.1D). Alternatively, canyon treefrog populations may be so isolated and gene flow so low that genetic drift results in genetically isolated populations (Fig. 1.1A). Finally, we predicted an isolation-by-distance pattern (Fig. 1.1E) or panmixia pattern (Fig. 1.1F) for Mexican spadefoots where gene flow is likely to be diffuse and relatively unimpeded by landscape factors.

1D. Methods

The study region is the Madrean Sky Islands of southeastern Arizona (USA), characterized by many high mountain ranges separated by arid valley scrubland. The region's landscape is remarkably heterogeneous with large gradients in elevation, water permanence, precipitation, vegetation, and temperature. Our study focused on the Huachuca Mountains and surrounding mountain ranges and valleys, including the Santa Rita, Whetstone, Dragoon, and Mule Mountains. Summer monsoon rains and flash floods in our study region are seasonally predictable but spatially variable. Some areas may receive rain early in the season and stay wet during the entire monsoon while others may receive no rain all season. For these reasons, we used an opportunistic but spatially stratified sampling approach in order to maximize the chance of finding amphibians while attempting to balance the extent of our study, the density of sample locations, and the evenness of sampling locations on the landscape. Adult and larval amphibians were sampled during the spring and summer monsoon seasons of 2010, 2011, and 2012. A single toe clip (adult) or tail clip (larvae) was taken from each individual for DNA extraction and

genotyping. Where possible, sampling sites were visited across multiple years in order to maximize the chance of sampling multiple families. Other sites consisted of multiple isolated pools within 1 km of each other to maximize the chance of sampling multiple families. Additional sampling details and effects of sampling strategy are reported in Appendix 1.A.

Genetic methods

Microsatellite marker information, genotyping details, marker screening procedures, and sibling removal procedures for larval samples are provided in Appendix 1.A. Briefly, population genetic diversity estimates of expected heterozygosity (H_E), observed heterozygosity (H_O), and allelic richness (AR) were estimated with the program MSA 4.05 (Dieringer and Schlötterer 2003). We estimated effective population size (N_e) using the linkage disequilibrium method of Waples and Do (2008), as implemented in NeEstimator V2 (Do et al. 2014). Global genetic differentiation for each species was estimated using G'_{ST}, a standardized measure of genetic differentiation appropriate for multiple species comparisons (Hedrick 2005). Pairwise genetic distance (between each pair of sample sites) was calculated using D_{ps}, a method of measuring genetic differentiation based on proportion of shared alleles (Bowcock et al. 1994). Both G'_{ST} and D_{ps} were calculated with MSA 4.05. Individual-based hierarchical population structure was analyzed using the Bayesian clustering program STRUCTURE 2.3.4 (Pritchard et al. 2000). The most likely number of genetic clusters (K) for each species was determined using the delta-K method (Evanno et al. 2005). Genetic clustering methods are further described in Appendix 1.A, and genotype data are available through figshare (http://dx.doi.org/10.6084/m9.figshare.1205533).

Landscape Genetics

Hypothesized landscape connectivity surfaces were built using CIRCUITSCAPE (McRae 2006). CIRCUITSCAPE uses circuit theory to simulate gene flow (i.e., "current") through a resistance surface in which landscape features hypothesized to promote gene flow are assigned low resistances, and landscape features hypothesized to inhibit gene flow are assigned high resistances. CIRCUITSCAPE allows gene flow across multiple pathways and reports pairwise summations of resistance between sampling locations. Modeling multiple pathways is appropriate for dryland anurans with high dispersal ability (Chan and Zamudio 2009). A geographic information system (ArcGIS 10.1, Environmental Systems Research Institute) was used to catalog and manipulate landscape data, and landscape resistance models, data, and sources are described in detail in Appendix 1.B. Nine landscape resistance surfaces in four broad structural connectivity categories were examined (Table 1.3). The first category was terrestrial and included three resistance surfaces: Canopy (resistance decreased with canopy cover), Urban (resistance increased with development), and LandCov (combination Canopy and Urban for which resistance was lowest with high canopy cover and highest for high development). The second category was aquatic and included three resistance surfaces: Stream (resistance was lowest for perennial/intermittent streams and ponds, moderate for ephemeral streams, and highest for areas with no aquatic habitat), PrecipET (resistance decreased as summer precipitation-evapotranspiration increased), and AvgWat (combination Stream and PrecipET for which resistance was lowest where both precipitation was high and aquatic habitat was available, and for which resistance was highest for dry areas with no aquatic habitat). The third category was topography and included Slope (resistance increased with slope). The fourth category was isolation-by-distance and included pairwise Euclidean distance between sampling locations (Euclidean) and one uniform, non-zero resistance surface (Null).

We evaluated relationships between pairwise genetic distance and pairwise landscape resistances using a mixed-effects modeling approach (van Strien et al. 2012). Through mixed-effects modeling, explanatory variables (pairwise landscape resistances) are treated as fixed effects, and sampling locations are treated as random effects to account for non-independent values in distance matrices (Yang 2004). Model fit was evaluated with the R^2_β statistic (Edwards et al. 2008) that compares a model with fixed and random effects (pairwise landscape distance or resistance and sampling location) to a null model with only the random effect (sampling location) and an intercept. Comparison of model performance metrics, such as p-values, allows for evaluating significant differences between models; however, no formal method of comparison has been developed or agreed upon for evaluating R^2_β values of different models. Therefore, we compared R^2_β values to one another directly as is common to-date in studies using this approach (van Strien et al. 2012). We also used multiple regression with distance matrices (MRDM) (Holzhauer et al. 2006, Balkenhol et al. 2009) as a complementary method to evaluate relationships between genetic and structural connectivity. MRDM methods are described in Appendix 1.B. All analyses were performed in R version 2.14.0 (R Development Core Team, 2012), using a modified version of lme4 (Bates et al. 2012) for mixed-effects modeling, PBKRTEST (Halekoh and Højsgaard 2012) for R^2_β calculation as described in van Strien et al. (2012), and ecodist (Goslee and Urban 2007) for MRDM.

1E. Results

We found support for the hypothesis that population structure (genetic differentiation) was correlated with species' water requirements. Global genetic differentiation was highest for canyon treefrogs (G'_{ST} = 0.57), intermediate for red-spotted toads (G'_{ST} = 0.31), and lowest for

spadefoots (G'_{ST} = 0.09). We found strong hierarchical clustering for canyon treefrogs (Fig. 1.2A) with spatial clustering by mountain range (Fig. 1.2D). Red-spotted toads had moderate hierarchical structure (Fig. 1.2B) with complex spatial patterns of genetic connectivity (Fig. 1.2E). Mexican spadefoots had little hierarchical structure (Fig. 1.2C) with diffuse spatial clustering (Fig. 1.2F). Delta-*K* results for all species and genetic clusters are included in Appendix 1.A. Sampling information and population genetic metrics are summarized in Table 1.2 and described in full in Appendix 1.A.

Landscape resistances and distances in three of four categories (terrestrial, aquatic and isolation-by-distance) were moderately to highly correlated for each species (Appendix 1.B, Table 1.B.3). We evaluated correlated landscape resistances independently in a mixed-effects modeling framework to insure that collinear variables were not included in the same model. Mixed-effects models revealed a large difference in the strength of correlation between genetic and structural connectivity across species. R^2_β values for canyon treefrogs were more than double those for red-spotted toads and Mexican spadefoots (Table 1.3). Within species, R^2_β values for canyon treefrogs were highest for models in the terrestrial and aquatic categories, with AvgWater having the highest correlation across models (R^2_β = 0.70). For red-spotted toads, Urban had the strongest correlation with genetic connectivity (R^2_β = 0.33). However, R^2_β for other terrestrial resistances (Canopy and LandCov) were lower than overall aquatic resistances, and Urban was highly correlated (r > 0.9) with Null (isolation-by-distance category). Thus, the R^2_β for urban resistance may reflect the effects of null resistance rather than a true terrestrial effect. Finally, Mexican spadefoot genetic connectivity was most closely related to Euclidean distance in the isolation-by-distance category (R^2_β = 0.31).

We also examined relationships between genetic and structural connectivity within major genetic clusters for each species. For canyon treefrogs, we examined two nested clusters: the western cluster (CT-W) and the Huachuca Mountains cluster (CT-H) (Fig. 1.2D). Results for the two nested clusters did not differ greatly from results for all canyon treefrog sites, though the support for isolation-by-distance increased marginally at finer scales (Appendix 1.B, Table 1.B.4). The same was true for the only major genetic cluster of Mexican spadefoots (MS-E, Fig. 1.2F) in which results differed only slightly by scale (Appendix 1.B, Table 1.B.4). However, the two major genetic clusters for red-spotted toads were spatially complex, with one spatially clustered group (the Huachuca Mountains group, RT-H) and a larger, spatially diffuse group (the northern group, RT-N) (Fig. 1.2E). Hierarchical structure was not found in RT-H and was moderate for RT-N. We found strong support for a relationship between genetic structure and topographic resistance for RT-N. Conversely, genetic structure of populations in the RT-H group had no relationship with landscape structure, indicating panmictic population structure (Table 1.3).

Combining topographic resistance with other landscape resistances provides a context for interpreting how the physical template (topography) and landscape features (e.g., streams, canopy cover, and urbanization) interact and affect genetic connectivity. Topographic resistance (slope) was not correlated with other landscape resistance surfaces, and for that reason we evaluated couplet models combining topography with landscape resistances in other categories (terrestrial, aquatic, and isolation-by-distance). R^2_β values for couplet models were higher than single resistance models across all species, and R^2_β values increased by the widest margin for red-spotted toads and Mexican spadefoots (Table 1.3). Perhaps most notably, the best couplet model for each species and within the northern red-spotted toad (RT-N) genetic cluster included

both topographic and aquatic resistances. Canyon treefrogs had equivalent and high R^2_β values (0.85) for the couplet models combining topography + aquatic resistance and topography + isolation-by-distance. However, rather than the expected negative correlation with genetic connectivity, topographic resistance was positively correlated with genetic connectivity for canyon treefrogs. This was also true for the two finer-scale genetic clusters examined for canyon treefrogs (Appendix 1.B, Table 1.B.4). This may indicate gene flow across high slope areas, such as mountain ranges and ridgelines, rather than across flat landscapes. Urbanization resistances were highly correlated with uniform resistance values (the isolation-by-distance hypothesis) for both genetic clusters of canyon treefrogs due to very low urban development within the spatial extent of those clusters, and R^2_β values for models incorporating urbanization resistances should be interpreted with this in mind.

Finally, MRDM results for each species and their genetic clusters largely corroborated mixed-effects modeling results, although there were some differences. Canyon treefrog genetic distances were most highly correlated with uniform landscape resistance, with the highest support for uniform landscape resistance (isolation-by-distance hypothesis) model. When accounting for high collinearity between the uniform and aquatic resistances within genetic clusters of canyon treefrogs (*vif* > or near to 10), conservative interpretation of the MRDM results also supports the uniform resistance-only model for both genetic clusters. For red-spotted toads (both overall and for the northern group), the best model included low resistance along river networks and ponds, topographic resistance, and uniform resistance. However, the correlation with uniform resistance was negative, indicating no support for the isolation-by-distance hypothesis. Finally, we found support for the aquatic hypothesis for Mexican spadefoots at multiple spatial scales. Results are summarized in Appendix 1.B.

1F. Discussion

Characterizing the influences of species ecology and the landscape on genetic connectivity among populations contributes to fundamental ecological and evolutionary knowledge and is an important part of successful conservation of species (Allendorf and Luikart 2007, Manel and Holderegger 2013). Our findings highlight the utility and potential of species' ecological traits – in our case water dependency – in characterizing relationships between genetic and structural (landscape) connectivity across taxa. We found a positive relationship between population differentiation and increasing water requirements across three aquatic species. When considered independently, landscape drivers of genetic connectivity were largely predicted by hypothesized models built upon knowledge of water requirements, a defining characteristic of species ecology for desert amphibians. Aquatic connectivity had the strongest relationship with genetic connectivity across species when landscape drivers were combined with topography. This supports the notion that in arid environments, water and aquatic habitat are major factors in gene flow and landscape permeability for all aquatic species – from perennial to ephemeral specialists.

Desert anurans utilize a range of ecological strategies to survive in areas characterized by a spatial mosaic of perennial, intermittent, and ephemeral waters embedded in an arid landscape. Larval development periods restrict species' breeding habitats, and desiccation risk is a known driver of amphibian movements in arid environments (Tingley and Shine 2011). High mobility is one possible strategy for capitalizing on unpredictable availability of water and may drive high genetic connectivity observed in some desert anurans in the American Southwest (Mexican spadefoots in this study; Chan and Zamudio 2009). The high mobility of Mexican spadefoots and other ephemeral specialists in the region (e.g., Couch's spadefoot, *Scaphiopus couchii*, and the

Great Plains toad, *Bufo cognatus*) may provide greater resiliency to temporal or spatial changes in habitat availability, and high genetic connectivity between populations may buffer the genetic consequences of some habitat loss.

High mobility, however, is only one end of a spectrum of potential strategies for aquatic desert life; other species may instead exhibit site fidelity to isolated pools with perennial or longer-term intermittent water. Both canyon treefrogs and red-spotted toads exhibit some degree of site fidelity and had greater population structure than Mexican spadefoots. Proximity to water is the hypothesized mechanism by which canyon treefrogs meet necessary water requirements for thermoregulation (Snyder and Hammerson 1993). Red-spotted toads also exhibit non-random occupancy of suitable breeding habitat (Dayton and Fitzgerald 2001) and fidelity for particular sites (Turner 1959, Weintraub 1974). These findings support our hypothesis of greater population structure with increasing water requirements. Aquatic habitat in the Sky Islands region is threatened by human water use (Marshall et al. 2010), a warming and drying climate (Seager et al. 2007), and an increased risk of catastrophic disturbances such as extreme fires (Brown et al. 2004). A drier landscape and loss of an already limited number of breeding sites may result in a greater risk of loss of genetic diversity for amphibians such as red-spotted toads, canyon treefrogs and others with small population sizes and/or high water requirements (e.g., Chiricahua leopard frogs, *Lithobates chiricahuensis*; Arizona treefrog, *Hyla wrightorum*; and Sonoran tiger salamander, *Ambystoma mavortium stebbinsi*).

Considered independently, the importance of different connectivity models varied across species. As predicted, terrestrial and aquatic connectivity were highly correlated with genetic connectivity for canyon treefrogs in mixed-effects models. But, the null resistance model (isolation-by-distance) performed similarly, and MRDM models provided strong support for an

isolation-by-distance-only model. This indicates that distance alone may be an important driver of population genetic structure in this species. This may be particularly true at the spatial scale of a single mountain range where high elevation, lower temperature, and greater precipitation provide a high density and availability of permeable landscape. This is supported by the marginal increase in support for isolation-by-distance at a finer scale for canyon treefrogs. Two things may explain this result. First, distance may in fact be the primary driver of genetic connectivity between populations, particularly within a mountain range. Second, if landscape attributes such as aquatic connectivity are important for dispersal, the high permeability of the landscape may make it difficult to detect the importance of such features using a landscape genetics approach (Cushman et al. 2013).

For red-spotted toads, all mixed-effects models performed similarly with the exception of poorly supported Euclidean distance-only model. However, when major genetic clusters were considered independently, topographic resistance had the highest R^2_β for the northern red-spotted toad group (RT-N) as predicted, and the Huachuca group (RT-H) was panmictic, highlighting the variability of important landscape drivers of genetic connectivity introduced by spatial scale and extent of a study. Finally, mixed-effects models supported distance alone (Euclidean) as the best explanatory factor in Mexican spadefoot genetic connectivity.

Topography is the physical template upon which organisms interact with other landscape factors, and high slope is known to reduce genetic connectivity in some amphibians (Lowe et al. 2006). When topographic resistance was considered alongside other landscape factors, aquatic connectivity emerged as a dominant driver of genetic connectivity for all species. However, for canyon treefrogs, the correlation between topographic resistance and genetic connectivity was opposite the expected relationship, with high slope correlated with high genetic connectivity.

Though canyon treefrogs have the highest water requirements of the three species we examined they are relatively well-adapted to dry conditions (Snyder and Hammerson 1993). Complex topography and high elevation ridges may not completely inhibit canyon treefrog gene flow, and our results suggest some genetic resilience to temporarily dewatered or disturbed habitat (e.g., from fires or a dry year) at finer spatial scales where individuals may be capable of recolonizing breeding habitat. Furthermore, mountain ranges may provide more refugia and less stressful environmental conditions for dispersing individuals due to wetter monsoon conditions, higher canopy cover, and lower temperatures than valley regions. Similar patterns of isolation-by-mountain range are described for sympatric insects described as headwater specialists (Finn et al. 2007, Phillipsen and Lytle 2013).

The relationship between genetic and aquatic connectivity for red-spotted toads may be driven by the species' affinity for bedrock pools. In ephemeral areas, adults might disperse along riparian networks in which refugia and the likelihood of finding suitable breeding habitat are greatest, and they may be deterred by the high slope of canyons, incised channels, or valley walls. Longitudinal connectivity may also be the result of rare but important downstream dispersal when larvae in these shallow bedrock reaches are displaced and washed downstream by flash floods.

Finally, the relationship between genetic and aquatic connectivity in a topographic context for Mexican spadefoots supports the idea that aquatic connectivity may be important for aquatic species with even the most ephemeral water requirements. Mexican spadefoots have the lowest hydrologic requirements of the three species in this study, but aquatic habitat remains a critical part of their life cycle. Furthermore, high slope topography may represent a barrier, may not

provide adequate breeding habitat or underground refugia, or may be too energetically costly to navigate.

These findings highlight the potential predictive power of species biology and ecology in understanding population connectivity. Still, there are inherent limitations with this methodology. Gene flow estimates derived from microsatellite data reflect gene flow over the last few decades to centuries and do not always reflect present-day demographic or genetic processes (Waples and Gaggiotti 2006). Secondary contact after removal of a historical barrier may manifest as a cryptic genetic signal unrelated to current landscape processes (Landguth et al. 2010). Our study extent may have encompassed two major lineages of red-spotted toads that diverged during the late Pleistocene (Bryson et al. 2012). However, studies suggest similar or even increased landscape permeability for at least the last 1000 generations for this species (Holmgren et al. 2003, Pigati et al. 2009). Moreover, global genetic differentiation of red-spotted toads in this study was moderate to low, and with many populations in this study estimated to have modest N_e it is unlikely that the signal from secondary contact is detectable in this study (Whitlock and McCauley 1999).

Challenges stemming from collinearity, resistance surface parameterization, and spatial scale can also complicate detection and interpretation of relationships between genetic and structural connectivity. This is not unique to our study as collinearity among landscape resistance values is a persistent challenge in landscape genetics (Balkenhol et al. 2009). Our ability to account for collinearity in resistance values is limited because formal comparisons of R^2_β have yet to be developed. Thus, comparisons of close R^2_β values can make interpretation – and determining the "true" landscape driver – difficult. Therefore, though interpreting results in an ecological context does provide valuable insight (Cushman and Landguth 2010), R^2_β values must be interpreted

with these correlations in mind. Defining landscape resistance values is a recognized challenge in landscape genetics (Spear et al. 2010, Cushman et al. 2013). It is likely that true landscape resistances are more complex than the simple resistance values used in our study, and non-linear relationships may exist between genetic and landscape connectivity (e.g., Peterman et al. 2014). However, our goal was to compare hypothesized relationships between genetic structure of populations and a suite of landscape factors, and we created simple landscape resistance layers that reflect our hypotheses and that were easily compared across species.

Our study's spatial extent captured meaningful genetic structure across all three species, but landscape effects may change at different spatial scales (Anderson et al. 2010, Murphy et al. 2010). Spatial patterns of genetic diversity indicated clean hierarchical structure for canyon treefrogs and clear isolation-by-distance patterns for spadefoots; however, red-spotted toads displayed spatially complex structure, and genetic connectivity within genetic clusters varied in its relationship to the landscape. Though we do not know the underlying cause of that spatial variability in red-spotted toads, complex effects of spatial scale highlight the need to carefully interpret patterns observed in one portion of a species' range when drawing management-relevant conclusions outside the study area. The landscape is often heterogeneous across a species' range, and edge verses central populations may have different population dynamics and undergo different selective pressures (Hardie and Hutchings 2010, Trumbo et al. 2013). The ranges of the three study species extend beyond the area of this study and encompass areas with drier climate, greater urbanization, and lower canopy cover than the geographic extent of this study. The variability observed for red-spotted toads emphasizes that relationships between landscape variables and genetic connectivity are not necessarily consistent across a range or at

different spatial scales, and relationships may be fundamentally different in areas where the matrix between populations is drier, harsher, or offers fewer refugia.

In conclusion, we found that patterns of population structure, connectivity, and their landscape drivers are predicted by the water dependencies of anurans in dryland ecosystems. Our work supports recent studies highlighting the utility of multi-species inference and ecologically derived hypotheses (e.g., Hughes et al. 2013). Genetic diversity is often a missing component in conservation planning and resource allocation despite its recognized role in species persistence (Laikre et al. 2010). With increasing human demand for aquatic resources in arid environments, environmental change and habitat alteration will likely outpace the resources and time necessary for single-species population genetics studies for many species of conservation concern. When single-species studies are not feasible, the use of species' ecological information to predict relationships between genetic and structural connectivity may provide a promising alternative.

1G. Acknowledgements

We extend our sincerest gratitude to the following individuals, agencies, and organizations that helped make this work possible. This study was funded by the Department of Defense Strategic Environmental Research and Development Program (RC-1724). Sheridan Stone assisted with study design, logistics, and sampling efforts throughout the duration of the project. Jessica Hale, Kristen Jaeger, Britta Padgham, Tom Miscione, and Robert Troup provided extensive help with sampling efforts. David Armstrong, Jan Armstrong, Michael Bogan, Ken Charters, Merce Dostale, Caren Goldberg, Matt Kaplan, Lanie Levick, Jesi Miscione, Eric Moody, Mike Sredl, Katherine Strickler, Michael Tarachow, and Eric Wallace assisted with *H. arenicolor* sampling. Brooke Gebow and The Nature Conservancy Ramsey Canyon helped with field work logistics.

Martin Schlaepfer and Mike Sredl assisted with study design, Dale Turner provided spatial riparian data for Mexico, and Martin van Strien provided assistance with mixed-effects modeling. Lorenz Hauser, Adam Leaché, Joshua Lawler, and three anonymous reviewers provided helpful comments on the manuscript. Additional funding for MCM was provided by a National Science Foundation Graduate Research Fellowship (Grant No. DGE-0718124).

1H. References

Allendorf, F. W., and G. Luikart. 2007. Conservation and the genetics of populations. Blackwell Publishing, Malden, Massachusetts, USA.

Anderson, C. D., B. K. Epperson, M. Fortin, R. Holderegger, P. M. A. James, M. S. Rosenberg, K. T. Scribner, and S. Spear. 2010. Considering spatial and temporal scale in landscape-genetic studies of gene flow. Molecular Ecology **19**:3565-3575.

Balkenhol, N., L. P. Waits, and R. J. Dezzani. 2009. Statistical approaches in landscape genetics: an evaluation of methods for linking landscape and genetic data. Ecography **32**:818-830.

Bates, D., M. Maechler, B. Bolker,and S. Walker. 2014. lme4: Linear mixed-effects models using Eigen and S4. R package version 1.1-7. http://CRAN.R-project.org/package=lme4

Bowcock, A. M., A. Ruiz-Linares, J. Tomfohrde, E. Minch, J. R. Kidd, and L. L. Cavalli-Sforza. 1994. High resolution human evolutionary trees with polymorphic microsatellites. Nature **368**:455-457.

Bradbury, I. R., B. Laurel, P. V. Snelgrove, P. Bentzen, and S. E. Campana. 2008. Global patterns in marine dispersal estimates: the influence of geography, taxonomic category, and life history. Proceedings of the Royal Society B **275**:1803-1809.

Brennan, T. C., and A. T. Holycross. 2006. A field guide to amphibians and reptiles in Arizona. Arizona Game and Fish Department, Phoenix, Arizona, USA.

Brown, T., B. L. Hall, and A. L. Westerling. 2004. The impact of twenty-first century climate change on wildland fire danger in the Western United States: an applications perspective. Climatic Change. **62**:365-388.

Bryson, R. W., J. R. Jaeger, J. A. Lemos-Espinal, and D. Lazcano. 2012. A multilocus perspective on the speciation history of a North American aridland toad (*Anaxyrus punctatus*). Molecular Phylogenetics and Evolution **64**:393-400.

Buchholz, D. R., and T. B. Hayes. 2000. Larval period comparison for the spadefoot toads *Scaphiopus couchii* and *Spea multiplicata* (Pleobatidae: Anura). Herpetologica **56**:455-468.

Cadena, C. D., N. Gutiérrez-Pinto, N. Dávila, and R. T. Chesser. 2011. No population genetic structure in a widespread aquatic songbird from the Neotropics. Molecular Phylogenetics and Evolution **58**:540-545.

Chan, L. M., and K. R. Zamudio. 2009. Population differentiation of temperate amphibians in unpredictable environments. Molecular Ecology **18**:3185-3200.

Cushman, S. A., and E. L. Landguth. 2010. Spurious correlations and inference in landscape genetics. Molecular Ecology **19**:3592-3602.

Cushman, S. A., A. J. Shirk, and E. L. Landguth. 2013. Landscape genetics and limiting factors. Conservation Genetics **14**:263-274.
Dayton, G. H., and L. A. Fitzgerald. 2001. Competition, predation, and the distribution of four desert anurans. Oecologia **129**:430-435.
Dieringer, D., and C. Schlötterer. 2003. Microsatellite analyser (MSA): a platform independent analysis tool for large microsatellite data sets. Molecular Ecology Notes **3**:167-169.
Dimmitt, M. A., and R. Ruibal. 1980. Environmental correlates of emergence in spadefoot toads (*Scaphiopus*). Journal of Herpetology **14**:21-29.
Do, C., R. S. Waples, D. Peel, G. M. Macbeth, B. J. Tillett, and J. R. Ovenden. 2014. NeEstimator v2: re-implementation of software for the estimation of contemporary effective population size (N_e) from genetic data. Molecular Ecology Resources **14**:209-214.
Edwards, L. J., K. E. Muller, R. D. Wolfinger, B. F. Qaqish, and O. Schabenberger. 2008. An R^2 statistic for fixed effects in the linear mixed model. Statistics in Medicine **27**:6137-6157.
Evanno, G., S. Regnaut, and J. Goudet. 2005. Detecting the number of clusters of individuals using the software STRUCTURE: a simulation study. Molecular Ecology **14**:2611-2620.
Finn, D. S., M. S. Blouin, and D. A. Lytle. 2007. Population genetic structure reveals terrestrial affinities for a headwater stream insect. Freshwater Biology **52**:1881-1897.
Goslee, S.C. and D. L. Urban. 2007. The ecodist package for dissimilarity-based analysis of ecological data. Journal of Statistical Software **22**:1-19.
Halekoh, U., and S. Højsgaard. PBKRTEST: parametric bootstrap and Kenward Roger based methods for mixed model comparison. R package version 0.3-2. http://CRAN.R-project.org/package=pbkrtest.
Hardie, D. C., and J. A. Hutchings. 2010. Evolutionary ecology at the extremes of species' ranges. Environmental Reviews **18**:1-20.
Hedrick, P. W. 2005. A standardized genetic differentiation measure. Evolution **59**:1633-1638.
Holmgren, C. A., M. C. Peñalba, K. A. Rylander, and J. L. Betancourt. 2003. A 16,000 ^{14}C yr B.P. packrat midden series from the USA-Mexico Borderlands. Quaternary Research **60**:319-329.
Holzhauer, S. I. J., K. Ekschmitt, A. Sander, J. Dauber, and V. Wolters. 2006. Effect of historic landscape change on the genetic structure of the bush-cricket *Metrioptera roeseli*. Landscape Ecology **21**:891-899.
Hughes, J. M., J. A. Huey, and D. J. Schmidt. 2013. Is realised connectivity among populations of aquatic fauna predictable from potential connectivity? Freshwater Biology **58**:951-966.
Imbert, E., and F. Lefèvre. 2003. Dispersal and gene flow of *Populus nigra* (Salicaceae) along a dynamic river system. Journal of Ecology **91**:447-456.
Jaeger, K. L., J. D. Olden, and N. A. Pelland. 2014. Climate change poised to threaten hydrologic connectivity and endemic fishes in dryland streams. Proceedings of the National Academy of Sciences, USA **111**:13894-13899.
Kingsford, R. T., K. M. Jenkins, and J. T. Porter. 2004. Imposed hydrological stability on lakes in arid Australia and effects on waterbirds. Ecology **85**:2478-2492.
Laikre, L., F. W. Allendorf, L. C. Aroner, C. S. Baker, D. P. Gregovich, M. M. Hansen, J. A. Jackson, K. C. Kendall, K. McKelvey, M. C. Neel, I. Olivieri, N. Ryman, M. K. Schwartz, R. Short Bull, J. B. Stetz, D. A. Tallmon, B. L. Taylor, C. D. Vojta, D. M. Waller, and R. S. Waples. 2010. Neglect of genetic diversity in implementation of the Convention on Biological Diversity. Conservation Biology **24**:86-88.

Landguth, E. L., S. A. Cushman, M. K. Schwartz, K. S. McKelvey, M. Murphy, and G. Luikart. 2010. Quantifying the lag time to detect barriers in landscape genetics. Molecular Ecology **19**:4179-4191.

Lowe, W. H., G. E. Likens, M. A. McPeek, and D. C. Buso. 2006. Linking direct and indirect data on dispersal: isolation by slope in a headwater stream salamander. Ecology **87**:334-339.

Manel, S., and R. Holderegger. 2013. Ten years of landscape genetics. Trends in Ecology and Evolution **28**:614-621.

Manel, S., M. K. Schwartz, G. Luikart, and P. Taberlet. 2003. Landscape genetics: combining landscape ecology and population genetics. Trends in Ecology and Evolution **18**:189-197.

Marshall, R. M., M. D. Robles, D. R. Majka, and J. A. Haney. 2010. Sustainable water management in the southwestern United States: reality or rhetoric? PLoS ONE **5**:e11687.

McRae, B. H. 2006. Isolation by resistance. Evolution **60**:1551-1561.

Murphy, M. A., J. S. Evans, and A. Storfer. 2010. Quantifying *Bufo boreas* connectivity in Yellowstone National Park with landscape genetics. Ecology **91**:252-261.

Nilsson, C., R. L. Brown, R. Jansson, and D. M. Merritt. 2010. The role of hydrochory in structuring riparian and wetland vegetation. Biological Reviews **85**:837-858.

Peterman, W. E., G. M. Connett, R. D. Semlitsch, and L. S. Eggert. 2014. Ecological resistance surfaces predict fine-scale genetic differentiation in a terrestrial woodland salamander. Molecular Ecology **23**:2402-2413.

Phillipsen, I. C., and D. A. Lytle. 2013. Aquatic insects in a sea of desert: population genetic structure is shaped by limited dispersal in a naturally fragmented landscape. Ecography **36**:731-743.

Pigati, J. S., J. E. Bright, T. M. Shanahan, and S. A. Mahan. 2009. Late Pleistocene paleohydrology near the boundary of the Sonoran and Chihuahuan Deserts, southeastern Arizona, USA. Quaternary Science Reviews **28**:286-300.

Pritchard, J. K., M. Stephens, and P. Donnelly. 2000. Inference of population structure using multilocus genotype data. Genetics **155**:945-59.

Richardson, J. L. 2012. Divergent landscape effects on population connectivity in two co-occurring amphibian species. Molecular Ecology **21**:4437-4451.

Robertson, H. L., M. T. Guzik, and N. P. Murphy. 2014. Persistence in the desert: ephemeral waterways and small-scale gene flow in the desert spring amphipod, *Wangiannachiltonia guzikae*. Freshwater Biology **59**:653-665.

Seager, R., M. Ting, I. Held, Y. Kushnir, J. Lu, G. Vecchi, H. Huang, N. Harnik, A. Leetmaa, N. Lau, C. Li, J. Velez, and N. Naik. 2007. Model projections of an imminent transition to a more arid climate in southwestern North America. Science **316**:1181-1184.

Snyder, G. K., and G. A. Hammerson. 1993. Interrelationships between water economy and thermoregulation in the canyon treefrog *Hyla arenicolor*. Journal of Arid Environments **25**:321-329.

Sodhi, N. S., D. Bickford, A. C. Diesmos, T. M. Lee, L. P. Koh, B. W. Brook, C. H. Sekercioglu, and C. J. A. Bradshaw. 2008. Measuring the meltdown: drivers of global amphibian extinction and decline. PLoS ONE **3**:e1636.

Spear, S. F., N. Balkenhol, M. Fortin, B. H. McRae, and K. Scribner. 2010. Use of resistance surfaces for landscape genetic studies: considerations for parameterization and analysis. Molecular Ecology **19**:3576-3591.

Stebbins, R. C. 2003. Western reptiles and amphibians. Third Edition. Houghton Mifflin, Singapore.

Stuart, S. N., J. S. Chanson, N. A. Cox, B. E. Young, A. S. L. Rodrigues, D. L. Fischman, and R. W. Waller. 2004. Status and trends of amphibian declines and extinctions worldwide. Science **306**:1783-1786.

Taylor, P.D., L. Fahrig, K. Henein, and G. Merriam. 1993. Connectivity is a vital element of landscape structure. Oikos **68**:571–573.

Tevis, L. 1966. Unsuccessful breeding by desert toads (*Bufo punctatus*) at the limit of their ecological tolerance. Ecology **47**:766-775.

Tingley, R., and R. Shine. 2011. Desiccation risk drives the spatial ecology of an invasive anuran (*Rhinella marina*) in the Australian semi-desert. PLoS ONE **6**:e25979.

Trumbo, D. R., S. F. Spear, J. Baumsteiger, and A. Storfer. 2013. Rangewide landscape genetics of an endemic Pacific northwestern salamander. Molecular Ecology **22**:1250-1266.

Turner, F. B. 1959. Some features of the ecology of *Bufo punctatus* in Death Valley, California. Ecology **40**:175-181.

van Strien, M. J., D. Keller, and R. Holderegger. 2012. A new analytical approach to landscape genetic modelling: least-cost transect analysis and linear mixed models. Molecular Ecology **21**:4010-4023.

Vörösmarty, C. J., P. B. McIntyre, M. O. Gessner, D. Dudgeon, A. Prusevich, P. Green, S. Glidden, S. E. Bunn, C. A. Sullivan, C. Reidy Liermann, and P. M. Davies. 2010. Global threats to human water security and river biodiversity. Nature **467**:555-561.

Waples, R. S., and C. Do. 2008. LDNE: a program for estimating effective population size from data on linkage disequilibrium. Molecular Ecology Resources **8**:753-756.

Waples, R. S., and O. Gaggiotti. 2006. What is a population? An empirical evaluation of some genetic methods for identifying the number of gene pools and their degree of connectivity. Molecular Ecology **15**:1419-1439.

Weintraub, J. D. 1974. Movement patterns of the red-spotted toad, *Bufo punctatus*. Herpetologica **30**:212-215.

Whitlock, M. C., and D. E. McCauley. 1999. Indirect measures of gene flow and migration: $F_{ST} \neq 1/(4Nm + 1)$. Heredity **82**:117-125.

Yang, R. C. 2004. A likelihood-based approach to estimating and testing for isolation by distance. Evolution **58**:1839-1845.

Zweifel, R. G. 1961. Larval development of the tree frogs *Hyla arenicolor* and *Hyla wrightorum*. American Museum Novitates **2056**:1-20.

1I. Tables

Table 1.1. Genetic and landscape connectivity hypotheses. Hypothesized genetic connectivity models for each species (CT = canyon treefrog, RT = red-spotted toad, and MS = Mexican spadefoot) are indicated by "**X**". Hypotheses are visualized in Fig. 1.1.

Hypotheses	**Species predictions**			**Description**	**Population genetics patterns**	**Landscape drivers and genetic connectivity correlation (+/-)**
	CT	RT	MS			
Isolated populations	**X**			High differentiation; no relationship with distance.	All populations distinct from one another; high population differentiation.	None: local processes (e.g., genetic drift) dominate.
Terrestrial	**X**			Canopy cover promotes genetic connectivity; development reduces connectivity.	Populations cluster within areas of high canopy cover; distinct populations in developed areas.	Canopy cover (+) and urban land use (-).
Aquatic	**X**	**X**		Connectivity correlated with hydrologic network (streams, ponds), precipitation.	Populations cluster along riparian networks and in areas with high precipitation.	Hydrologic network: streams and ponds (+); precipitation (+).
Topography		**X**	**X**	Slope (rise over run) negatively correlated with genetic connectivity.	Isolated populations in areas with steep terrain; high connectivity along flat ground.	Topography: slope (-).
Isolation-by-distance			**X**	Differentiation correlated with distance.	Population differentiation increases proportionally with distance.	Distance (+).
Panmixia			**X**	Low differentiation; no relationship with distance.	Little/no population differentiation.	None: migration/connectivity dominate.

Table 1.2. Sample size, microsatellite information, and population genetics metrics for each species. Sample sizes are given as number of sampling locations (*N*), total individuals (*n*), *n* with all but one full sibling (sib) from each family removed, *n* with reconstructed parents included (described in Appendix 1.A), and average *n* ($\bar{n}$) per sampling location with all siblings, with only one full sibling, and with reconstructed parents. Microsatellite information includes loci count and average allelic richness (AR, averaged across populations, and adjusted for smallest sample size). Population genetic metrics include expected heterozygosity (H_E) and observed heterozygosity (H_O) calculated as averages of all populations, with reconstructed parents; median effective population size across populations ($\overline{N_e}$); and overall population differentiation (G'_{ST}). More information, including population genetic metrics by population and locus, is included in Appendix 1.A.

Species	**Sample size**				**Average *n***			**Loci**		**Population genetics**			
	N	*n*	*n*, no sibs	*n*, with parents	$\bar{n}$	$\bar{n}$, no sibs	$\bar{n}$, with parents	Count	AR	H_E	H_O	$\overline{N_e}$	G'_{ST}
Canyon treefrog	15	575	175	202	42.2	11.7	13.5	12	5.09	0.73	0.74	30.7	0.57
Red-spotted toad	15	660	233	252	41.1	15.9	16.8	14	5.29	0.76	0.74	83.0	0.31
Mexican spadefoot	26	1163	781	784	38.3	30.0	30.2	8	5.26	0.67	0.67	5951.7	0.09

Table 1.3. Mixed-effects modeling results for each species (CT = canyon treefrog, RT = red-spotted toad, MS = Mexican spadefoot) and major genetic clusters of red-spotted toads (RT-N = north, RT-H = Huachuca Mountains; Fig. 1.2). Spatial data are described in full in Appendix 1.B. Single explanatory variable models are included above the line, and couplet models are below. Top R^2_β values are highlighted in bold font. Isolated populations and panmixia hypothesize no landscape effect, indicated by poor model performance across all other models. A dash indicates no support for isolated populations and panmixia. All R^2_β correlation coefficients are positive except those underlined. Slope is negatively correlated with D_{PS} for CT in all couplet models, and Euclidean is negatively correlated with D_{PS} for RT-N in the IBT + T couplet model.

Hypotheses	**Resistance layers/ distance**	**R^2_β, mixed-effects models**				
Species		**CT**	**RT**	**MS**	**RT-N**	**RT-H**
Isolated populations	*N/A*	-	-	-	-	-
Terrestrial (TE)	Canopy	0.68	0.26	0.28	0.06	0.02
	Urban	0.68	**0.33**	0.27	0.06	<0.01
	LandCov	0.69	0.27	0.28	0.07	<0.01
Aquatic (A)	Stream	0.67	0.32	0.28	0.10	<0.01
	PrecipET	0.68	0.30	0.28	0.06	<0.01
	AvgWater	**0.70**	0.31	0.28	0.09	<0.01
Topography (T)	Slope	0.35	0.27	0.29	**0.48**	0.01
Isolation-by-distance (IBD)	Euclidean	0.57	0.14	**0.31**	0.02	<0.01
	Null	0.67	0.30	0.28	0.06	<0.01
Panmixia	*N/A*	-	-	-	-	**Yes**
TE + T	Best of TE + Slope	0.78	0.58	0.49	0.62	0.04
A + T	Best of A + Slope	**0.85**	**0.61**	**0.50**	**0.66**	0.03
IBD + T	Euclidean + Slope	0.76	0.32	0.39	0.37	0.02
	Null + Slope	**0.85**	0.56	0.48	0.36	0.03

1J. Figures

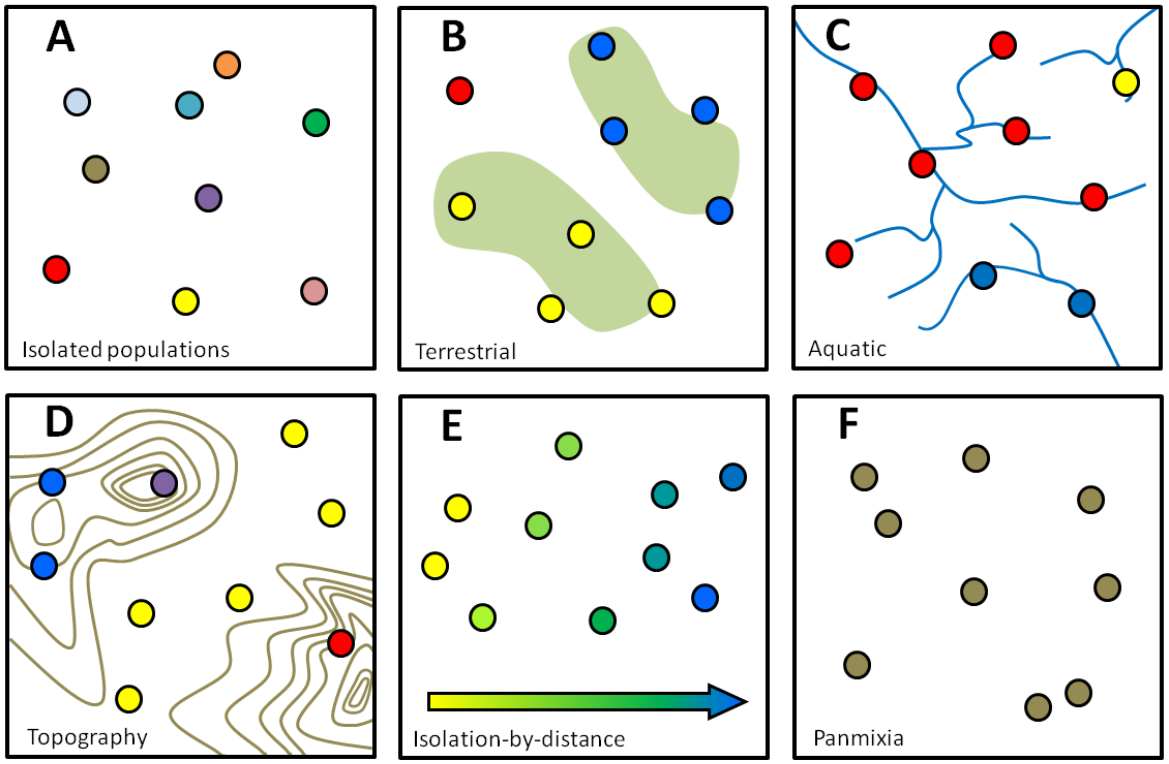

Figure 1.1. Genetic connectivity hypotheses (see Table 1.1). Populations (circles) of the same color are genetically similar. Panels illustrate: isolated populations (A) with no landscape drivers of population differentiation; rather, local processes such as genetic drift drive genetic differentiation of populations. Terrestrial (B) describes genetic connectivity associated with low resistance land cover, such as areas with high canopy cover (shown in green). Aquatic (C) describes connectivity within riparian networks (shown as blue lines) or in areas with high precipitation. Topography (D) is characterized by high connectivity along flat ground (low slope) and high differentiation of populations separated by high slope, as shown with brown contour lines. Isolation-by-distance (E) describes an increase in genetic differentiation between populations as distance increases or along a cline (arrow). Panmixia (F) is characterized by genetically similar populations across the sampling range with no relationship to landscape.

Figure 1.2.

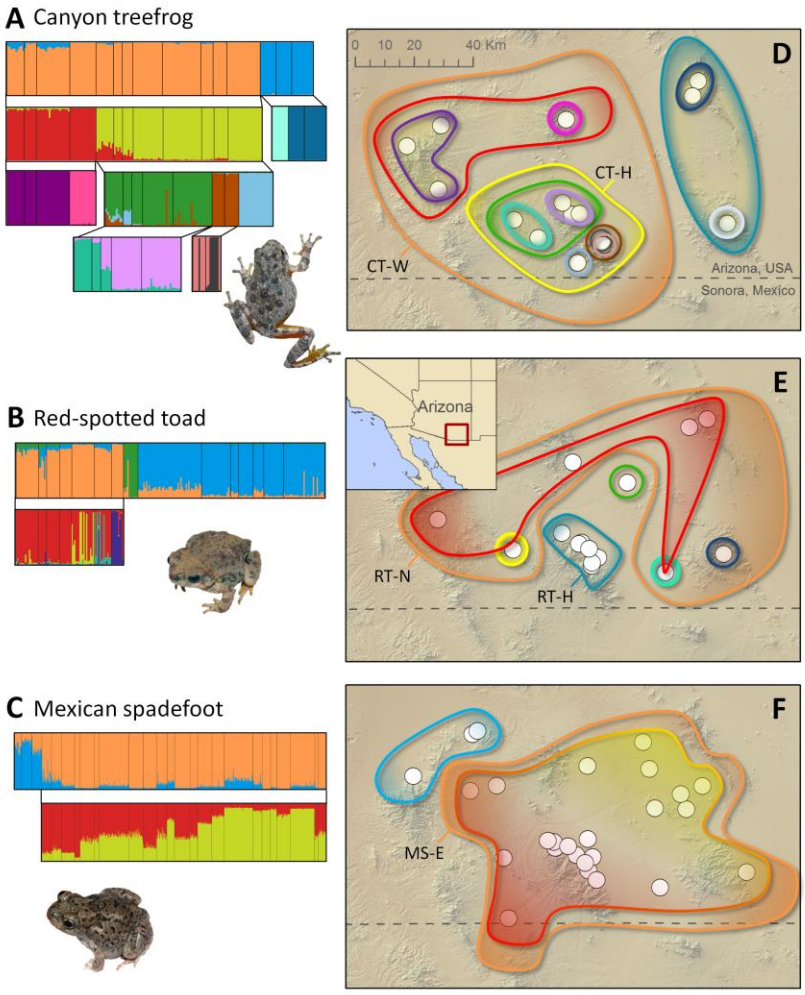

Fig. 1.2. Spatial and individual hierarchical population structure for each species. Individual-based STRUCTURE results are shown in Panels A, B, and C. Each vertical bar represents one individual. Colors indicate the most likely genetic cluster assignments. Black vertical bars denote individuals from the same sampling locations. Each cluster was hierarchically analyzed for nested structure; nested structure results are shown directly below the original cluster. Hierarchical analyses were repeated until terminal clusters (K = 1) were reached. Panels D, E, and F: nested outlines group sampling locations into genetic clusters shown in panels A, B, and C, with study extent shown in black box of inset map (Panel E). Outline color corresponds to population clusters. Red to yellow shading in Panel F represents the transition between two clusters shown in Panel C (Mexican spadefoots). Major genetic clusters include: canyon treefrog-west (CT-W) and canyon treefrog - Huachuca Mountains (CT-H) (Panel D); red-spotted toad-north (RT-N) and red-spotted toad - Huachuca Mountains (RT-H) (Panel E); Mexican spadefoot - east (MS-E) (Panel F).

1K. Chapter 1 Supplemental Material

Appendix 1.A. Sampling and genetic methods.

Description of sampling and genetic methods as well as assessment of potential bias due to different sampling methods. Appendix 1.A also includes sampling maps for all three species and tables describing sampling and genetic information by site and by species, microsatellite loci for red-spotted toads and canyon treefrogs, results from Hardy Weinberg exact tests, microsatellite loci characteristics, STRUCTURE results, and results of assessment of bias across sampling methods.

Amphibian sampling

Sample sites for each species are shown in Fig. 1.A.1, A2, and A3, and sample-specific information is summarized by location in Table 1.A.1. Adults were collected at breeding sites and along roadways, and larval samples were collected with dip nets from breeding ponds. Where possible, multiple spatial or temporal replicates from a given sampling locale were collected (described in the main text). These temporal and spatial replicates ("Reps") were tallied and are presented in Table 1.A.1, and the genetic implications of variability in the number of replicates are discussed later in this appendix.

Microsatellite amplification and screening

Whole genomic DNA extractions were performed using DNeasy 96 Blood & Tissue Kit (QIAGEN), and extractions were performed at the Molecular Ecology Research Lab at the University of Washington's School of Aquatic and Fishery Sciences. Mexican spadefoot loci

were compiled from previously published microsatellite markers (Rice et al. 2008, Van Den Bussche et al. 2009). Canyon treefrog and red-spotted toad marker sets were developed by the Evolutionary Genetics Core Facility at Cornell University and are described in Table 1.A.2. Polymerase chain reaction (PCR) was used to amplify DNA for multiplexed loci using Multiplex PCR kits (QIAGEN). PCR products were genotyped using an ABI 3730 sequencer (Applied Biosystems) at the Oregon State University's Center for Genome Research and Biocomputing (Corvallis, OR). Genotypes were analyzed using the software GENEMAPPER 4.1 (Applied Biosystems), and alleles were binned using the program TANDEM (Matschiner and Salzburger, 2009). Loci were screened for the presence of linkage disequilibrium using the log likelihood ratio statistic for each pair of loci in each population was found (GenePop, Raymond and Rousset 1995). No evidence of consistent linkage between loci was found. Any significant pairwise linkage results occurred in < 13% of all populations for a given species; results not shown but available upon request. Loci were also screened for deviations from Hardy-Weinberg equilibrium (HWE) using the exact p-test (results presented in Table 1.A.3) as implemented in GenePop (Raymond and Rousset 1995), and the presence of null alleles was evaluated with Micro-Checker (Van Oosterhout et al. 2004) using adults only (spadefoots) or larval samples from which all but one full sibling were removed. With a Bonferroni correction applied, no significant deviations from HWE were observed for any locus in a given population for canyon treefrogs or Mexican spadefoots. Three significant deviations from HWE were observed for red-spotted toads (Table 1.A.3); however, because these deviations did not represent a considerable proportion of tests for any given population or locus, all markers and populations were retained in our analyses. Summary statistics for all retained loci (all species) are included in Table 1.A.4, including *F*-statistics calculated using MSA 4.05 (Dieringer and Schlötterer 2003).

Larval samples can bias population genetics findings by artificially inflating genetic differentiation due to family structure (Goldberg and Waits 2010); therefore, we screened all larval samples for full siblings using the program COLONY (Wang 2009). One sibling was retained from each family with fewer than six siblings. For families with six or more full siblings, there is a 98.4% chance of detecting both parental alleles for each locus, and we manually reconstructed two parental genotypes for use in population-based analyses for samples < 25 in order to achieve the maximum sample size. For individual-based analyses, only a single sibling was retained. This was confirmed by re-genotyping rare alleles (in < 3 individuals). We estimated statistical power of our final marker sets using POWSIM, a simulation-based computer program that estimates power (and α error) for chi-square and Fisher's exact tests when evaluating the hypothesis of genetic homogeneity (Ryman and Palm 2006). Sample sizes, number of samples, loci and allelic information, and number of generations can be combined under various scenarios to produce a hypothetical degree of genetic differentiation (measured as F_{ST}). We ran simulations for each species and used our actual sample size and number of samples (conservatively calculated without reconstructed parents), our median estimated N_e, numbers of loci and alleles, and allele frequency for simulations. Number of generations was then adjusted to approximate observed F_{ST}. Each species was simulated at a range of numbers of generations from 10 to 500 to calculate power at a range of F_{ST} output values, including one that approximated the observed $F_{ST.}$ Proportion of significant differences observed (200 runs) was 1.0 for all species in almost all scenarios. The 10-generation spadefoot simulations were the only scenario with a proportion of significant differences observed that fell below 1.0. However, the estimated F_{ST} for that run was roughly 1/10 the observed F_{ST}, indicating that a 10-generation simulation is not sufficiently long to reflect actual observed genetic differentiation for this

species. These results indicate satisfactory statistical power given the loci and sample sizes in our dataset.

Hierarchical population structure and clustering

Individual-based hierarchical population structure was analyzed using the Bayesian clustering program STRUCTURE 2.3.4 (Pritchard et al. 2000). Each sampling site was treated as an independent putative population with a total of *n* putative populations for each species. Ten iterations of each *K* from 1 to *n* + 1 for each species were run for 1,000,000 cycles with a burn-in of 200,000 cycles. We used the locprior model with admixture and correlated allele frequencies. The most likely *K* was determined using the delta-*K* method (Evanno et al. 2005) in which the most likely value of *K* is assessed by the second-order rate of change in the log-likelihood. A delta-*K* value cannot be calculated for $K = 1$; thus, for cases in which $K = 1$ has the greatest log-likelihood, 1 is assumed to be the most likely *K* (Spear et al. 2012). This analysis was repeated for genetic clusters in which both $K > 1$ and $n > 1$ to identify hierarchical population structure until terminal clusters were described (Phillipsen et al. 2013). All STRUCTURE output and delta-*K* calculations are included in Table 1.A.5. STRUCTURE output was visualized using the program DISTRUCT 1.1 (Rosenberg 2004).

Assessment of potential sampling bias from variable sampling methods

Despite accounting for larval family structure, it is possible that variable sampling methods may introduce biases into genetic inference of population structure and connectivity. For example, COLONY accounts for full-sibling groups, but it is possible that half-siblings or other distant family structure inflates genetic differentiation between larval samples relative to adult samples.

Also, Mexican spadefoot adults were collected along roadways in addition to breeding sites. It is not well known whether adults of this species exhibit breeding site fidelity or homing behavior; if they do, particularly for their larval pond, it is reasonable to expect that adults collected at breeding sites may be more genetically similar than those collected along roads. To examine whether we see evidence of large bias from these variable sampling methods, we paired larval samples with nearby adult samples for red-spotted toads and spadefoots. Canyon treefrogs were not included because we did not have enough adult samples to generate a sufficient number of adult-larval paired samples. We then examined genetic diversity and overall genetic differentiation within each group of samples collected by a given method (larval samples, adult samples, breeding site adults, and roadside adults).

Allelic richness and heterozygosity were similar across sampling methods within species. We found some evidence for higher differentiation among larval samples than adult samples for red-spotted toads, where G'_{ST} increased by 62% for larval samples compared to adult samples (Table 1.A.6). N_e was also lower for larval samples than adults. However, for spadefoots, there was modest evidence of lower genetic differentiation among larval samples than for adult samples, with G'_{ST} reduced by 34% for larval samples compared to adult samples. N_e was also lower for adult samples than for larvae for which the median N_e value was 10,000 (the estimate for infinite population sizes). Genetic differentiation between spadefoot adult sampling methods was minimal. However, for both species, not all "pairs" of larval and adult samples were spatially congruent. Some adult and larval red-spotted toad pairs were selected based on similar sample sizes and similar spatial locations, but with local processes identified as important for this species (for example, low N_e in some populations), the pattern of higher G'_{ST} may be spurious and requires further exploration.

We also explored the effects of multiple sampling replicates ("Reps") in space and time on genetic diversity indices. To do this, we used a paired sample approach for populations of all three species with two or more replicates (from which at least 10 % of the sampled individuals represented an additional replicate). These included 3 populations of canyon treefrogs, 6 populations of red-spotted toads, and 12 populations of spadefoots. Due to low sample sizes for two of the three species, we did not explore effects of sampling replicates on genetic differentiation between populations. Genetic diversity metrics (H_O, H_E, AR, N_e and the upper confidence limit of N_e (N_e high) calculated using a jackknifing approach and estimated as 10,000 for infinite values) were calculated with only one replicate and with multiple replicates. To control for sample size, multiple replicate samples were reduced to match sample sizes of one replicate only. Where possible, equal numbers of individuals were included from each replicate in the reduced sample. A paired t-test was then used to compare differences in H_O, H_E and AR, and a Wilcoxon signed-rank test was used to compare differences in N_e and the upper confidence interval of N_e given the non-normal distribution of differences for these values. Local processes such as drift due to low N_e or low migration rates as well as possible metapopulation dynamics were identified as playing a greater role in population genetic structure of canyon treefrogs and red-spotted toads, and the effect of multiple sampling replicates may be more apparent in species such as these with low N_e and greater family structure among larval samples. For that reason, the effect of replicates on these genetic diversity metrics was calculated for all species as well as for canyon treefrogs and red-spotted toads combined.

We found little evidence that sample replicates biased the results of this study (Table 1.A.7). We found no significant differences in genetic diversity measures between single and replicate samples for all species, and we found only one significant difference for canyon treefrog and red-

spotted toads alone (H_E, p-value = 0.024). If a Bonferroni correction for multiple comparisons is applied, the result for H_E is not significant.

In summary, although we saw differences in estimates of genetic differentiation between larval and adult samples for both species, the range of G'_{ST} values within species were comparatively low. These potential biases did not result in overlap of G'_{ST} between species, and thus for this study we suspect that the potential bias did not affect the outcome of this study. We also found little support for the effect of number of spatial or temporal sampling replicates on the genetic diversity metrics of this study. However, our results are limited to our study species in a subsection of their ranges, and bias due to different sampling methods may be more substantial for other species or regions. Future consideration of biases from sampling methods both in empirical and simulation studies may be particularly important for development of predictive models in which small differences in connectivity estimates may have implications for resistance surface parameterization or management actions.

References

Bowcock, A. M., A. Ruiz-Linares, J. Tomfohrde, E. Minch, J. R. Kidd, and L. L. Cavalli-Sforza. 1994. High resolution human evolutionary trees with polymorphic microsatellites. Nature **368**:455-457.

Dieringer, D., and C. Schlötterer. 2003. Microsatellite analyser (MSA): a platform independent analysis tool for large microsatellite data sets. Molecular Ecology Notes **3**:167-169.

Evanno, G., S. Regnaut, and J. Goudet. 2005. Detecting the number of clusters of individuals using the software STRUCTURE: a simulation study. Molecular Ecology **14**:2611-2620.

Goldberg, C. S., and L. P. Waits. 2010. Quantification and reduction of bias from sampling larvae to infer population and landscape genetic structure. Molecular Ecology Resources **10**:304-313.

Matschiner, M., and W. Salzburger. 2009. TANDEM: integrating automated allele binning into genetics and genomics workflows. Bioinformatics **25**:1982-1983.

Phillipsen, I. C., and D. A. Lytle. 2013. Aquatic insects in a sea of desert: population genetic structure is shaped by limited dispersal in a naturally fragmented landscape. Ecography **36**:731-743.

Pritchard, J. K., M. Stephens, and P. Donnelly. 2000. Inference of population structure using multilocus genotype data. Genetics **155**:945-959.

Raymond, M. and F. Rousset. 1995. GENEPOP (version 1.2): population genetics software for exact tests and ecumenicism. Journal of Heredity **86**:248-249.

Rice, A. M., D. E. Pearse, T. Becker, R. A. Newman, C. Lebonville, G. R. Harper, and K. S. Pfennig. 2008. Development and characterization of nine polymorphic microsatellite markers for Mexican spadefoot toads (*Spea multiplicata*) with cross-amplification in plains spadefoot toads (*S. bombifrons*). Molecular Ecology Resources **8**:1386-1389.

Rosenberg, N. A. 2004. Distruct: a program for the graphical display of population structure. Molecular Ecology Notes **4**:137-138.

Ryman, N., and S. Palm. 2006. POWSIM: a computer program for assessing statistical power when testing for genetic differentiation. Molecular Ecology **6**:600-602.

Spear, S. F., C. M. Crisafulli, and A. Storfer. 2012. Genetic structure among coastal tailed frog populations at Mount St. Helens is moderated by post-disturbance management. Ecological Applications **22**:856-869.

Van Den Bussche, R. A., J. B. Lack, C. E. Stanley, J. E. Wilkinson, P. S. Truman, L. M. Smith, and S. T. McMurry. 2009. Development and characterization of 10 polymorphic tetranucleotide microsatellite markers for New Mexico spadefoot toads (*Spea multiplicata*). Conservation Genetics Resources **1**:71-73.

Van Oosterhout, C., W. F. Hutchinson, D. P. M. Wills, and P. Shipley. 2004. MICRO-CHECKER: software for identifying and correcting genotyping errors in microsatellite data. Molecular Ecology Notes **4**:535-538.

Wang, I. J. 2009. A new method for estimating effective population sizes from a single sample of multilocus genotypes. Molecular Ecology **18**:2148-2164.

Fig. 1.A.1. Canyon treefrog sampling map.

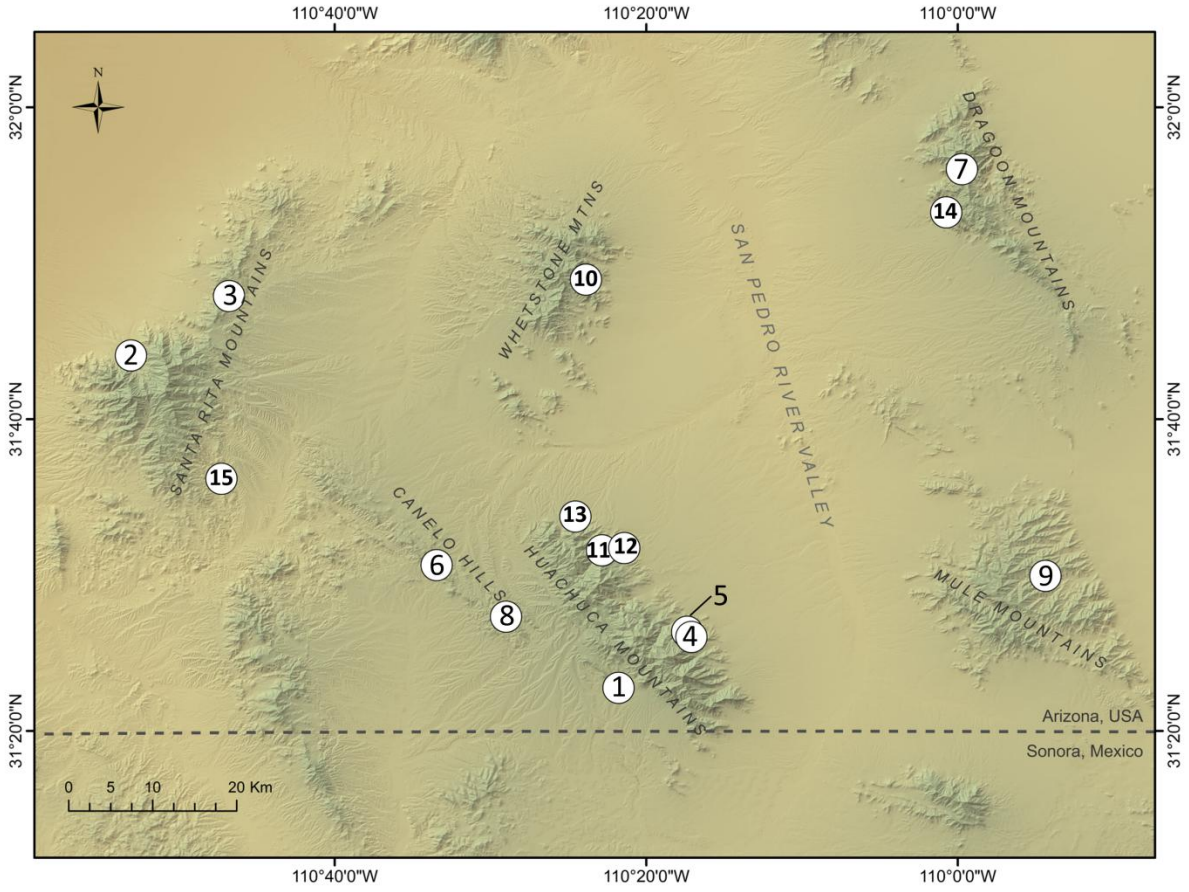

Fig. 1.A.2. Red-spotted toad sampling map.

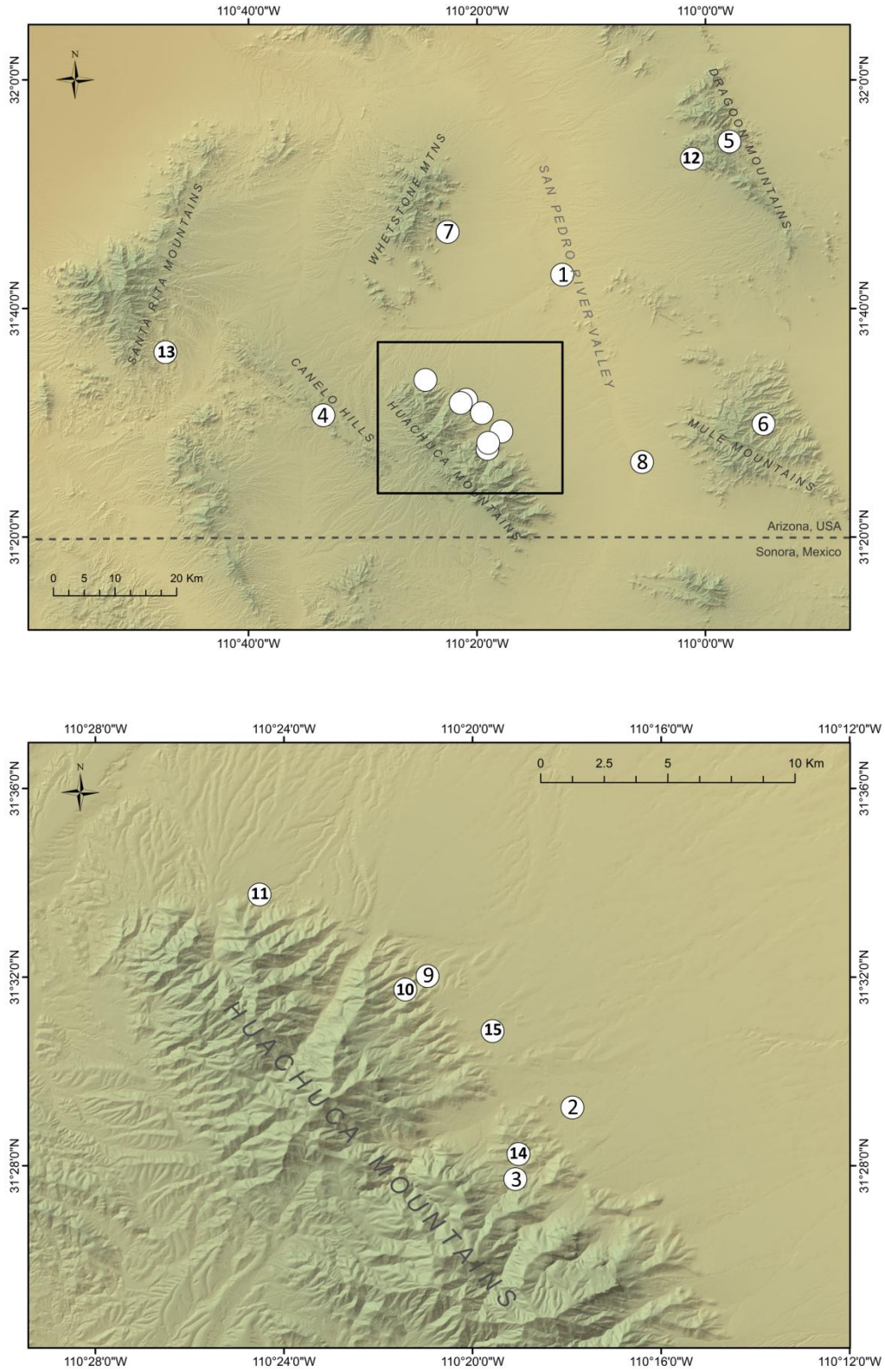

Fig. 1.A.3. Mexican spadefoot sampling map.

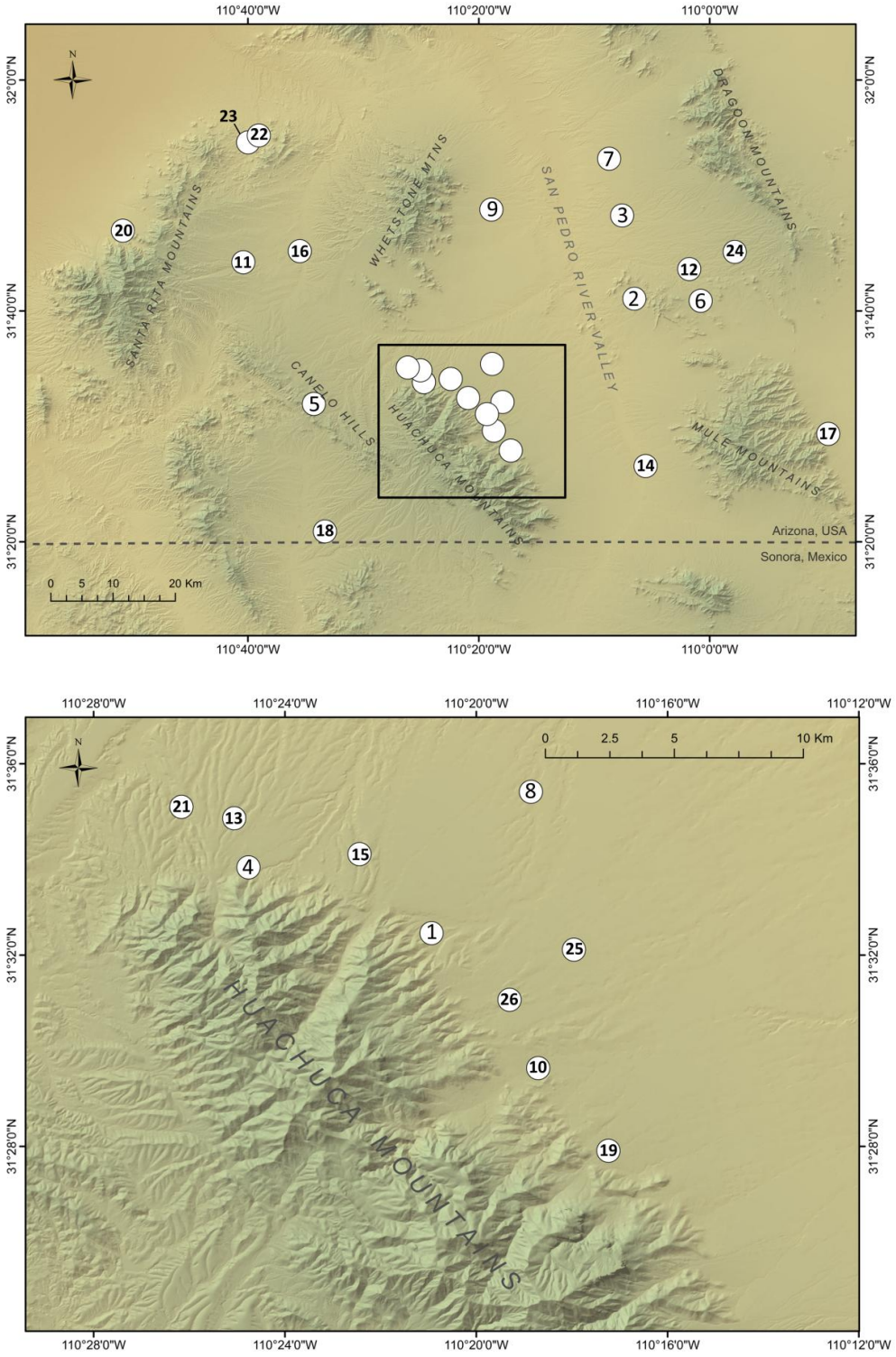

Table 1.A.1. Sample number and locations (UTM Zone 12); sample size with siblings removed (*N* All), with reconstructed parents (*N* with P), and with number and percent of adults; replicates (temporal or spatial); allelic richness (based on minimum sample size); expected and observed heterozygosity; effective population size (N_e) and the 95% confidence intervals for N_e calculated via a jackknifing method where "*Inf*" represents infinity; and F_{IS} values averaged over all loci. Results from Hardy Weinberg exact tests are included in Table 1.A.3. Additional information by locus and/or population are available from M.C. Mims upon request.

Canyon treefrog

Site	UTM Northing	UTM Easting	*N* All	*N* with P	*N* Adults	Percent Adults	Reps	AR	H_E	H_O	N_e	C.I.s for N_e		F_{IS}
1	560558	3471841	19	19	15	79	1	4.96	0.71	0.75	17.9	12.7	27.4	-0.07
2	510906	3511050	10	11	2	20	1	6.45	0.81	0.84	*Inf*	52.2	*Inf*	-0.06
3	520834	3518105	7	8	2	29	2	5.26	0.78	0.81	13.5	8.7	24.4	-0.09
4	567504	3478529	7	11	0	0	1	4.58	0.71	0.73	7.5	3.1	16.2	-0.05
5	567930	3477919	8	10	0	0	1	4.66	0.74	0.78	7.4	3.7	13.4	-0.09
6	541988	3486290	5	7	0	0	1	5.50	0.72	0.68	*Inf*	26.2	*Inf*	0.08
7	594936	3533556	12	12	4	33	1	4.53	0.63	0.58	17.6	8.7	64.2	0.09
8	549066	3480211	10	12	3	30	2	5.65	0.79	0.81	33.1	15.5	348	-0.05
9	603435	3485393	9	13	1	11	2	3.06	0.54	0.54	2.7	1.8	6.7	-0.02
10	556976	3520186	15	16	0	0	1	4.33	0.70	0.74	*Inf*	75.7	*Inf*	-0.08
11	558781	3488127	17	17	17	100	1	5.54	0.80	0.81	30.7	18.7	67.5	-0.02
12	561038	3488403	22	23	0	0	2	5.62	0.79	0.75	323.1	72.3	*Inf*	0.04
13	556064	3492110	6	9	0	0	1	5.79	0.79	0.84	75.1	25.9	*Inf*	-0.11
14	593398	3528429	9	12	0	0	1	4.35	0.64	0.60	19.7	9.6	83.5	0.04
15	520105	3496453	19	22	0	0	1	6.05	0.80	0.83	94.4	35.1	*Inf*	-0.05

Table 1.A.1, continued.

Red-spotted toad

Site	UTM Northing	UTM Easting	*N* All	*N* with P	*N* Adults	Percent Adults	Reps	AR	H_E	H_O	N_e	C.I.s for N_e		F_{IS}
1	574944	3509235	11	12	0	0	2	3.88	0.65	0.69	6.9	3.3	11.7	-0.09
2	566670	3483820	8	8	0	0	1	5.81	0.83	0.78	*Inf*	287.2	*Inf*	0.03
3	564771	3481006	15	15	0	0	1	5.55	0.79	0.75	302.1	49.1	*Inf*	0.05
4	542015	3486332	17	18	0	0	3	5.05	0.76	0.70	20	14.4	30.1	0.07
5	597845	3530951	9	11	0	0	1	5.99	0.80	0.82	*Inf*	49.9	*Inf*	-0.05
6	603007	3485338	9	11	0	0	2	4.36	0.67	0.68	2.9	2.3	4.9	-0.03
7	559054	3516045	6	9	0	0	1	5.28	0.77	0.73	*Inf*	180.6	*Inf*	0.02
8	586216	3479036	13	13	13	100	1	5.08	0.75	0.76	7.8	5	11.8	-0.04
9	561774	3488938	22	24	17	77	3	4.87	0.72	0.67	37.6	25.2	65.8	0.06
10	561034	3488404	6	6	0	0	1	5.93	0.79	0.72	*Inf*	*Inf*	*Inf*	0.05
11	556119	3492102	48	48	25	52	5	5.61	0.80	0.82	46.4	37.7	58.5	-0.04
12	592703	3528123	10	15	0	0	1	5.52	0.76	0.74	83	37.2	*Inf*	0.00
13	520105	3496453	17	18	2	12	1	5.75	0.78	0.72	144.6	55.6	*Inf*	0.05
14	564872	3481987	31	33	27	87	3	5.54	0.78	0.80	81.5	50.8	176.4	-0.04
15	563972	3486799	11	11	2	18	2	5.22	0.76	0.76	641.9	34.8	*Inf*	-0.02

Table 1.A.1, continued.

Mexican spadefoot

Site	UTM Northing	UTM Easting	*N* All	*N* with P	*N* Adults	Percent Adults	Reps	AR	H_E	H_O	N_e	C.I.s for N_e		F_{IS}
1	561802	3489747	36	36	17	47	3	5.26	0.67	0.64	1903.3	87.1	*Inf*	0.03
2	584463	3505799	21	21	21	100	1	4.86	0.68	0.67	12.2	4.6	41.2	0.00
3	582676	3519097	23	23	0	0	1	5.31	0.69	0.72	*Inf*	63.7	*Inf*	-0.06
4	555732	3492251	12	12	12	100	1	5.56	0.67	0.75	*Inf*	48	*Inf*	-0.14
5	540672	3488698	33	33	0	0	2	5.40	0.65	0.66	*Inf*	314.2	*Inf*	-0.01
6	593537	3505547	34	34	0	0	1	5.05	0.65	0.62	*Inf*	10400	*Inf*	0.04
7	580834	3528180	72	72	0	0	3	5.21	0.67	0.67	1157.8	132.2	*Inf*	-0.01
8	565055	3495225	36	36	0	0	2	5.41	0.69	0.67	377.7	78.6	*Inf*	0.07
9	564804	3519926	31	31	0	0	1	5.16	0.67	0.65	1845	64.3	*Inf*	0.02
10	565362	3484554	39	39	18	46	2	5.35	0.68	0.69	*Inf*	105	*Inf*	-0.01
11	530935	3511341	24	24	0	0	1	4.92	0.65	0.64	*Inf*	44.8	*Inf*	0.01
12	591925	3510598	16	16	16	100	2	5.08	0.67	0.70	*Inf*	32.7	*Inf*	-0.06
13	555249	3494145	36	36	0	0	1	5.47	0.68	0.65	*Inf*	67.5	*Inf*	0.03
14	586216	3479036	9	9	9	100	1	5.00	0.68	0.65	*Inf*	24.7	*Inf*	0.01
15	559400	3492783	34	34	20	59	3	5.16	0.65	0.65	82.5	32.7	*Inf*	-0.02
16	538646	3513134	25	25	25	100	1	5.30	0.64	0.60	618.9	50.5	*Inf*	0.05
17	611229	3484426	19	20	0	0	1	5.15	0.67	0.69	63.9	24.2	*Inf*	-0.05
18	542257	3468315	14	16	0	0	1	5.00	0.61	0.66	49.8	17.3	*Inf*	-0.09
19	567709	3481377	19	19	19	100	3	5.30	0.66	0.69	74.7	26.4	*Inf*	-0.06
20	514446	3516357	17	17	0	0	1	5.32	0.72	0.70	58.4	23.4	*Inf*	0.03
21	553502	3494577	74	74	9	12	3	5.34	0.66	0.65	*Inf*	147.3	*Inf*	0.01
22	531529	3530515	26	26	0	0	2	5.65	0.73	0.71	83.5	36.5	*Inf*	0.04
23	532978	3531631	25	25	0	0	1	5.26	0.69	0.68	*Inf*	160.3	*Inf*	0.00
24	598126	3513429	61	61	0	0	2	5.25	0.69	0.66	*Inf*	77.7	*Inf*	0.08
25	566518	3489137	19	19	4	21	1	5.52	0.69	0.68	79.1	28.9	*Inf*	0.01
26	564400	3487189	26	26	9	35	3	5.39	0.68	0.70	*Inf*	72.8	*Inf*	-0.03

Table 1.A.2. Locus, repeat length (di-, tri- or tetranucleotide), and primer sequences for the final microsatellite loci for red-spotted toads (*Anaxyrus punctatus*) and canyon treefrogs (*Hyla arenicolor*), developed by the Evolutionary Genetics Core Facility at Cornell University.

Canyon treefrog			
Locus	Repeat	Forward primer (5' - 3')	Reverse primer (5' - 3')
ha40	tet	ACAACTCCCAGCATATATCTCTC	GTTCACTGTACTCAAATGGCCTC
ha280	tri	TCCTTCACACTCTAAGGTTGCTC	CGCACTTTATGAACAGATTTGCC
ha311	tet	ATAATTACAGTGATGCCGCCTTG	CAAGCAACCATCAACATATGTAGG
ha357	tet	TTGTATCACTTGTGCTATTGGGC	TAGTGCTGCATTTATGTGGAAGG
ha479	tet	GCATTGTTCAAGTATTACCAGGC	TGTTCTCACTTTGCAGTTGAAGG
ha568	tet	GAGGCAGATTAATAGGTGAACGG	CATCCAAACACATACATCAGGGC
ha664	tet	AATGCCACATGTAACTGAGTGTG	TCCATTACTAAAGTACACCAGCC
ha703	tet	AGGTAGGTAGGTGTGCTTACATG	ACACTTGTGTCTTGAGTCATTGAC
ha705	tet	ACAGAAGCTACACCTAACACCTC	AAATATTAACCACCGGAGTACCC
ha1435	tet	ACTAGGTCATTCATTAGATGTGGG	TGAAAGGCTTAACTCTTCCAAGC
ha1997	tet	TTCTAACAAAGCCTGAGACATCC	TTGGACCCTTTATGACTTGCTTG
ha2144	tet	TGGCCGGTGAGTGTATATCTATC	TTGGATACCTACCTCACAGTCTG
Red-spotted toad			
Locus	Repeat	Forward primer (5' - 3')	Reverse primer (5' - 3')
ap71	tet	AACCCTTTGTGACAGAATGGTTC	TTTGGTTGTTCACATCTCTCTGG
ap213	tet	ATCTCATTTCCCTCAAACTGTGC	GAAACAGTGAGCCAAACATTCCC
ap360	tet	TGCTCAACACTACTGAAGACATC	AGGATCTGTCAGGAGCAGTTATC
ap1904	tri	CACGATGTGTCCCTCTTTGTTTG	GGAGTAGCAGAAGGAATGTTGTG
ap2524	di	CCAGAAGTCATATGATCAGCGTG	ATTCCACTGTTGTTACCACTGAC
ap3396	tet	GGCAAATGTCCACAAATGTACAG	TGAGTCAGATAAGCTAGATGTGGG
ap3587	tri	GACGGATGAGACCAACATAGAAC	GATTGAACAAGACAAGCCCAAAC
ap3591	tet	CCACATTAAATACTGGCGCCTAG	GACCGATTCTGCCATATCTGC
ap4565	tet	TGCATGCCACTGTAGATAATAGG	TAGAGATAGCACTTACACCTGGG
ap5418	tet	ACAAGTGGGTAGAAAGATATGGG	CAGGAGCTGCTGGAGAGTATTC
ap5818	tet	ACCTTGAATTCTTTGTCATGTTCC	CCAGGGAGCCATTATTTCAGATG
ap6204	tet	CTGCTGCAACTGACACTG	AAACATACAAGGCTGACTATGGG
ap9886	tri	TGCGTGTTTCCATGTACCATATG	CAGTACAGTGTGGATGTGAAAGG
ap10273	tri	ACCAATATCTATCCTCCGACGTC	ATGTGAGAATAGGTTAGCGTTCC

Table 1.A.3. *P*-values for Hardy Weinberg exact test for each population (rows) and locus (columns). Significant *p*-values with a Bonferroni correction applied are shown in bold. No data (*na*) indicates that only one allele was present for a given locus in a given population, or two alleles were detected but one was represented by only one copy.

Canyon treefrog

	280	357	40	664	1435	2144	311	705	1997	479	568	703
1	0.353	0.223	0.291	0.490	0.344	0.642	0.937	0.338	0.841	0.515	0.739	0.064
2	0.483	0.501	0.208	0.779	0.910	0.624	0.783	0.255	1.000	0.823	0.576	1.000
3	0.404	0.745	0.424	0.291	0.106	0.617	1.000	0.991	0.819	0.739	1.000	0.867
4	0.764	0.782	0.182	0.345	0.159	0.266	0.142	0.127	0.021	0.273	0.391	0.263
5	0.409	0.786	0.496	0.667	0.654	0.367	0.219	0.810	0.198	0.900	0.113	0.944
6	0.007	0.011	0.106	0.232	0.305	0.440	0.849	1.000	0.433	0.805	0.559	0.661
7	*na*	1.000	0.039	0.140	0.071	0.255	0.343	0.160	0.802	0.429	0.928	0.555
8	0.769	0.482	0.619	0.314	0.881	0.608	1.000	0.178	0.989	0.321	0.008	0.812
9	1.000	1.000	0.028	0.938	0.263	0.036	0.566	0.457	0.015	0.089	0.026	0.119
10	0.889	0.821	0.261	1.000	0.479	0.400	0.372	0.886	0.353	0.872	0.823	0.972
11	0.912	0.756	0.126	0.834	0.024	0.957	0.368	0.580	0.189	0.849	0.687	0.399
12	0.550	0.228	0.630	0.443	0.026	0.330	0.016	0.857	0.421	0.183	0.115	0.037
13	0.251	0.026	0.741	0.152	0.591	0.683	0.245	0.442	0.766	0.315	0.101	0.016
14	*na*	0.595	0.080	0.341	1.000	0.404	0.909	0.158	0.035	0.725	0.133	0.823
15	0.780	0.057	0.521	0.892	0.588	0.078	0.355	0.688	0.713	0.377	0.653	0.862

Table 1.A.3,
continued.

Red-spotted toad

	10273	2524	3396	5818	3591	360	6204	71	213	3587	1904	4565	5418	9886
1	0.304	0.227	0.400	0.119	0.653	0.219	*na*	0.722	0.471	0.174	1.000	0.774	0.258	0.530
2	0.089	0.378	0.759	0.696	0.866	0.887	0.434	1.000	0.223	0.191	0.069	0.855	0.189	0.766
3	0.384	0.032	0.622	**0.001**	0.971	0.996	0.047	0.749	0.188	0.071	1.000	0.672	0.250	0.117
4	0.853	0.032	0.934	0.047	0.375	0.139	1.000	0.965	0.584	0.317	0.116	0.256	0.620	0.260
5	0.983	0.795	0.775	0.271	0.715	0.516	1.000	0.980	0.680	0.053	0.932	0.679	1.000	0.754
6	0.511	0.098	0.140	0.076	0.182	0.568	1.000	0.739	0.669	0.160	1.000	0.011	0.084	0.654
7	0.742	0.665	0.627	0.878	0.688	0.652	1.000	0.345	0.527	1.000	1.000	0.339	0.463	0.648
8	0.982	0.063	0.552	0.454	1.000	0.027	0.602	0.110	0.037	0.057	0.743	0.215	0.173	0.468
9	0.322	0.385	0.607	0.127	0.095	0.275	1.000	0.148	0.537	0.025	0.173	0.052	0.218	0.693
10	0.148	0.655	1.000	**0.003**	0.430	0.709	1.000	0.760	0.163	0.379	1.000	0.213	1.000	0.585
11	**0.002**	0.077	0.284	0.804	0.933	0.053	0.867	0.854	0.267	0.046	0.057	0.076	0.362	0.224
12	0.438	1.000	0.116	0.193	0.209	0.115	0.729	0.516	0.366	0.388	1.000	0.283	0.644	0.896
13	0.008	0.033	0.941	0.008	0.274	0.688	1.000	0.112	0.411	0.053	1.000	0.605	0.830	0.335
14	0.310	0.128	0.150	0.826	0.740	0.987	0.091	0.834	0.281	0.483	0.549	0.013	0.260	1.000
15	0.881	0.461	0.163	0.857	0.719	0.076	0.538	0.364	0.125	0.342	0.554	0.760	0.897	0.188

Table 1.A.3, continued.

Mexican spadefoot								
	C7	D125	H115	D103	D111	D7	H129	20
1	0.942	0.081	0.563	0.057	0.804	1.000	0.884	0.564
2	0.072	0.443	0.026	0.409	0.400	1.000	0.234	0.228
3	0.906	0.337	0.828	0.133	0.918	1.000	0.496	0.504
4	0.012	0.874	0.259	0.260	0.724	*na*	0.293	0.387
5	0.809	0.072	0.883	0.534	0.747	*na*	0.348	0.448
6	0.300	0.073	0.888	0.106	0.588	*na*	0.408	0.766
7	0.698	0.016	0.340	0.547	0.100	1.000	0.309	0.487
8	0.363	0.046	0.281	0.419	0.710	0.084	0.522	0.351
9	0.275	0.521	0.135	0.829	0.980	*na*	0.188	0.740
10	0.717	0.811	0.898	0.166	0.763	*na*	0.157	0.941
11	0.129	0.687	0.350	0.002	0.997	*na*	0.094	0.893
12	0.660	0.840	0.465	0.492	0.499	*na*	0.232	0.591
13	0.415	0.652	0.382	0.039	0.312	*na*	0.496	0.378
14	0.842	0.650	0.421	0.099	0.879	*na*	0.302	0.976
15	0.423	0.339	0.015	0.210	0.457	*na*	1.000	0.268
16	0.529	0.323	0.664	0.255	0.167	*na*	0.018	0.462
17	0.585	0.086	0.127	0.965	0.828	*na*	0.442	0.642
18	0.411	0.519	0.305	0.465	0.340	*na*	1.000	0.083
19	0.831	0.666	0.129	0.916	0.401	*na*	0.327	0.361
20	0.818	0.181	0.071	0.902	0.955	0.431	0.725	0.745
21	0.589	0.576	0.252	0.526	0.807	*na*	0.613	0.468
22	0.902	0.332	0.217	0.197	0.607	0.297	0.462	0.991
23	0.832	0.237	0.284	0.355	0.554	1.000	0.574	0.000
24	0.967	0.907	0.300	0.160	0.902	0.002	0.147	0.732
25	0.879	0.574	0.831	0.657	0.831	*na*	0.239	0.286
26	0.963	0.835	0.208	0.897	0.710	*na*	0.865	0.322

Table 1.A.4. Characteristics of final microsatellite loci datasets for each species. Expected heterozygosity, observed heterozygosity, variability in PCR product size (Var), variability in PCR repeat number (VarRepN), allelic characteristics, and *F*-statistics are shown. Additional information available upon request from M.C. Mims.

Canyon treefrog											
Locus	H_E	H_O	Var	VarRepN	Allele				F_{IS}	F_{ST}	F_{IT}
					Min	Mean	Max	Richness			
40	0.79	0.77	151.5	9.47	305	383.88	413	7.75	0.03	0.11	0.14
280	0.52	0.48	39.02	4.34	261	269.16	279	3.82	0.06	0.12	0.17
311	0.75	0.79	69.76	4.36	199	210.7	235	6.6	-0.05	0.13	0.08
357	0.66	0.71	21.85	1.37	204	214.81	232	4.62	-0.08	0.10	0.03
479	0.78	0.77	159.47	9.97	275	300.22	335	8.11	0.00	0.15	0.15
568	0.79	0.8	383.77	23.99	332	384.07	432	9.2	0.00	0.15	0.15
664	0.68	0.72	201.42	12.59	291	315.27	369	7.16	-0.06	0.19	0.14
703	0.84	0.83	644.4	40.28	305	397.43	499	9.19	0.00	0.09	0.10
705	0.77	0.79	394.52	24.66	320	360.16	416	7.33	-0.03	0.11	0.09
1435	0.77	0.77	298.06	18.63	178	307.3	375	7.32	0.02	0.13	0.14
1997	0.78	0.84	459.77	28.74	243	271.88	327	7.74	-0.09	0.14	0.07
2144	0.62	0.62	21.26	1.33	174	180.43	198	4.46	0.01	0.16	0.17
Red-spotted toad											
Locus	H_E	H_O	Var	VarRepN	Allele				F_{IS}	F_{ST}	F_{IT}
					Min	Mean	Max	Richness			
71	0.84	0.85	123.98	7.75	233	335.74	365	6.58	-0.01	0.04	0.03
213	0.87	0.83	2266.66	141.67	258	367.51	430	7.27	0.02	0.04	0.06
360	0.83	0.85	86.57	5.41	376	396.41	416	6.55	-0.01	0.05	0.04
1904	0.56	0.58	15.53	1.73	280	291.49	298	3.33	-0.06	0.04	-0.02
2524	0.72	0.69	17.44	4.36	365	382.32	391	5.05	0.05	0.05	0.10
3396	0.86	0.9	154.33	9.65	242	266.35	310	7.33	-0.04	0.04	0.00
3587	0.72	0.67	21.67	2.41	132	143.51	159	4.85	0.09	0.08	0.16
3591	0.72	0.75	155.3	9.71	316	332.05	438	5.51	-0.05	0.03	-0.02
4565	0.87	0.85	344.37	21.52	324	361.4	424	7.7	0.02	0.04	0.06
5418	0.91	0.89	1864.16	116.51	286	359.4	490	9.28	0.01	0.03	0.05
5818	0.86	0.73	135.15	8.45	408	435.82	496	6.01	0.10	0.02	0.12
6204	0.44	0.42	75.94	4.75	159	184.95	191	2.57	-0.02	0.07	0.05
9886	0.62	0.59	71.82	7.98	203	217.94	233	3.73	0.02	0.04	0.07
10273	0.83	0.78	156.83	17.43	325	355.76	376	5.87	0.06	0.04	0.10

Table 1.A.4, continued.

Mexican Spadefoot											
Locus	H_E	H_O	Var	VarRepN	Allele				F_{IS}	F_{ST}	F_{IT}
					Min	Mean	Max	Richness			
20	0.86	0.86	82.69	5.17	150	178.23	202	7.86	0.00	0.01	0.02
C7	0.8	0.81	89.23	5.58	232	243.26	268	6.3	-0.01	0.01	0.00
D103	0.69	0.68	77.36	4.84	133	140.55	169	5.24	0.03	0.00	0.03
D111	0.84	0.86	144.76	9.05	84	103.07	136	7.18	-0.01	0.02	0.00
D125	0.79	0.77	77.11	4.82	198	210.66	242	6.42	0.03	0.01	0.04
D7	0.07	0.06	4.77	0.3	212	212.4	232	1.56	0.14	0.02	0.16
H115	0.7	0.71	16.11	1.01	84	95.06	112	4.61	-0.01	0.01	0.00
H129	0.64	0.62	59.25	3.7	186	195.91	218	4.49	0.04	0.01	0.05

Table 1.A.5. STRUCTURE results and delta-*K* calculations for each species. Results are presented for each genetic cluster with best delta-*K* in bold.

Canyon treefrog - all populations

K	Mean LnP(*K*)	Stdev LnP(*K*)	Ln'(*K*)	|Ln"(*K*)|	Delta *K*
1	-9093.82	0.18	NA	NA	NA
2	**-8537.00**	**1.04**	**556.82**	**167.31**	**160.66**
3	-8147.49	2.23	389.51	181.21	81.12
4	-7939.19	14.73	208.30	7.21	0.49
5	-7738.10	15.62	201.09	46.76	2.99
6	-7583.77	25.84	154.33	116.84	4.52
7	-7546.28	108.98	37.49	101.37	0.93
8	-7610.16	741.54	-63.88	190.59	0.26
9	-7483.45	523.98	126.71	10.71	0.02
10	-7367.45	95.81	116.00	187.83	1.96
11	-7439.28	134.99	-71.83	16.60	0.12
12	-7494.51	138.59	-55.23	22.23	0.16
13	-7571.97	91.26	-77.46	35.08	0.38
14	-7684.51	270.39	-112.54	66.86	0.25
15	-7730.19	186.78	-45.68	14.96	0.08
16	-7760.91	300.21	-30.72	NA	NA

Canyon treefrog - western group

K	Mean LnP(*K*)	Stdev LnP(*K*)	Ln'(*K*)	|Ln"(*K*)|	Delta *K*
1	-7356.15	0.39	NA	NA	NA
2	**-6973.11**	**0.63**	**383.04**	**167.45**	**264.43**
3	-6757.52	12.86	215.59	18.68	1.45
4	-6560.61	17.87	196.91	39.79	2.23
5	-6403.49	6.76	157.12	123.87	18.33
6	-6370.24	18.98	33.25	22.25	1.17
7	-6314.74	33.30	55.50	87.91	2.64
8	-6347.15	25.78	-32.41	77.86	3.02
9	-6457.42	124.04	-110.27	88.56	0.71
10	-6479.13	85.90	-21.71	8.46	0.10
11	-6509.30	70.28	-30.17	31.15	0.44
12	-6570.62	102.93	-61.32	56.82	0.55
13	-6688.76	189.85	-118.14	NA	NA

Canyon treefrog - northwestern group

K	Mean LnP(*K*)	Stdev LnP(*K*)	Ln'(*K*)	|Ln"(*K*)|	Delta *K*
1	-2462.50	0.57	NA	NA	NA
2	**-2248.47**	**0.94**	**214.03**	**253.09**	**268.76**
3	-2287.53	17.77	-39.06	23.63	1.33
4	-2302.96	14.28	-15.43	16.94	1.19
5	-2301.45	13.78	1.51	NA	NA

Canyon treefrog - Santa Rita group

K	Mean LnP(*K*)	Stdev LnP(*K*)	Ln'(*K*)	|Ln"(*K*)|	Delta *K*
1	**-1690.58**	**0.38**	**NA**	**NA**	**NA**

Table 1.A.5, continued.

2	-1693.03	3.14	-2.45	0.12	0.04
3	-1695.36	4.32	-2.33	5.49	1.27
4	-1692.20	1.00	3.16	NA	NA

Canyon treefrog - southwestern group

K	Mean LnP(*K*)	Stdev LnP(*K*)	Ln'(*K*)	|Ln"(*K*)|	Delta *K*
1	-4457.82	0.24	NA	NA	NA
2	-4292.70	33.15	165.12	4.37	0.13
3	**-4131.95**	**11.36**	**160.75**	**105.96**	**9.33**
4	-4077.16	17.13	54.79	87.08	5.08
5	-4109.45	160.49	-32.29	84.61	0.53
6	-4057.13	24.78	52.32	99.66	4.02
7	-4104.47	56.91	-47.34	4.32	0.08
8	-4156.13	63.66	-51.66	44.54	0.70
9	-4252.33	121.29	-96.20	NA	NA

Canyon treefrog - Huachuca and Canelo group

K	Mean LnP(*K*)	Stdev LnP(*K*)	Ln'(*K*)	|Ln"(*K*)|	Delta *K*
1	-2770.95	0.54	NA	NA	NA
2	**-2754.07**	**5.33**	**16.88**	**53.81**	**10.09**
3	-2791.00	30.92	-36.93	10.50	0.34
4	-2817.43	36.99	-26.43	45.92	1.24
5	-2889.78	57.80	-72.35	110.59	1.91
6	-2851.54	29.00	38.24	NA	NA

Canyon treefrog - Canelo group

K	Mean LnP(*K*)	Stdev LnP(*K*)	Ln'(*K*)	|Ln"(*K*)|	Delta *K*
1	**-660.86**	**0.43**	**NA**	**NA**	**NA**
2	-662.53	2.25	-1.67	2.25	1.00
3	-661.95	1.16	0.58	NA	NA

Canyon treefrog - northern Huachuca group

K	Mean LnP(*K*)	Stdev LnP(*K*)	Ln'(*K*)	|Ln"(*K*)|	Delta *K*
1	-2001.53	0.46	NA	NA	NA
2	-2030.85	38.31	-29.32	22.21	0.58
3	-2037.96	43.77	-7.11	25.50	0.58
4	-2019.57	28.44	18.39	NA	NA

Canyon treefrog - Carr Canyon group

K	Mean LnP(*K*)	Stdev LnP(*K*)	Ln'(*K*)	|Ln"(*K*)|	Delta *K*
1	-546.61	0.40	NA	NA	NA
2	**-490.71**	**3.44**	**55.90**	**69.73**	**20.24**
3	-504.54	13.51	-13.83	NA	NA

Canyon treefrog - eastern group

K	Mean LnP(*K*)	Stdev LnP(*K*)	Ln'(*K*)	|Ln"(*K*)|	Delta *K*
1	-1125.51	0.46	NA	NA	NA
2	**-938.96**	**0.60**	**186.55**	**223.24**	**369.57**
3	-975.65	20.74	-36.69	4.19	0.20
4	-1008.15	23.66	-32.50	NA	NA

Table 1.A.5, continued.

Canyon treefrog - Dragoons group					
K	Mean LnP(*K*)	Stdev LnP(*K*)	Ln'(*K*)	|Ln"(*K*)|	Delta *K*
1	**-687.94**	**0.69**	**NA**	**NA**	**NA**
2	-689.36	1.76	-1.42	1.81	1.03
3	-688.97	1.51	0.39	0.18	0.12
4	-688.76	1.94	0.21	NA	NA
Red-spotted toad - all populations					
K	Mean LnP(*K*)	Stdev LnP(*K*)	Ln'(*K*)	|Ln"(*K*)|	Delta *K*
1	-13215.02	0.46	NA	NA	NA
2	-12971.37	13.98	243.65	102.01	7.30
3	**-12829.73**	**8.44**	**141.64**	**63.70**	**7.55**
4	-12751.79	27.19	77.94	36.58	1.35
5	-12710.43	29.91	41.36	0.06	0.00
6	-12669.01	71.29	41.42	49.47	0.69
7	-12677.06	43.01	-8.05	30.23	0.70
8	-12654.88	64.53	22.18	116.90	1.81
9	-12749.60	178.93	-94.72	177.69	0.99
10	-13022.01	407.90	-272.41	298.99	0.73
11	-12995.43	403.13	26.58	325.88	0.81
12	-13294.73	468.77	-299.30	300.26	0.64
13	-13894.29	867.01	-599.56	929.46	1.07
14	-13564.39	505.81	329.90	753.24	1.49
15	-13987.73	953.76	-423.34	113.54	0.12
16	-14297.53	757.84	-309.80	NA	NA
Red-spotted toad - Huachuca group					
K	Mean LnP(*K*)	Stdev LnP(*K*)	Ln'(*K*)	|Ln"(*K*)|	Delta *K*
1	**-7728.50**	**0.40**	**NA**	**NA**	**NA**
2	-7739.63	9.16	-11.13	5.23	0.57
3	-7745.53	76.76	-5.90	104.14	1.36
4	-7855.57	181.07	-110.04	125.11	0.69
5	-7840.50	283.73	15.07	293.10	1.03
6	-8118.53	159.93	-278.03	11.19	0.07
7	-8407.75	350.29	-289.22	442.65	1.26
8	-8254.32	234.76	153.43	NA	NA
Red-spotted toad - Northern group					
K	Mean LnP(*K*)	Stdev LnP(*K*)	Ln'(*K*)	|Ln"(*K*)|	Delta *K*
1	-4553.32	0.32	NA	NA	NA
2	-4449.05	8.94	104.27	18.66	2.09
3	-4363.44	29.85	85.61	20.58	0.69
4	**-4298.41**	**5.18**	**65.03**	**72.03**	**13.90**
5	-4305.41	16.50	-7.00	26.40	1.60
6	-4338.81	52.72	-33.40	3.73	0.07
7	-4375.94	36.93	-37.13	59.32	1.61

Table 1.A.5, continued.

8	-4472.39	58.42	-96.45	9.56	0.16
9	-4559.28	174.10	-86.89	NA	NA

Red-spotted toad - Northern sub-group

K	Mean LnP(*K*)	Stdev LnP(*K*)	Ln'(*K*)	|Ln"(*K*)|	Delta *K*
1	**-2372.74**	**0.48**	**NA**	**NA**	**NA**
2	-2430.49	33.76	-57.75	35.43	1.05
3	-2452.81	87.30	-22.32	79.44	0.91
4	-2395.69	26.53	57.12	52.34	1.97
5	-2390.91	33.63	4.78	NA	NA

Mexican spadefoot - all populations

K	Mean LnP(*K*)	Stdev LnP(*K*)	Ln'(*K*)	|Ln"(*K*)|	Delta *K*
1	-19503.12	0.18	NA	NA	NA
2	**-19351.07**	**6.00**	**152.05**	**68.00**	**11.33**
3	-19267.02	11.99	84.05	104.55	8.72
4	-19287.52	41.90	-20.50	110.89	2.65
5	-19418.91	160.98	-131.39	59.02	0.37
6	-19491.28	197.55	-72.37	1.44	0.01
7	-19565.09	289.89	-73.81	51.89	0.18
8	-19587.01	270.93	-21.92	9.04	0.03
9	-19617.97	181.86	-30.96	130.94	0.72
10	-19779.87	355.34	-161.90	284.66	0.80
11	-19657.11	235.36	122.76	277.71	1.18
12	-19812.06	273.94	-154.95	139.42	0.51
13	-19827.59	271.40	-15.53	212.04	0.78
14	-19631.08	210.34	196.51	250.04	1.19
15	-19684.61	217.28	-53.53	36.77	0.17
16	-19774.91	149.92	-90.30	158.59	1.06
17	-19706.62	130.22	68.29	258.44	1.98
18	-19896.77	365.91	-190.15	310.33	0.85
19	-19776.59	168.08	120.18	17.39	0.10
20	-19673.80	185.09	102.79	136.42	0.74
21	-19707.43	107.20	-33.63	8.41	0.08
22	-19732.65	220.54	-25.22	100.37	0.46
23	-19657.50	80.49	75.15	90.43	1.12
24	-19672.78	127.48	-15.28	59.26	0.46
25	-19747.32	242.03	-74.54	9.78	0.04
26	-19812.08	334.43	-64.76	NA	NA

Mexican spadefoot - Santa Rita group

K	Mean LnP(*K*)	Stdev LnP(*K*)	Ln'(*K*)	|Ln"(*K*)|	Delta *K*
1	**-1758.44**	**0.53**	**NA**	**NA**	**NA**
2	-1797.04	29.55	-38.60	14.24	0.48
3	-1821.40	37.96	-24.36	1.36	0.04
4	-1847.12	29.46	-25.72	NA	NA

Table 1.A.5, continued.

Mexican spadefoot - Huachuca group

K	Mean LnP(*K*)	Stdev LnP(*K*)	Ln'(*K*)	|Ln"(*K*)|	Delta *K*
1	-17565.59	0.07	NA	NA	NA
2	**-17497.87**	**10.61**	**67.72**	**129.18**	**12.17**
3	-17559.33	32.91	-61.46	24.50	0.74
4	-17596.29	83.92	-36.96	128.06	1.53
5	-17761.31	154.30	-165.02	0.93	0.01
6	-17927.26	178.78	-165.95	141.40	0.79
7	-17951.81	204.93	-24.55	95.89	0.47
8	-18072.25	302.79	-120.44	260.18	0.86
9	-17932.51	263.72	139.74	245.68	0.93
10	-18038.45	226.66	-105.94	96.13	0.42
11	-18048.26	243.41	-9.81	84.39	0.35
12	-17973.68	275.75	74.58	120.49	0.44
13	-18019.59	335.17	-45.91	109.97	0.33
14	-17955.53	137.98	64.06	69.75	0.51
15	-17961.22	154.04	-5.69	100.90	0.66
16	-18067.81	303.65	-106.59	266.85	0.88
17	-17907.55	147.00	160.26	261.14	1.78
18	-18008.43	248.44	-100.88	31.08	0.13
19	-18140.39	380.27	-131.96	285.94	0.75
20	-17986.41	220.01	153.98	87.47	0.40
21	-17919.90	158.72	66.51	41.97	0.26
22	-17895.36	169.39	24.54	52.57	0.31
23	-17923.39	144.17	-28.03	74.31	0.52
24	-17877.11	110.27	46.28	NA	NA

Table 1.A.6. Comparison of allelic richness, observed and expected heterozygosity, N_e (median estimate and the count of upper confidence intervals that include infinite population sizes), and genetic differentiation (G'_{ST}) between sampling methods for red-spotted toads and spadefoots.

Red-spotted toad						
	Allelic richness	H_O	H_E	N_e	N_e infinite C. I.	G'_{ST}
Adults	5.781	0.776	0.764	81.8	2 of 4	0.235
Larvae	5.673	0.749	0.772	35.0	1 of 4	0.380
Mexican spadefoot						
	Allelic richness	H_O	H_E	N_e	N_e infinite C. I.	G'_{ST}
Adults	4.985	0.667	0.664	618.90	10 of 11	0.103
Larvae	5.020	0.654	0.673	*Infinite*	10 of 11	0.077
Breeding Adults	4.937	0.656	0.667	732.10	6 of 6	0.102
Roadside Adults	5.024	0.677	0.661	197.60	4 of 5	0.099

Table 1.A.7. Spatial and temporal sampling replicates and genetic diversity (expected and observed heterozygosity, allelic richness, N_e, and the upper confidence interval for N_e estimate calculated via a jackknifing method). Significant results shown in bold font.

All species		
Paired t-test	*t*	*p-val*
H_E	1.723	0.100
H_O	-1.128	0.273
AR	1.191	0.248
Wilcoxon signed-rank test	*V*	*p-val*
N_e	101	0.5136
N_e *(upper C.I.)*	22	1
Canyon treefrog and red-spotted toads		
Paired t-test	*t*	*p-val*
H_E	**2.777**	**0.024**
H_O	-0.378	0.715
AR	1.707	0.126
Wilcoxon signed-rank test	*V*	*p-val*
N_e	19	0.944
N_e *(upper C.I.)*	9	0.447

Appendix 1.B. Landscape resistance methods and additional landscape genetics results

Additional description of landscape resistance methods and tables describing landscape resistance values and source data, correlation coefficients between resistance/distance values, mixed-effects modeling results for major genetic clusters of canyon treefrogs and Mexican spadefoots, and results of multiple regression with distance matrices.

Landscape resistance and distance details and construction

We hypothesized relationships between genetic and structural connectivity along a gradient of species water requirements. Final hypotheses were organized into six categories. Two categories imply no correlation with landscape factors: isolated populations (high genetic differentiation between sampling locations driven primarily by low migration, genetic drift, and/or small populations) and panmixia (low genetic differentiation due to high gene flow between all sampling locations and/or large populations). The other four categories imply a specific relationship between genetic connectivity and some landscape factor. These categories are summarized in Table 1.B.1. Each category – terrestrial, aquatic, topography, and isolation-by-distance – was evaluated using one or multiple landscape resistance surfaces built with spatial data. These resistance surfaces and data are summarized in Table 1.B.1, and details for data layers and sources are included in Table 1.B.2.

Hypothesized resistances of structural connectivity between sampling locations were built using CIRCUITSCAPE (McRae 2006), a program utilizing circuit theory to simulate gene flow through a resistance surface. CIRCUITSCAPE allows for gene flow (i.e., "current") to travel across multiple pathways, reporting pairwise summations of resistance between sampling locations. To generate these pairwise data, we built raster maps of resistance (low to high) using

data in Table 1.B.2. A geographic information system (ArcGIS 10.1, Environmental Systems Research Institute) was used to catalog and manipulate landscape data and generate resistance raster maps. Each resistance map was scaled for hypothesized landscape resistance to gene flow from 1 - 100 where 1 indicates low resistance and 100 indicates high resistance. The scale of resistance values was arbitrary and was designed to reflect hypothesized relationships between landscape features and genetic connectivity. We examined two additional scales of resistance (1 - 1000 and 1 - 10,000), but resistances and the relationships with genetic connectivity were highly correlated ($r > 0.99$). Thus only results for resistances from 1 – 100 are included in this manuscript.

To balance demand for computational resources with maintaining enough detail to realistically examine structural connectivity, all resistance maps were scaled to 60 m resolution, which involved resampling of some data layers. The spatial extent of resistance rasters ensured a buffer of at least 30 km from the edge of the raster to a given sample site. With this grain and extent, we were able to perform all CIRCUITSCAPE analyses in the pairwise source/ground modeling mode and using a cell connection scheme of eight neighbors, allowing maximum freedom of current flow. Due to the location of one Mexican spadefoot sampling site near the US-Mexico border, the 30 km buffer required use of spatial data from the US and Mexico. Data are generally more widely available and higher resolution for the US, and in some cases in our study Mexico's data are courser resolution (Table 1.B.2). However, it is unlikely that the resolution of data for Mexico would skew structural connectivity estimates between populations of any species, particularly with only one sample site very near the border.

Some landscape resistance layers had moderate to strong correlations with one another. These correlations are summarized in Table 1.B.3 and were taken into account in all analyses of genetic and structural connectivity relationships.

Mixed-effects modeling results for canyon treefrog and Mexican spadefoot genetic clusters

Mixed-effects modeling results (individual factors and couplet models) for canyon treefrog and Mexican spadefoot genetic clusters are presented in Table 1.B.4. Methods and results are presented in the main text.

Multiple regression with distance matrices (MRDM) methods and results

MRDM evaluates relationships between one or many explanatory distance matrices and a response distance matrix and uses permutation to determine statistical significance of the overall model. MRDM also informs significance of each explanatory variable in a model, and those significance values can help elucidate drivers among correlated structural connectivity hypotheses. We included one distance matrix (with the highest R^2_β value as calculated by mixed-effects modeling) from each structural connectivity category to build global MRDM models. For cases in which multiple variables were included in the supported model, we evaluated the variance inflation factor of each predictor variable. A variance inflation factor > 10 is considered a threshold at which collinearity of variables is problematic for interpreting model results (Kutner et al. 2004). Variance inflation factor was evaluated using the linear form of each model with the R package "car" (Fox and Weisberg 2011). Pairwise landscape resistances were then dropped according to significance (least significant dropped first) until only one resistance layer remained. We inferred strength of model fit by evaluating overall R^2 and the significance of

explanatory variables (pairwise landscape resistances) included in the model. MRDM results are summarized in the main text of the manuscript and are presented in Table 1.B.4 of this appendix.

References

Fox, J., and S. Weisberg. 2011. An R Companion to Applied Regression, Second Edition. Thousand Oaks CA: Sage. URL: http://socserv.socsci.mcmaster.ca/jfox/Books/Companion

Kutner, M., C. Nachsheim, and J. Netter. 2004. Applied Linear Regression Models. McGraw-Hill, New York, NY.

McRae, B. H. 2006. Isolation by resistance. Evolution **60**:1551-1561.

Table 1.B.1. Descriptions and data used to construct resistance layers for each connectivity hypothesis (data described in Table 1.B.2, and note that data used often include different sources for Arizona and Mexico). Isolated population and panmixia hypotheses presented in text are not included here because they are not associated with effects of any particular landscape driver. Additional details available upon request from M.C. Mims.

Resistance layers	Description	Data used	Type
Terrestrial			
Canopy	Resistance decreases with increased canopy cover.	Canopy Cover - Arizona; Canopy Cover - Mexico	Categorical
Urban	Resistance increases with development.	Urbanization - Arizona; Urbanization - Mexico	Categorical
LandCov	Resistance is lowest with high canopy cover and highest for high development.	Combination of Canopy and Urbanization resistance layers (reclassified)	Categorical
Aquatic			
Stream	Resistance is lowest for streams and ponds, moderate for ephemeral streams, and highest for areas with no aquatic habitat.	Streams - Arizona; Streams - Mexico; Ponds and lakes - Arizona; Geology - Arizona; Geology - North America; Streamflow permanence - geological inference; Streamflow permanence - known perennial reaches	Categorical
PrecipET	Resistance decreases as summer precipitation-evapotranspiration increases.	Precipitation - Arizona; Precipitation - Mexico; Evapotranspiration	Continuous
AvgWater	Resistance is lowest where precipitation is highest and aquatic habitat is available and is highest in dry areas with no aquatic habitat.	Average Stream and PrecipET resistance layers	Categorical + Continuous
Topography			
Slope	Resistance increases with slope.	Slope from digital elevation model (DEM)	Continuous
Isolation-by-Distance			
Euclidean	Pairwise Euclidean distance between sampling locations.	Euclidean distance	Continuous
Null	Uniform landscape resistance.	Null model	Uniform

Table 1.B.2. Data, details, resolution, and source information for spatial and environmental data used to create resistance layers (Table 1.B.1).

Data	Details	Resolution	Source
Canopy cover - Arizona	2001 NLCD canopy density dataset.	30m	http://www.mrlc.gov/nlcd01_data.php
Canopy cover - Mexico	USGS Land Cover Institute.	250m	http://landcover.usgs.gov/nalcms.php
Urbanization - Arizona	2006 NLCD land cover dataset.	30m	http://www.mrlc.gov/nlcd2006.php
Urbanization - Mexico	USGS Land Cover Institute.	250m	http://landcover.usgs.gov/nalcms.php
Streams - Arizona	NHDPlus Version 2, downloaded from National Map Viewer (USGS).	*shapefile*	http://viewer.nationalmap.gov/viewer/
Streams - Mexico	Stream network supplied by Dale Turner, The Nature Conservancy.	*shapefile*	Dale Turner, The Nature Conservancy, personal request.
Ponds and lakes - Arizona	NHDPlus Version 2, downloaded from National Map Viewer (USGS).	*shapefile*	http://viewer.nationalmap.gov/viewer/
Geology - Arizona	Surface deposits identified for characterization of ephemeral streams.	*shapefile*	http://mrdata.usgs.gov/geology/state/state.php?state=AZ
Geology - North America	Surface deposits identified for characterization of ephemeral streams.	*shapefile*	http://ngmdb.usgs.gov/gmna/
Streamflow permanence - geological inference	Steamflow permanence records (Huachuca Mountains) as a function of geology.	*N/A*	Kristin Jaeger and Julian Olden, unpublished data.
Streamflow permanence - known perennial reaches	The Nature Conservancy, US Fish and Wildlife Service: documented and well-known perennial stream reaches.	*N/A*	http://azconservation.org/map_gallery/san_pedro_river_surface_water http://www.fws.gov/southwest/federal_assistance/pdfs/chapter%2010%20santa%20cruz%20river%20watershed.pdf
Precipitation - Arizona	PRISM: 30-year precipitation averages for months of June-Oct, 1981-2010.	800m	http://prism.nacse.org/normals/
Precipitation - Mexico	Climate Wizard: 50+ year precipitation averages, June-Oct, 1951-2002.	50km	http://www.climatewizard.org/

Table 1.B.2, continued.

Data	Details	Resolution	Source
Evapotranspiration	MODIS Global Terrestrial Evapotranspiration Data Set, June-Oct, 2000-2010.	5km	http://www.ntsg.umt.edu/project/mod16
Slope	Calculated with 9-m Digital Elevation Model from National Elevation Dataset.	9m	http://ned.usgs.gov/downloads.asp
Euclidean distance	Pairwise distances calculated using UTM location data in PASSaGE 2.	*distance*	http://www.passagesoftware.net/
Null model	Uniform resistance layer.	*flexible*	

Table 1.B.3. Pearson correlation coefficients between pairwise resistance/distance values for each species and their major genetic clusters, identified in Figure 1.2 of the main text.

Canyon treefrog

	AvgWat	Canopy	Urban	LandCov	PrecipET	Slope	Stream	Null
Canopy	0.811							
Urban	0.967	0.745						
LandCov	0.859	0.990	0.794					
PrecipET	0.946	0.853	0.906	0.897				
Slope	0.167	-0.066	0.265	-0.026	0.024			
Stream	0.955	0.707	0.920	0.756	0.811	0.278		
Null	0.971	0.748	0.998	0.798	0.913	0.245	0.922	
Eucl	0.965	0.744	0.995	0.794	0.904	0.239	0.921	0.997

Red-spotted toad

	AvgWat	Canopy	Urban	LandCov	PrecipET	Slope	Stream	Null
Canopy	0.842							
Urban	0.894	0.800						
LandCov	0.898	0.988	0.873					
PrecipET	0.945	0.876	0.857	0.913				
Slope	0.394	0.047	0.357	0.159	0.311			
Stream	0.966	0.758	0.845	0.820	0.830	0.412		
Null	0.946	0.826	0.951	0.894	0.925	0.446	0.883	
Eucl	0.906	0.797	0.894	0.861	0.882	0.457	0.848	0.949

Mexican spadefoot

	AvgWat	Canopy	Urban	LandCov	PrecipET	Slope	Stream	Null
Canopy	0.842							
Urban	0.894	0.800						
LandCov	0.898	0.988	0.873					
PrecipET	0.945	0.876	0.857	0.913				
Slope	0.394	0.047	0.357	0.159	0.311			
Stream	0.966	0.758	0.845	0.820	0.830	0.412		
Null	0.946	0.826	0.951	0.894	0.925	0.446	0.883	
Eucl	0.906	0.797	0.894	0.861	0.882	0.457	0.848	0.949

Canyon treefrog - west

	AvgWat	Canopy	Urban	LandCov	PrecipET	Slope	Stream	Null
Canopy	0.724							
Urban	0.955	0.648						
LandCov	0.786	0.991	0.707					
PrecipET	0.911	0.795	0.859	0.849				
Slope	0.080	-0.237	0.234	-0.189	-0.176			
Stream	0.950	0.595	0.900	0.658	0.738	0.247		
Null	0.960	0.649	0.998	0.710	0.871	0.209	0.899	
Eucl	0.872	0.591	0.922	0.639	0.751	0.306	0.846	0.923

Table 1.B.3, continued.

Canyon treefrog - Huachuca Mountains

	AvgWat	Canopy	Urban	LandCov	PrecipET	Slope	Stream	Null
Canopy	0.523							
Urban	0.948	0.412						
LandCov	0.637	0.981	0.513					
PrecipET	0.933	0.700	0.836	0.798				
Slope	-0.284	-0.588	-0.106	-0.542	-0.497			
Stream	0.935	0.285	0.914	0.406	0.747	-0.039		
Null	0.956	0.401	0.998	0.506	0.850	-0.133	0.918	
Eucl	0.846	0.348	0.886	0.431	0.756	-0.204	0.804	0.894

Red-spotted toad - north

	AvgWat	Canopy	Urban	LandCov	PrecipET	Slope	Stream	Null
Canopy	0.877							
Urban	0.894	0.754						
LandCov	0.926	0.984	0.851					
PrecipET	0.956	0.798	0.908	0.851				
Slope	0.093	-0.225	0.194	-0.091	0.086			
Stream	0.966	0.887	0.802	0.923	0.849	0.067		
Null	0.892	0.752	1.000	0.849	0.907	0.199	0.800	
Eucl	0.819	0.642	0.968	0.751	0.868	0.256	0.700	0.966

Red-sotted toad - Huachuca Mountains

	AvgWat	Canopy	Urban	LandCov	PrecipET	Slope	Stream	Null
Canopy	0.585							
Urban	0.927	0.363						
LandCov	0.687	0.985	0.494					
PrecipET	0.972	0.548	0.956	0.665				
Slope	-0.271	-0.427	0.036	-0.397	-0.204			
Stream	0.983	0.603	0.865	0.688	0.914	-0.324		
Null	0.915	0.324	0.998	0.457	0.943	0.064	0.855	
Eucl	0.786	0.182	0.913	0.311	0.864	0.090	0.689	0.918

Mexican spadefoot - east

	AvgWat	Canopy	Urban	LandCov	PrecipET	Slope	Stream	Null
Canopy	0.821							
Urban	0.881	0.779						
LandCov	0.881	0.988	0.856					
PrecipET	0.941	0.858	0.846	0.900				
Slope	0.265	-0.139	0.197	-0.028	0.207			
Stream	0.961	0.728	0.827	0.795	0.814	0.278		
Null	0.940	0.805	0.941	0.878	0.923	0.299	0.867	
Eucl	0.904	0.782	0.879	0.848	0.883	0.291	0.837	0.948

Table 1.B.4. Mixed-effects modeling results for major genetic clusters for canyon treefrogs (CT-W: canyon treefrog – west; CT-H canyon treefrog - Huachucas) and Mexican spadefoot (MS-E: Mexican spadefoot - east). Genetic clusters are identified in Figure 1.2 of the main text. Top R^2_β values for single-resistance (top) and couplet-resistance (below) models are highlighted in bold font. IP and P hypothesize no landscape effect, indicated by poor model performance across all other models. A dash indicates no support for IP or P. All R^2_β correlation coefficients are positive with the exception of a negative relationship with Slope in models denoted with underlined text.

Hypotheses	Resistance layers/distance	R^2_β, mixed-effects models		
Species		CT-W	CT-H	MS-E
Isolated populations (IP)	*N/A*	-	-	-
Terrestrial (TE)	Canopy	0.64	0.06	0.22
	Urban	0.73	**0.80**	0.21
	LandCov	0.68	0.51	0.23
Aquatic (A)	Stream	0.71	0.79	0.23
	PrecipET	**0.74**	0.76	0.22
	AvgWater	0.73	0.79	0.23
Topography (T)	Slope	0.46	0.61	0.16
Isolation-by-distance (IBD)	Eucl	0.61	0.58	**0.29**
	Null	0.72	**0.80**	0.22
Panmixia (P)	*N/A*	-	-	-
TE + T	Best of TE + Slope	**0.86**	**0.85**	0.44
A + T	Best of A + Slope	0.85	0.84	0.22
IBD + T	Eucl + Slope	0.73	0.67	0.39
	Null + Slope	**0.86**	**0.85**	**0.46**

Table 1.B.5. MRDM results by species. Correlation between genetic distance and landscape resistance were consistent within a species or group and are shown as positive (+) or negative (-). R^2 and p-values generated from permutation tests are shown for the overall model, and p-values for each factor are included. Best models shown in bold font, and for best models with > 2 factors, variance inflation factors (*vif*) are included in italicized text just below each factor in the model. *For Mexican spadefoots, the Stream-only and Euclidean-only models performed similarly. A partial mantel test was used to evaluate correlation between genetic distance and either Stream or Euclidean while controlling for the other. The partial mantel statistic was more significant for Stream (p = 0.030) than for Euclidean (p = 0.093). †*vif* > 10 indicates high collinearity among predictor variables. Note that for both canyon treefrog clusters, *vif* values suggest interpreting results with caution.

Canyon treefrog						
	Null	AvgWat	Slope	LandCov	R^2	p-val
correlation	+	+	-	-		
1	0.201	0.980	0.945	0.915	0.54	0.001
2	0.002		0.954	0.915	0.54	0.001
3	0.002			0.928	0.54	0.001
4	**0.001**				**0.54**	**0.001**
Red-spotted toad						
	Null	Stream	Slope	Urban	R^2	p-val
correlation	-	+	+	+		
1	0.097	0.001	0.019	0.335	0.62	0.002
2	**0.009**	**0.001**	**0.023**		**0.61**	**0.001**
vif	*6.0*	*5.58*	*1.39*			
3	0.121	0.009			0.47	0.003
4		0.001			0.40	0.001
Mexican spadefoot						
	Eucl	Stream	Slope	LandCov	R^2	p-val
correlation	+	+	+	+		
1	0.256	0.179	0.668	0.956	0.44	0.001
2	0.234	0.129	0.51		0.44	0.001
3	0.138	0.095			0.43	0.001
4*		**0.001**			**0.40**	**0.001**
5	**0.001**				**0.38**	**0.001**
Red-spotted toad - north						
	Null	Stream	Slope	Lan	R^2	p-val
correlation	-	+	+	+		
1	0.068	0.259	0.034	0.928	0.73	0.027
2	**0.026**	**0.017**	**0.025**		**0.73**	**0.007**
vif	*2.95*	*2.85*	*1.07*			
3		0.15	0.059		0.48	0.046
4			0.061		0.40	0.061

Table 1.B.5, continued.

Red-spotted toad - Huachuca Mountains						
	Null	Stream	Slope	Lan	R^2	p-val
correlation	-	+	+	+		
1	0.303	0.383	0.237	0.552	0.42	0.582
2	0.179	0.171	0.302		0.36	0.384
3	0.527	0.593			0.08	0.737
4	0.731				0.01	0.731
Canyon treefrog - west						
	Null	PrecipET	Slope	Urban	R^2	p-val
correlation	+	-	-	-		
1	0.109	0.001	0.003	0.465	0.72	0.001
2	**0.001**	**0.001**	**0.002**		**0.71**	**0.001**
vif	*9.50*	*9.37*	*2.36*			
3	0.001	0.173			0.51	0.001
4	0.001				0.45	0.001
Canyon treefrog - Huachuca Mountains						
	Null	AvgWat	Slope	Urban	R^2	p-val
correlation	+	-	-	-		
1	0.006	0.006	0.256	0.047	0.78	0.001
2	**0.005**	**0.006**		**0.019**	**0.74**	**0.001**
vif†	*15.39*	*16.44*		*1.44*		
3	0.014	0.071			0.55	0.012
vif†	*11.65*	*11.65*				
4	0.001				0.34	0.001
Mexican spadefoot - east						
	Eucl	AvgWat	Slope	LandCov	R^2	p-val
correlation	+	+	-	-		
1	0.594	0.048	0.167	0.305	0.36	0.006
2		0.028	0.186	0.36	0.36	0.006
3		0.001	0.345		0.34	0.001
4		**0.001**			**0.31**	**0.001**

Chapter 2: Landscape genetics and multispecies conservation: the case for a traits-based revolution

Authors: M.C. Mims, E.E. Hartfield Kirk, D.A. Lytle, J.D. Olden

2A. "In a Nutshell"

- Landscape and population genetic studies often play critical roles in single-species conservation planning and management, yet the transferability of landscape genetic findings across species and regions and the potential for predictive frameworks remain largely unexplored.
- Traits, or measurable attributes of individuals, populations, or species, are employed in many ecological disciplines as a common currency for comparison across species and regions and may offer a promising platform for multispecies comparison and inference in landscape genetics.
- Traits-based approaches could expand significantly the contribution of many landscape genetic studies to species and regions for which genetic evaluations of taxa are not available or feasible for a wide variety of logistical reasons.
- Formal development, testing, and generalization of traits-based frameworks represent a significant step toward advancing the utility, efficiency, and effectiveness of landscape genetic inference in contemporary ecology and conservation.

2B. Abstract

Recent calls for rapid, efficient, and reliable evaluation of species vulnerability to environmental change necessitate frameworks for the simultaneous assessment of multiple species. Here, we

propose traits-based frameworks to enhance the utility of landscape genetics in multispecies conservation. Traits are measurable attributes of individuals, populations, or species, and are used in many ecological disciplines as a common currency for comparison across species and regions. The utility of traits in multispecies vulnerability assessments is recognized increasingly, and many traits are known to modulate relationships between species, their genetics, and the environment. Here, we propose guiding principles for the formal development, testing, and generalization of traits-based frameworks to advance the utility, efficiency, and effectiveness of genetic inference in contemporary ecology and conservation. Traits-based frameworks may ultimately improve the transferability and relevance of landscape genetics in science, management, and policy.

2C. Introduction

Rapid environmental change and limited resources necessitate robust conservation planning in which knowledge of population attributes, such as structure, connectivity, and genetic integrity, play a fundamental role (Williams *et al.* 2008). For decades, population genetic approaches have been used to identify scenarios that may compromise the health, resilience, or persistence of a species and its populations, such as inbreeding and outbreeding depression, or accumulation of deleterious alleles (Amos and Balmford 2001). Population genetics has also informed designation of management units (Palsbøll *et al.* 2007), particularly for species that are difficult to monitor using traditional approaches (Schwartz *et al.* 2007). In recent years, the field of landscape genetics has integrated population genetics with emerging spatial statistics to examine how the environment affects population genetic structure, diversity, and differentiation (Manel *et al.* 2003). New technologies and increasing focus on adaptive genetic variance continue to

expand the contribution of population and landscape genetics to conservation biology (Segelbacher *et al.* 2010; Manel and Holderegger 2013).

Increasing emphasis has been placed on using species' attributes – or traits – to identify at-risk species to environmental change when species-specific approaches are not feasible (Foden *et al.* 2013; Pacifici et al. 2015). Traits are species attributes measurable at the individual level, including morphological traits (body size or gape), life history traits (fecundity, age at maturation, or longevity), behavioral traits (parental care or aestivation), and other characteristics that broadly enable an organism to cope with ecological challenges. Such traits can be summarized for a given individual, population, or species and can be used as a "common currency" for comparison across species. The utility of traits-based approaches is widely recognized in community ecology, where traits are often used to investigate patterns across taxa and ecosystems (McGill *et al.* 2006). Opportunities for multispecies, traits-based studies in landscape genetics continues to increase as analytical approaches converge (Bolliger *et al.* 2014) and open communication, data sharing, and collaboration are increasingly prioritized (Balkenhol *et al.* 2009). Concurrently, calls for hypothesis-driven inquiry (Segelbacher *et al.* 2010) and multispecies inference (Manel and Holderegger 2013) underscore the need for strategic approaches that promote generalized frameworks in population and landscape genetics. Here, we discuss steps and strategies for the formal development, testing, and application of traits-based frameworks for multispecies inference in landscape genetics.

2D. Principles of Application

Species, population genetics, and the environment are connected mechanistically by traits

A traits-based framework for the generalization of population and landscape genetics builds upon long-recognized mechanistic connections between traits and population genetics. Population size and migration rates were among the first factors identified as fundamental to population genetic structure (Wright 1943), and both are primarily governed by traits, such as fecundity, longevity, generation time, and dispersal ability. Recent evidence suggests that genetic diversity is negatively related to life span and positively related to fecundity, illustrating the strong linkages between genetic diversity and life history attributes (Romiguier *et al.* 2014). The same traits affecting population genetic structure are also associated with the vulnerability of species to environmental change (Williams *et al.* 2008).

Mechanistic linkages between organismal attributes and ecological processes imply that some traits or combination of traits may better explain patterns of population and landscape genetics than implicit indicators, such as predicted abundance (Peterman *et al.* 2014). Some "focal traits", i.e., traits with strong hypothesized links to population genetic processes, may provide useful predictive frameworks for population and landscape genetic patterns across species. For example, dispersal ability is perhaps one of the most important and widely recognized drivers of landscape genetic patterns across a range of taxa, including amphibians in the northeastern United States (Richardson 2012), woodland birds in Australia (Amos *et al.* 2014), freshwater fishes in the southeastern United States (Fluker *et al.* 2014), and aquatic insects in western Switzerland (Alp *et al.* 2012). In addition to dispersal, other traits, such as life history attributes and behavior, may also influence population and landscape genetic structure. The traits of breeding site fidelity and generation time explained differences in population genetic differentiation, landscape associations, effective population size, and sensitivity to land-use change for two otherwise ecologically similar salamander species in eastern United States

(Whiteley *et al.* 2014). Territorial social organization, a behavioral trait, was associated strongly with population genetic diversity of two woodland lizard species following fire disturbance in Australia (Smith *et al.* 2014). Increasingly, combinations of traits that include dispersal ability, behavior and other ecologically limiting factors have proven useful in explaining differential landscape genetic patterns between species (e.g., Goldberg and Waits 2010; Kelly and Palumbi 2010).

Traits provide currency for multispecies inference in population and landscape genetics

The extent to which patterns and processes are generalizable across species is a unifying research theme in ecology, with critical importance to managers seeking to build comprehensive multispecies or community-level conservation plans with relatively limited information. Recent multispecies genetic studies highlight the utility of considering many species at once in attributing patterns of population genetic structure to environmental gradients (Manel *et al.* 2012) or particular geographic "hot spots" of genetic diversity (Thomassen *et al.* 2011). We propose traits-based inference as a formal organizing framework for multi-taxa inference in population and landscape genetics. Evidence for a range of freshwater organisms suggests that traits may provide the basis for multispecies generalization of population genetic structure. For example, dispersal and life history traits predicted population genetic structure in almost three-quarters of >100 fish and aquatic macroinvertebrate species in Australia (Hughes *et al.* 2013). Population genetic structure for a diverse suite of aquatic taxa in the southwestern United States was also closely linked to dispersal and aquatic habitat requirements (Mims *et al.* 2015; Phillipsen *et al.* 2015, Panel 1), thus providing new opportunities to broadly transfer these associations to other aquatic taxa in the region (Figure 2. 1).

A framework for multispecies population and landscape genetic inference provides an important tool for managers and conservation practitioners tasked with applying the best available data to managing many species at once. For example, the two studies highlighted in Panel 1 provide the foundation for conservation prioritization of regional aquatic fauna. Dewatering of perennial springs and streams due to climate change and human water use in the southwestern United States (Sabo *et al.* 2010) may result in local extinction of genetically distinct populations of the canyon treefrog (*Hyla arenicolor*) and the giant water bug (*Abedus herberti*) with little chance of recolonization (Bogan and Lytle 2011). Alternatively, predaceous diving beetles (*Boreonectes aequinoctialis*) and Mexican spadefoots (*Spea multiplicata*) are well adapted to capitalize on ephemeral aquatic habitats that are temporally and spatially variable in availability, and population genetic analysis revealed high gene flow for both species within the range of these studies. These ephemeral-adapted species and others like them may be less vulnerable to changes in aquatic habitat or landscape features.

Traits offer a promising framework toward generalization of landscape genetic studies, but efforts toward multispecies inference must consider challenges inherent to population and landscape genetics. For example, the spatial scale (Balkenhol *et al.* 2009), grain size (Galpern *et al.* 2012), and study extent (Trumbo *et al.* 2013) can have profound effects on the outcomes, and thus interpretation, of population and landscape genetic studies. Landscape genetics must also be interpreted in the context of temporal scale, considering both the imprinting of former landscape processes and the lag time to detect the effects of contemporary environments (Landguth *et al.* 2010). These challenges should be carefully and explicitly considered (Balkenhol *et al.* 2009), particularly when employing multispecies inference or developing predictive frameworks. At the same time, traits and multi-taxa inference may ultimately help identify scenarios in which

species or populations are particularly sensitive to the spatial or temporal elements of a study design. We may find that the effects of space and time differ, and are possibly predicted, by species traits such as dispersal ability or generation time. For example, the temporal lag of landscape genetic signals is directly affected by population size and generation time (Whitlock and McCauley 1999; Landguth *et al.* 2010). Thus, traits may provide a powerful way forward to reduce uncertainty due to the spatial and temporal challenges of genetic approaches.

Traits enhance the utility of genetics studies for management and conservation goals

Traits may ultimately help elucidate the opportunities and limitations of genetic approaches to inform management actions. Population and landscape genetics are employed to address a wide range of management goals (DeSalle and Amato 2004; Bolliger *et al.* 2014), and the relevance of genetic information to achieve these objectives is constrained by the degree and nature of population structure (Table 2.1). Technological developments in the field (Allendorf *et al.* 2010), increasing focus on adaptive genetic variance (Manel and Holderegger 2013), and careful study design (Segelbacher *et al.* 2010) may effectively expand or shift the management goals informed under different trait scenarios (Figure 2. 2). But focal traits, such as species dispersal ability, life histories, environmental tolerances, and phenology, are increasingly linked to population genetic structure – and the degree to which this structure is influenced by the landscape. Traits can reveal situations in which interactions between population genetic structure and the landscape are likely, identifying valuable and informative pursuits in landscape genetics, such as estimating landscape resistance to gene flow or identifying dispersal corridors or barriers (Figure 2. 2, central oval). Alternatively, if traits suggest that population genetic structure will not be closely tied to the landscape (for example, panmixia or completely isolated populations, Figure 2. 2,

outer-most oval), then genetic inference may have limited utility in quantifying landscape effects but could inform other management goals such as identifying genetically unique populations or estimating population risk due to inbreeding depression.

2E. Future Directions

Traits-based frameworks to identify linkages between and across species, genes, and environments show promise; however, more rigorous and systematic evaluations of the geographic and taxonomic generalizations of population and landscape genetics will be required. Here, we explore three focal areas fundamental to furthering and refining the use of traits in testing ecological processes across taxa and geography and for the rapid, efficient, and generalizable incorporation of landscape genetics into management and conservation practice.

Selecting informative traits: which ones and how many?

With many traits to choose from, a useful strategy may be to first select "focal" response traits that determine species resilience and resistance to environmental change (McGill *et al.* 2006). In some cases, one or two focal traits may be intuitive drivers of population genetic patterns; in other cases, multivariate analyses will facilitate the simultaneous consideration and comparison among a suite of focal traits. Some examples of focal traits might include life history traits or traits that characterize ecological limitations. Life history traits, such as fecundity, generation time, and longevity, influence the growth rate of populations, can affect overall genetic diversity, and may ultimately shape population structure and species response to environmental change (Romiguier *et al.* 2014). Traits that characterize ecological or physiological limitations, such as dispersal potential, thermal tolerance, or physicochemical requirements may also predict

associations between genetic structure and the landscape. Several ecologically limiting traits have been related to population genetic structure, particularly for aquatic organisms including invertebrate position in the intertidal zone (Kelly and Palumbi 2010), rate of water loss in salamanders (Peterman *et al.* 2014), and water dependency of aquatic organisms in an arid environment (Mims *et al.* 2015; Phillipsen *et al.* 2015). Ecologically limiting traits also provide the framework for inference of landscape genetic structure for other taxa facing similar environmental challenges (Figure 2. 1).

Empirical examples of traits-based inference in landscape genetics often report trait values as categorical or relative measures, leaving considerable uncertainty about the strength of such relationships. Coupling technological advances in genetic resolution with more rigorous traits-based analyses will be necessary to realize the predictive potential of a traits framework. Opportunities for comparisons among many species are increasing, allowing for more formal evaluation of traits-based models to complement the largely qualitative evaluations to-date (but see Hughes *et al.* 2013). Predicting population structure via a uni- or bivariate trait framework already shows promise, and multivariate trait approaches will likely continue to refine and improve such models, capturing species that fall outside relationships built upon one or two focal traits. For example, though the two studies featured in Panel 1 support the potential of a traits-based framework for multi-taxa inference, they also highlight important future directions to improve this framework. The barking frog (*Craugastor augusti*) has no aquatic larval life stage but also has low dispersal tendencies (Goldberg and Schwalbe 2004) and is thus not well-represented by the bivariate trait framework (Figure 2.1). Additional traits such as generation time, habitat specificity, or breeding seasonality may better describe the population genetics of species poorly predicted by one or two focal traits.

Uncertainty and the importance of intraspecific trait variability

Intraspecific trait variability can have profound effects in community ecology (Bolnick *et al.* 2011) and may be particularly important in linking traits to population genetic structure, as extreme trait values (versus the mean) may have a disproportionately high effect on gene flow and population genetic structure. For example, maximum – not mean – fish dispersal is hypothesized to be decisive for the rate of exchange of individuals between populations, and thus maximum dispersal ability is likely more closely related to gene flow and recolonization processes than mean dispersal (Albanese *et al.* 2009). In many cases, a single value – typically a mean or maximum observed value – may be sufficient to distinguish species from one another (e.g., Blanck and Lamouroux 2006). However, trait variability is not well understood or quantified for many species. For example, a recent meta-analysis found quantitative dispersal estimates for only 62 stream fish species globally (Radinger and Wolter 2014), suggesting knowledge gaps of important traits such as dispersal ability even for species-rich groups. In the studies highlighted in Panel 1, the traits of dispersal potential and water dependency were considered as relative metrics (amphibians, Mims *et al*. 2015) or categorical variables (invertebrates, Cañedo-Argüelles *et al.* 2015).

Availability of trait data may be limited for many taxa, and quantifying intraspecific trait variability for many species may not be feasible. Classification of a species' habitat requirements often aim to characterize a species' environmental niche, but a single summary trait value (such as a mean) does not capture trait plasticity that may bound the true environmental tolerance of a species. For example, larval development period for some amphibian species is plastic, where increased developmental rates aid in avoiding desiccation as aquatic habitats dry (e.g., Denver *et*

al. 1998). Simulation-based approaches (Epperson *et al.* 2010) and consideration of well-studied taxa may provide valuable opportunities to determine whether, and if so how, intraspecific trait variability affects the ability to relate traits, population genetic structure, and the landscape. We argue that landscape and conservation genetics would benefit from recent methodological advances in community ecology that incorporate intraspecific trait variation into predictive models (Laughlin *et al.* 2012).

Operationalizing traits-based multispecies inference in landscape genetics

Species' traits may provide the foundation to further integrate landscape genetics with the broader fields of ecology, conservation, and restoration that increasingly rely upon traits-based inference to inform multispecies management and conservation planning. Formal exploration of the strengths, limitations, and uncertainty of such a framework may promote rapid, efficient, and generalizable incorporation of landscape genetics knowledge in management and policy. We propose the following milestones that, if achieved, will aid in operationalizing how a traits-based framework will contribute to multispecies inference and conservation application of landscape genetic studies. First, *conceptual work* and *pioneering research* already provide support for using traits as the basis of a promising multispecies framework in population and landscape genetics (Kelly and Palumbi 2010; Hughes *et al.* 2013). Next, we require the *integration of existing knowledge* into the framework. This step includes both coalescence of existing landscape genetic studies as well as the development, collection, refinement, and evaluation of traits databases for many taxa. As landscape genetic studies become more numerous, accessible, and powerful, opportunities for *testing* traits-based frameworks across taxa and regions will ultimately inform the power and limitations of *operationalizing* predictive frameworks for species for which

landscape genetic studies are not feasible. These steps are critical in the timely and efficient utilization of traits-based approaches for multispecies landscape genetic inference, and evaluation of this framework will ultimately further the utility of landscape genetics in science, management, and policy.

2F. Conclusions

Traits provide a promising framework for geographic transferability, cross-species comparison, and broader testing of ecological theories in landscape genetics. Here we propose leveraging available and ongoing landscape genetics research to formally explore, develop, and test traits as a common currency across taxa, geography, and disciplines. Such research would focus and unify emerging support of traits as important drivers of population and landscape genetic patterns. Moving forward, more rigorous, systematic evaluations of traits-based frameworks for population and landscape genetics will help evaluate their potential in addressing fundamental ecological, evolutionary, and conservation goals.

2G. Acknowledgements

We thank Erin Landguth for providing helpful comments on the manuscript. This research was funded by the Department of Defense Strategic Environmental Research and Development Program (RC-1724). Additional funding was provided by a National Science Foundation Graduate Research Fellowship (Grant No. DGE-0718124) to MCM and the H. Mason Keeler Endowed Professorship (School of Aquatic and Fishery Sciences, University of Washington) to JDO.

2H. References

Albanese B, Angermeier PL, and Peterson JT. 2009. Does mobility explain variation in colonisation and population recovery among stream fishes? Freshw Biol **54**: 1444–1460.

Allendorf FW, Hohenlohe PA, and Luikart G. 2010. Genomics and the future of conservation genetics. Nat Rev Genet **11**: 697–709.

Alp M, Keller I, Westram AM, and Robinson CT. 2012. How river structure and biological traits influence gene flow: a population genetic study of two stream invertebrates with differing dispersal abilities. Freshw Biol **57**: 969–81.

Amos W and Balmford A. 2001. When does conservation genetics matter? Heredity **87**: 257–65.

Amos JN, Harrisson KA, Radford JQ, et al. 2014. Species- and sex-specific connectivity effects of habitat fragmentation in a suite of woodland birds. Ecology **95**: 1556–68.

Balkenhol N, Gugerli F, Cushman SA, et al. 2009. Identifying future research needs in landscape genetics: where to from here? Landsc Ecol **24**: 455–63.

Blanck A and Lamouroux N. 2006. Large-scale intraspecific variation in life-history traits of European freshwater fish. J Biogeogr **34**: 862–75.

Bogan MT and Lytle DA. 2011. Severe drought drives novel community trajectories in desert stream pools. Freshw Biol **56**: 2070–81.

Bolliger J, Lander T, and Balkenhol N. 2014. Landscape genetics since 2003: status, challenges and future directions. Landsc Ecol **29**: 361–6.

Bolnick DI, Amarasekare P, Araújo MS, et al. 2011. Why intraspecific trait variation matters in community ecology. Trends Ecol Evol **26**: 183–92.

Cañedo-Argüelles M, Boersma KS, Bogan MT, et al. 2015. Dispersal strength determines meta-community structure in a dendritic riverine network. J Biogeogr **42**: 778–790.

Chan LM and Zamudio KR. 2009. Population differentiation of temperate amphibians in unpredictable environments. Mol Ecol **18**: 3185–200.

Denver RJ, Mirhadi N, and Phillips M. 1998. Adaptive plasticity in amphibian metamorphosis: response of Scaphiopus hammondii tadpoles to habitat desiccation. Ecology **79**: 1859–72.

DeSalle R and Amato G. 2004. The expansion of conservation genetics. Nat Rev Genet **5**: 702–12.

Epperson BK, McRae BH, Scribner K, et al. 2010. Utility of computer simulations in landscape genetics. Mol Ecol **19**: 3549–64.

Fluker BL, Kuhajda BR, and Harris PM. 2014. The effects of riverine impoundment on genetic structure and gene flow in two stream fishes in the Mobile River basin. Freshw Biol **59**: 526–43.

Foden WB, Butchart SHM, Stuart SN, et al. 2013. Identifying the world's most climate change vulnerable species: a systematic trait-based assessment of all birds, amphibians and corals. PLoS one **8**: e65427.

Galpern P, Manseau M, and Wilson P. 2012. Grains of connectivity: analysis at multiple spatial scales in landscape genetics. Mol Ecol **21**: 3996–4009.

Goldberg CS and Schwalbe CR. 2004. Habitat use and spatial structure of a barking frog (Eleutherodactylus augusti) population in southeastern Arizona. J Herpetol **38**: 305–12.

Goldberg CS and Waits LP. 2010. Comparative landscape genetics of two pond-breeding amphibian species in a highly modified agricultural landscape. Mol Ecol **19**: 3650–63.

Hedrick PW. 2005. A standardized genetic differentiation measure. Evolution **59**: 1633–8.

Hughes JM, Huey JA, and Schmidt DJ. 2013. Is realised connectivity among populations of aquatic fauna predictable from potential connectivity? Freshw Biol **58**: 951–66.
Kelly RP and Palumbi SR. 2010. Genetic structure among 50 species of the northeastern Pacific rocky intertidal community. PLoS One **5**: e8594.
Laughlin, DC, Joshi C, van Bodegom PM, et al. 2012. A predictive model of community assembly that incorporates intraspecific trait variation. Ecol Lett **15**: 1291–1299.
Landguth EL, Cushman SA, Schwartz MK, et al. 2010. Quantifying the lag time to detect barriers in landscape genetics. Mol Ecol **19**: 4179–91.
Manel S, Gugerli F, Thuiller W, et al. 2012. Broad-scale adaptive genetic variation in alpine plants is driven by temperature and precipitation. Mol Ecol **21**: 3729–38.
Manel S and Holderegger R. 2013. Ten years of landscape genetics. Trends Ecol Evol **28**: 614–21.
Manel S, Schwartz MK, Luikart G, and Taberlet P. 2003. Landscape genetics: combining landscape ecology and population genetics. Trends Ecol Evol **18**: 189–97.
McGill BJ, Enquist BJ, Weiher E, and Westoby M. 2006. Rebuilding community ecology from functional traits. Trends Ecol Evol **21**: 178–85.
Mims MC, Phillipsen IC, Lytle DA, et al. 2015. Ecological strategies predict associations between aquatic and genetic connectivity for dryland amphibians. Ecology.
Pacifici M, Foden WB, Visconti P, et al. 2015. Assessing species vulnerability to climate change. Nature Climate Change **5**: 215–224.
Palsbøll PJ, Bérubé M, and Allendorf FW. 2007. Identification of management units using population genetic data. Trends Ecol Evol **22**: 11–6.
Peterman WE, Connette GM, Semlitsch RD, and Eggert LS. 2014. Ecological resistance surfaces predict fine-scale genetic differentiation in a terrestrial woodland salamander. Mol Ecol **23**: 2402–13.
Phillipsen IC, Hartfield Kirk EE, Bogan MT, et al. 2015. Dispersal ability and habitat requirements determine landscape-level genetic patterns in desert aquatic insects. Mol Ecol **24**: 54–69.
Radinger J and Wolter C. 2014. Patterns and predictors of fish dispersal in rivers. Fish Fish **15**: 456–73.
Richardson JL. 2012. Divergent landscape effects on population connectivity in two co-occurring amphibian species. Mol Ecol **21**: 4437–51.
Romiguier J, Gayral P, Ballenghien M, et al. 2014. Comparative population genomics in animals uncovers the determinants of genetic diversity. Nature **515**: 261–3.
Sabo JL, Sinha T, Bowling LC, et al. 2010. Reclaiming freshwater sustainability in the Cadillac Desert. PNAS **107**: 21263–70.
Schwartz MK, Luikart G, and Waples RS. 2007. Genetic monitoring as a promising tool for conservation and management. Trends Ecol Evol **22**: 25–33.
Segelbacher G, Cushman SA, Epperson BK, et al. 2010. Applications of landscape genetics in conservation biology: concepts and challenges. Conserv Genet **11**: 375–85.
Smith AL, Bull CM, Gardner MG, and Driscoll DA. 2014. Life history influences how fire affects genetic diversity in two lizard species. Mol Ecol **23**: 2428–41.
Thomassen HA, Fuller T, Buermann W, et al. 2011. Mapping evolutionary process: a multi-taxa approach to conservation prioritization. Evol Appl **4**: 397–413.
Trumbo DR, Spear SF, Baumsteiger J, and Storfer A. 2013. Rangewide landscape genetics of an endemic Pacific northwestern salamander. Mol Ecol **22**: 1250–66.

Whiteley AR, McGarigal K, and Schwartz MK. 2014. Pronounced differences in genetic structure despite overall ecological similarity for two Ambystoma salamanders in the same landscape. Conserv Genet **15**: 573–91.
Whitlock MC and McCauley DE. 1999. Indirect measures of gene flow and migration: FST not equal to 1/(4Nm + 1). Heredity **82**: 117–25.
Williams SE, Shoo LP, Isaac JL, et al. 2008. Towards an integrated framework for assessing the vulnerability of species to climate change. PLoS Biol **6**: 2621–6.
Wright S. 1943. Isolation by distance. Genetics **28**.

2I. Panel 1

The landscape genetics of multiple aquatic species in a dryland environment

Two recent studies illustrate the potential of traits for multispecies inference in landscape genetics. Mims *et al.* (2015) and Phillipsen *et al.* (2015) evaluated the population and landscape genetics of aquatic taxa that span a range of water dependency and dispersal abilities in the Madrean Sky Islands of Arizona, USA. Water availability in this dryland region ranges from isolated perennial springs to ephemeral washes that contain water for only hours or days out of the year. Aquatic species in the region have adapted to this gradient of water availability with a diverse range of ecological strategies. Most strategies occur along the primary axes of dispersal and water dependency. Dispersal ability can range from 100s of meters to 10-100s of kilometers, and water dependency ranges from requiring water for only a short portion of the life cycle to requiring water for the entire life cycle. Both studies found strong support for relationships between water dependency, dispersal potential, and population genetic structure across taxa (Figure 2.1). Furthermore, species with intermediate dispersal and water dependency, such as Arizona snowfly, red-spotted toad, and canyon treefrog, had the strongest relationship with spatial (distance) and landscape factors (aquatic habitat and topography).

The species in these studies encompass a range of aquatic taxa spanning gradients of dispersal ability and habitat specificity. Trait databases characterizing the diverse assemblage of aquatic invertebrates in the Sky Islands region (e.g., Cañedo-Argüelles *et al.* 2015) may help infer population genetic structure for species with similar or intermediate trait values to those in this study. For example, the water scorpion (*Curicta pronotata*), water boatman (*Trichocorixa uhleri*), and predaceous diving beetle (*Rhantus atricolor*) are well-represented by the dispersal and water dependency traits of the three focal invertebrates in Phillipsen *et al*. (Figure 2.1).

Amphibian taxa such as the Great Plains toad (*Incilius alvarius*), Couch's spadefoot (*Scaphiopus couchii*), and Arizona treefrog (*Hyla wrightorum*) also fall along the same ecological strategies represented by amphibians in Mims *et al.*, and the inferred population genetic structure for the Great Plains toad and Couch's spadefoot (Figure 2.1) using this framework is supported by previous research (Chan and Zamudio 2009). Expansion of this framework to include traits such as habitat specificity, fecundity, trophic position, or others may help characterize species that are outliers along these two focal traits (e.g., Chiricahua leopard frog (*Lithobates chiricahuensis*) or barking frog (*Craugastor augusti*)).

2J. Tables

Table 2.1. Examples of management goals and considerations most relevant for different population genetic scenarios (isolated populations, isolation-by-distance, and panmixia).

Management goals	**Knowledge gaps and considerations**
Isolated populations	
- Identify unique and derivative populations - Prioritize conservation of populations with high genetic diversity - Identify populations at direct risk from low genetic diversity and its associated threats (e.g., inbreeding depression, mutational meltdown)	- Genetic drift obscures potential importance of landscape and local factors in population genetic attributes and connectivity - Distinguishing each population as an independent management unit may not be feasible or efficient
Isolation-by-distance or landscape	
- Implement metapopulation management strategies - Identify source populations and prioritize their conservation - Detect, maintain, and restore landscape corridors for population connectivity	- Genetic structure may not capture important contemporary landscape processes (e.g. land use change) due to temporal lag - Identifying "true" drivers among collinear landscape variables can be difficult
Panmixia	
- Determine whether management of individual units within panmictic group is necessary or effective in achieving goals - Manage for overall abundance on landscape	- High dispersal may obscure genetic signal of important local and landscape influences on demography - Panmictic neutral genetic variability may overlook important structure in adaptive genetic variance

2K. Figures

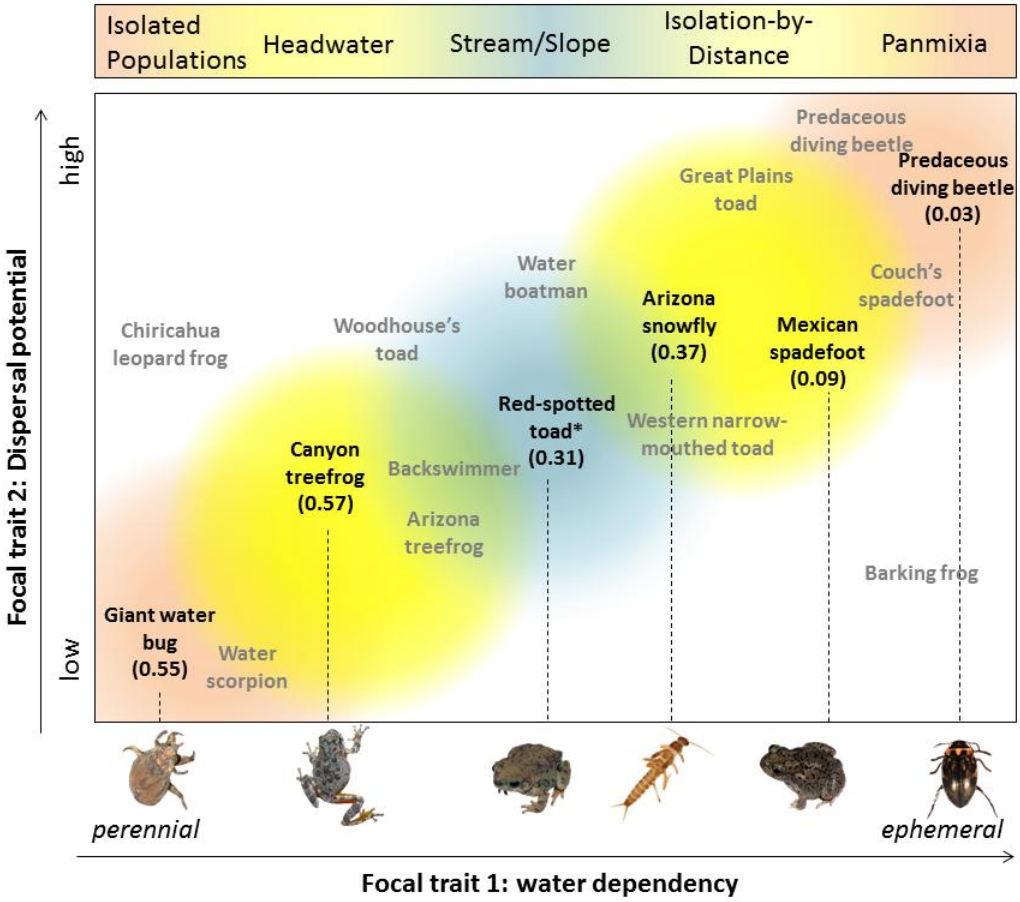

Figure 2.1. Population and landscape genetic structure along gradients of water dependency (focal trait 1: x-axis) and dispersal potential (focal trait 2: y-axis) to illustrate a traits-based multispecies inference framework. In this case, dispersal potential is a summary index comprising known dispersal distance, body size, and desiccation tolerance. Hypothesized models of population structure are shown as shaded circles with labels shown above the plot; more detail on these hypothesized models of population structure is available in Mims *et al*. (2015). Empirical results for six aquatic species – three anurans and three aquatic insects – are shown in black text within the plot and correspond to photos along the x-axis, connected by dashed line. Global G'_{ST}, a standardized value of genetic differentiation appropriate for comparison across species in which larger values indicate greater genetic differentiation (Hedrick 2005), is shown in parentheses below each study species. Additional aquatic species with distributions overlapping the six target taxa are shown in grey text according to their dispersal potential and water requirements. Common names are shown for all taxa. Red-spotted toads, marked with an asterisk (*), were also found to be panmictic in a subset of the study range; those results are not shown in this summary figure.

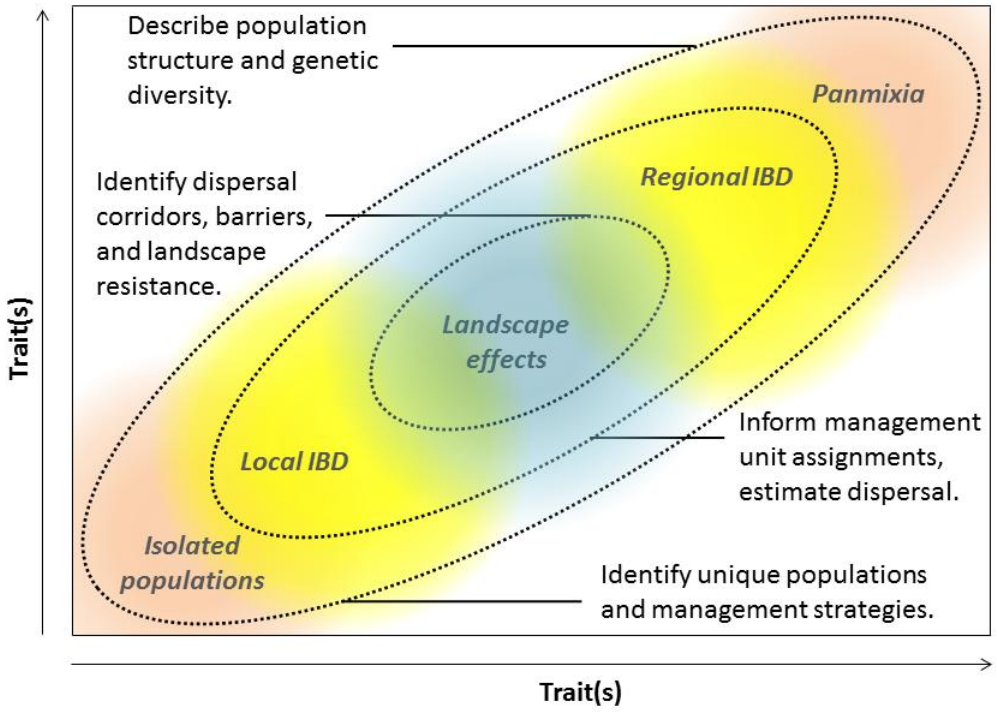

Figure 2.2. Population and landscape genetic structure along two focal trait axes. Models of population structure include, from lower left to upper right: isolated populations in which genetic drift dominates population structure ("Isolated populations" - red shading), genetically distinct groups of populations but local isolation-by-distance patterns ("Local IBD" - yellow shading), populations in which a landscape or environmental factor(s) drives population genetic structure ("Landscape effects" - blue shading), populations with isolation-by-distance structure throughout a region or species' range ("Regional IBD" - yellow shading), and panmictic populations ("Panmixia" - red shading). Regional and local isolation-by-distance patterns illustrate how the spatial scale of a study may reveal different population genetic patterns and processes. Nested ovals depict management-relevant information provided by population and landscape genetic approaches. For example, the outside oval encompasses all scenarios providing any baseline information on population structure and genetic diversity. The middle oval represents scenarios in which management units or dispersal ability may be informed. The central oval represents the core objectives of most landscape genetic studies – for example, to inform corridors and barriers to gene flow or estimate landscape resistance to dispersal.

Chapter 3: Significant differentiation, isolation-by-distance, and evidence of a metapopulation of the Arizona treefrog (*Hyla wrightorum*) in an isolated portion of its range

Authors: M.C. Mims, L. Hauser, J.D. Olden

3A. Abstract

Hyla wrightorum is an anuran native to the southwestern United States and Mexico, and a Distinct Population Segment (DPS) of the species exists in the Huachuca Mountains and Canelo Hills of southeastern Arizona, USA. Due to concerns about declining observations of the species within the DPS, its small geographic and isolated extent within the Huachuca Mountains and Canelo Hills, and presumably small population sizes, the DPS is currently a candidate for federal protection under the Endangered Species Act. Yet little is known about the status, connectivity, and genetic structure of populations within the Huachuca Mountains, which are critical components of planning for conservation efforts to promote the persistence of this anuran. We present results of a genetic study examining population diversity, structure, and connectivity within the Huachuca Mountains and Canelo Hills region of southeastern Arizona. We sampled DNA from *H. wrightorum* larvae and adults from 10 distinct locations, 8 of which were breeding sites and 4 of which were previously undescribed localities for the species. We developed and genotyped 17 polymorphic microsatellite loci and quantified genetic diversity, population differentiation, and influences of the landscape on population genetic structure. We found evidence of larger than expected effective population sizes, significant genetic differentiation between populations, and an isolation-by-distance pattern among populations. We found little

evidence of recent genetic bottlenecks, and individual-based analyses indicate gene flow between populations despite significant genetic differentiation. These patterns may indicate that the populations within the Huachuca Mountains constitute a metapopulation. We suggest that the DPS may be less vulnerable to extirpation than previously expected, but some small effective population sizes and the limited geographic extent of the DPS justify current concern for the persistence of this DPS. Efforts to ensure availability of high-quality breeding habitats and control for local threats such as predation by invasive predators may be critical to the persistence of this species within the Huachuca Mountains and Canelo Hills region.

Key words: dryland ecology, amphibians, Distinct Population Segment, conservation biology, Huachuca Mountains

3B. Introduction

Effective conservation of species vulnerable to extinction throughout some or all of their range requires knowledge of population attributes such as diversity, connectivity, and structure for successfully managing for long-term population viability (Williams et al. 2008). For decades, population genetic approaches have helped successfully identify scenarios that may compromise the health, resilience, or persistence of a species and its populations (Allendorf and Luikart 2007). Population genetic approaches have proven particularly useful in evaluating the status of amphibian species (Beebee 2005), many of which are declining globally due to a myriad of threats including habitat loss, invasive species, disease, and climate change (Stuart et al. 2004; Sodhi et al. 2009).

Hyla wrightorum, the Arizona treefrog, is an anuran native to the southwestern United States and Mexico, and it is currently a candidate species for federal protection by the U.S. Fish and Wildlife Service within a subset of its range (U.S. Fish and Wildlife Service 2013). *Hyla wrightorum* are most commonly associated with streams, cienegas (wetlands), and manmade ponds, particularly during the summer monsoon season when ephemeral or intermittent pools are used for breeding (Gergus 2000; Sredl et al. 2000). Its range includes three disjunct regions, with the majority of the species' range occurring in two disparate regions in the United States and in Mexico. Spatially intermediate to these two regions is an isolated portion of the species' range in the Huachuca Mountains and Canelo Hills region of southeastern Arizona, USA (Duellman 2001; Brennan and Holycross 2006). This distinct portion of the species' range is notable for its geographic isolation and for its phenotypic and genetic differentiation from the other two portions of the range (Gergus et al. 2004).

The *H. wrightorum* populations within the Huachuca Mountains and Canelo Hills region are of special conservation concern. In the past two decades, confirmed observations have been made at only half (8 of 16) of previously confirmed locations (Sredl et al. 2000; U.S. Fish and Wildlife Service 2013). The geographic range occupied by *H. wrightorum* in the Huachuca Mountains and Canelo Hills is small compared to the larger two portions of its distribution, with known breeding sites occurring within an area no larger than 8500 hectares. Based previous sampling efforts, population sizes within the Huachuca Mountains region are presumed to be small, with breeding choruses typically including 30 or fewer adults (Gergus 2000; U.S. Fish and Wildlife Service 2013). Potential threats to local persistence of this species include disease (Bradley et al. 2002) and predation by invasive American bullfrogs (*Lithobates catesbeianus*, Jones and Timmons 2010). In addition, available breeding habitat is believed to be scarce in the

region due to topographic constraints limiting suitable shallow breeding habitat (Gergus 2000). These factors contribute to concern regarding the vulnerability of these populations to regional processes such as dewatered habitat, catastrophic fires, and other manmade disturbances likely to increase in frequency and intensity with climate change and increasing human development (Westerling et al. 2006; Seager et al. 2007; Seager et al. 2012).

These concerns, coupled with the phenotypic, genetic, and geographic uniqueness of this group, have led to the designation of a Distinct Population Segment (DPS) of *H. wrightorum* in the Huachuca Mountains and Canelo Hills which is currently a candidate species for federal protection. Despite candidacy and concern for this species, the status of populations in this isolated range is generally unknown. It is difficult to determine whether apparent absences over the last two decades at roughly half of historical breeding sites are due to true declines, natural population fluctuations, or failure to detect the species. Because *H. wrightorum* may form breeding choruses only one or a few nights of the year, traditional census and survey efforts may fail to provide reliable information, particularly if populations are in fact in decline (Chadès et al. 2008). Genetic approaches provide promising alternatives to traditional census and survey efforts for evaluating population structure, size, and connectivity for many amphibians (Beebee 2005) and may offer valuable insight into the status of *H. wrightorum* in the Huachuca Mountains region.

We present results of a population genetic study for *H. wrightorum* in the Huachuca and Canelo Hills region of southeastern Arizona. The objectives of our study were to address current knowledge gaps regarding effective population sizes of this species, population genetic diversity and structure in the region, and whether spatial processes such as landscape attributes or distance affect population genetic structure. To achieve this, we used a combination of population-level

and individual-based approaches. Based on current knowledge of the species, we hypothesized small (< 30) effective population sizes for *H. wrightorum* in the Huachuca Mountains region. This was based on both small observed breeding choruses for this species (Gergus 2000; U.S. Fish and Wildlife Service 2013) as well as recent reported estimates of N_e for a sympatric congener (*H. arenicolor*, average $N_e = 30.7$, Mims et al. 2015). We also looked for evidence of any recent genetic bottlenecks. Finally, we tested five hypotheses regarding how spatial processes may influence gene flow. First, if populations are sufficiently small, genetic drift may result in complete decoupling of genetic structure and spatial processes, producing isolated populations. This has been observed for a pond breeding salamander sympatric to *H. wrightorum* in the Huachuca Mountains region (Storfer et al. 2014). Alternatively, an isolation-by-distance pattern may emerge in which closer populations have higher gene flow than those farther apart (Wright 1943). We also tested three additional hypotheses of landscape effects: isolation-by-slope, in which steep topography inhibits gene flow; connectivity-by-canopy, in which gene flow is higher along more shaded areas that may provide more cover from predation or desiccation; and connectivity-by-stream in which gene flow is higher along riparian corridors. Finally, we discuss how the findings of this research can help guide management and conservation efforts for this species.

3C. Methods

Amphibian sampling

Adult and larval *H. wrightorum* individuals were sampled during the summer monsoon season of 2014. We selected sampling locations using a combination of historical records of *H. wrightorum* occurrences as well as opportunistic visits to potentially suitable habitat (ponds and

wetlands) in the known range of the species. Sites were visited in the evenings, typically following thunderstorms, to maximize the chance of hearing breeding choruses. Sites were also visited during daylight hours when a combination of visual search and dip-netting were used to search for *H. wrightorum* larvae or adults near aquatic habitat. DNA was collected from each sampled individual via tail clip (larvae) or buccal swab (adult) (following Goldberg et al. 2003). Tail clips were immediately stored with a desiccant (Drierite), and buccal swabs were immediately placed in a vial with buffer ATL from a DNeasy Blood & Tissue DNA extraction kit (QIAGEN). Tail clips were then kept at room temperature and buccal swabs at -10°C until DNA was extracted.

DNA extraction, genotyping, and marker screening

Whole genomic DNA extractions were performed using DNeasy 96 Blood & Tissue Kit (QIAGEN) at the Molecular Ecology Research Lab at the University of Washington's School of Aquatic and Fishery Sciences. *Hyla wrightorum* microsatellite markers were developed by the Evolutionary Genetics Core Facility at Cornell University and are described in Table 3.A.1. Polymerase chain reaction (PCR) was used to amplify DNA for multiplexed loci using Multiplex PCR kits (QIAGEN). Primers for each loci in a multiplex set were combined in a primer mix that included a final concentration of 2μM of each primer. The volume for each PCR reaction was 10μl, consisting of 3μl water, 5μl multiplex master mix, 1μl primer mix, and 1μl DNA. PCR conditions followed QIAGEN guidelines and included an initial activation step of 15 minutes at 95°C, followed by 25 cycles through three steps: denaturation (30 seconds at 94°C), annealing (90 seconds at 60°C), and extension (90 seconds at 72°C). All PCR reactions were performed on C1000 Touch or S1000 thermal cyclers (Bio-RAD). PCR products were genotyped using

3730*xl* 96-Capillary Genetic Analyzer (Applied Biosystems) at Yale University's DNA Analysis Facility (New Haven, CT). Genotypes were analyzed using the software GENEMAPPER 4.1 (Applied Biosystems). Individuals with poor-quality genotype data were processed again through PCR and genotyping, and in a few cases DNA extractions were performed again provided sufficient tissue remained. Individuals with > 25% missing data after three genotyping attempts were discarded from downstream analyses.

Alleles were binned using the program TANDEM (Matschiner and Salzburger 2009). Any alleles occurring in < 3 individuals and > 1 repeat sequence from other alleles at the locus were confirmed by re-running the sample through PCR and genotyping. Loci were screened for the presence of linkage disequilibrium using the log likelihood ratio statistic for each pair of loci in each population (GenePop, Raymond and Rousset 1995). Loci were also screened for deviations from Hardy-Weinberg equilibrium (HWE) using the exact p-test as implemented in GenePop, and the presence of null alleles was evaluated with Micro-Checker (Van Oosterhout et al. 2004). All screening procedures were performed first using adults samples only (three populations) and then again with all population samples (adults and larvae) following full sibling removal (description follows).

Larval samples can bias population genetics findings by artificially inflating genetic differentiation due to family structure (Goldberg and Waits 2010); therefore, we screened all larval samples for full siblings using the program COLONY 2.0 (Jones and Wang 2009). Microsatellite loci were first screened for linkage disequilibrium or deviations from HWE using adult genotypes to identify any loci that may affect detection of siblings. When full siblings were detected, one sibling was retained from each family in the final dataset.

Genetic diversity and population structure

We calculated genetic diversity estimates of expected heterozygosity (H_E), observed heterozygosity (H_O), allelic richness (AR) rarified for the smallest number of sampled individuals per population and locus, and F_{IS} (Weir and Cockerham 1984). We also calculated two global measures of genetic differentiation, global F_{ST} (Weir and Cockerham 1984) and G'_{ST} (Hedrick 2005). We examined pairwise genetic distance (between each pair of sample sites) in two ways: D_{ps}, a method of measuring genetic differentiation based on proportion of shared alleles (Bowcock et al. 1994), and F_{ST} (Weir and Cockerham 1984) bootstrapped with 10,000 replicates to determine significance from zero. We used D_{ps} as the primary metric for genetic differentiation between populations because it based on allelic similarities and is not subject to equilibrium assumptions. We calculated genetic diversity, global genetic differentiation, and pairwise genetic differentiation metrics using MSA 4.05 (Dieringer and Schlötterer 2003). We also estimated effective population size (N_e) using the linkage disequilibrium method of Waples and Do (2008), as implemented in NeEstimator V2 (Do et al. 2014). Evidence of recent bottlenecks was evaluated using the program BOTTLENECK 1.2.02 (Piry et al. 1999). We performed a Wilcoxon signed rank test (10,000 iterations), which is appropriate for tests evaluating less than 20 loci (Piry et al. 1999), to determine if observed heterozygosity was higher than expected and indicated that a genetic bottleneck had occurred. We performed the test following four different mutation models: the infinite allele model (IAM), the strict one-step stepwise mutation model (SSM), and the two-phase model with 70% single step mutations and a variance among multiple steps of 30 (TPM70, program default) and with 95% single step mutations with a variance among multiple steps of 12 (TPM95, as recommended by Piry et al. (1999) for microsatellite loci). We also performed a mode-shift test to determine whether

distortion of the expected L-shape frequency distribution was detected and attributable to a recent bottleneck in any populations (Luikart et al. 1998).

To evaluate whether individuals sampled at a location likely originated from the local population, we used an individual assignment analysis as implemented in GeneClass2 (Piry et al. 2004). We used the Bayesian approach of Rannala and Mountain (1997) with 1,000 Monte Carlo-simulated individuals per sample. The designation of individuals as migrants was based on the likelihood of the individual genotype within the population where the individual was sampled (L_home), which is appropriate in cases where source populations may be missing from the samples (i.e., some populations may not have been sampled) (Piry et al. 2004). Individual-based hierarchical population structure was evaluated using the Bayesian clustering program STRUCTURE 2.3.4 (Pritchard et al. 2000). Each sampling site was treated as an independent putative population with a total of n putative populations. Ten iterations of each K from 1 to n + 1 were run for 500,000 cycles with a burn-in of 50,000 cycles. We incorporated sampling information using the LOCPRIOR model, and we allowed admixture and correlated allele frequencies. We determined the most likely K using the delta-K method (Evanno et al. 2005) in which the most likely value of K is assessed by the second-order rate of change in the log-likelihood. A delta-K value cannot be calculated for $K = 1$; thus, for cases in which $K = 1$ has the greatest log-likelihood, 1 is assumed to be the most likely K (Spear et al. 2012). This analysis was repeated for genetic clusters in which both $K > 1$ and $n > 1$ to identify hierarchical population structure until terminal clusters were described (Phillipsen and Lytle 2013). STRUCTURE output visualizations were constructed using the program DISTRUCT 1.1 (Rosenberg 2004).

Landscape genetic analysis

To evaluate possible landscape influences on population genetic structure, we first constructed four landscape connectivity surfaces using CIRCUITSCAPE (McRae 2006). CIRCUITSCAPE uses circuit theory to simulate gene flow (i.e., "current") through a resistance surface in which landscape features hypothesized to promote gene flow are assigned low resistances, and landscape features hypothesized to inhibit gene flow are assigned high resistances. CIRCUITSCAPE allows gene flow across multiple pathways and reports pairwise summations of resistance between sampling locations. Modeling multiple pathways is appropriate for dryland anurans with potentially high dispersal ability (Chan and Zamudio 2009; Mims et al. 2015). To generate pairwise resistance data, we built raster maps of resistance (low to high) using spatial data describing stream networks, canopy cover, and topography (slope). Four resistance surfaces were created to represent four simple models of landscape effects on gene flow: isolation-by-distance (uniform resistance across the landscape); isolation-by-slope (high resistance for steep regions, and low resistance across flat land), connectivity-by-canopy (low resistance with high canopy cover, high resistance in areas with low or no canopy), and connectivity-by-stream (low resistance along riparian corridors, defined as a 100 m buffer surrounding streams). All spatial data were obtained from publicly available sources and are described in detail in the Chapter 3 Appendix, Table 3.A.5. A geographic information system (ArcGIS 10.1, Environmental Systems Research Institute) was used to catalog and manipulate landscape data and generate resistance raster maps. Each resistance map was scaled for hypothesized landscape resistance to gene flow from 1 - 100 where 1 indicates low resistance and 100 indicates high resistance. The scale of resistance values was arbitrary and was designed to reflect hypothesized relationships between landscape features and genetic connectivity. All resistance surfaces were scaled to 30 m

resolution – the minimum resolution available for canopy cover (see Table 3.A.5). The spatial extent of resistance rasters ensured a buffer of at least 7 km from the edge of the raster to a given sample location. We selected a 7km buffer distance because 7km is the farthest nearest-neighbor distance between any sampling locations. With this grain and extent, we were able to perform all CIRCUITSCAPE analyses in the pairwise source/ground modeling mode and using a cell connection scheme of eight neighbors, allowing maximum freedom of current flow. Finally, we evaluated correlations between pairwise landscape resistances, reported these correlations in the Chapter 3Appendix (Table 3.A.6), and accounted for collinearity when relating landscape resistance to genetic distance.

We evaluated relationships between landscape resistance and population genetic differentiation (as measured by D_{ps}) in three ways. First, we first employed a causal modeling framework as implemented in Cushman et al. 2006. By calculating a series of Mantel tests (Mantel 1967) and partial Mantel tests, we assessed the relationship between each landscape resistance matrix and the genetic distance matrix while sequentially partialling out the influence of the other landscape resistance matrices. This approach is effective in identifying spurious correlations between genetic distance and landscape processes, particularly when landscape factors may be correlated (Cushman and Landguth 2010).

Second, we used multiple regression with distance matrices (MRDM) (Holzhauer et al. 2006, Balkenhol et al. 2009) as a complimentary method to evaluate relationships between genetic and landscape connectivity. MRDM evaluates relationships between one or many explanatory distance matrices and a response distance matrix and uses permutation to determine statistical significance of the overall model. MRDM also informs significance of each explanatory variable in a model, and those significance values can help elucidate drivers among correlated landscape

connectivity hypotheses. We first examined the global model with all four landscape resistances, and we then dropped factors according to significance (least significant dropped first) until only one factor remained. We inferred strength of model fit by evaluating overall R^2 and the significance of explanatory variables (pairwise landscape resistances) included in the model. We also evaluated the variance inflation factor of each predictor variable for models with multiple factors to screen for effects of collinearity. A variance inflation factor > 10 is considered a threshold at which collinearity of variables is problematic for interpreting model results (Kutner et al. 2004).

Finally, we also evaluated relationships between pairwise genetic distance and pairwise landscape resistances using a mixed-effects modeling approach (van Strien et al. 2012). Through mixed-effects modeling, explanatory variables (pairwise landscape resistances) are treated as fixed effects, and sampling locations are treated as random effects to account for non-independent values in distance matrices (Yang 2004). We evaluated model fit with the R^2_β statistic (Edwards et al. 2008) that compares a model with fixed and random effects (pairwise landscape distance or resistance and sampling location) to a null model with only the random effect (sampling location) and an intercept. Because no formal method of comparison has been developed or agreed upon for evaluating R^2_β values of different models, we compared R^2_β values to one another directly as is common to-date in studies using this approach (van Strien et al. 2012). All analyses were performed in R version 2.14.0 (R Development Core Team, 2012), using a modified version of lme4 (Bates et al. 2012) for mixed-effects modeling (van Strien et al. 2012), PBKRTEST (Halekoh and Højsgaard 2012) for R^2_β calculation as described in van Strien et al. (2012), and ecodist (Goslee and Urban 2007) for MRDM. We evaluated variance inflation factor using the linear form of each model with the R package "car" (Fox and Weisberg 2011).

3D. Results

We sampled *H. wrightorum* individuals at 10 locations for a total of N = 299 individuals sampled and genotyped, 82 of which were adults (Table 3.1, Figure 3.1). Four of the 10 sampling locations had no previous record of *H. wrightorum* presence (sites 2, 4, 5, and 10, Figure 3.2). Two locations had insufficient sample sizes for population-level analyses (populations 2 and 5); among the remaining 8 populations, the sample size mean was equal to 36.6, with a minimum of 19 and a maximum of 50. We identified 46 family groups among samples and retained only 1 full sibling from each, reducing the final sample size to a total of $N = 221$ (Table 3.2). Among the 8 populations with sufficient sample sizes for population level analyses, mean sample size was equal to 27.6, with a minimum of 19 and maximum of 40. Detailed information for sample size by population and with sibling adjustments is reported in Table 3.1.

All individuals were genotyped for 17 novel polymorphic microsatellite loci (Table 3.3; microsatellite loci described in Table 3.A.1). Genotyping failed for nine larval samples (not included in total sample size) in which individuals were missing > 25% genotype data despite multiple re-run attempts, in some cases with a second DNA extraction attempt. Some of these larvae were either very small when sampled or were found dead among live larvae and salvaged as voucher specimens. We suspect that species identification was incorrect for these individuals (in the case of very small larvae) or DNA was too degraded for successful genotyping (in the case of salvaged individuals). With a Bonferroni correction applied, we found only 5 instances of significant deviation from HWE (Table 3.A.2). Because these deviations occurred across five different loci and three different populations, we elected to retain all loci in our analyses. Significant LD for two markers pairs were found in only one of 8 populations each, and no

evidence of consistent LD was observed for any marker pair (Table 3.A.3). We also found no evidence of any null alleles.

Effective population size estimates averaged 116.7 individuals per population, with a minimum estimate of 32.5 and a maximum estimate of 277.9. Confidence intervals for N_e ranged from 23.1 to infinite values (Table 3.1). N_e estimates were lowest for Sites 8 and 10, where upper confidence intervals of N_e were < 100. In contrast, the largest estimate of N_e was for population 3, where N_e was estimated to be 277.9 individuals with an upper confidence interval of infinity. Observed heterozygosity averaged across all loci ranged from 0.647 (Site 4) to 0.695 (Site 7), and expected heterozygosity averaged across all loci ranged from 0.671 (Site 4) to 0.736 (Site 7). Allelic richness ranged from 5.47 (Site 4) to 6.24 (Site 8). Information for population and locus pairs, including observed heterozygosity, expected heterozygosity, allelic attributes, and F_{IS} are included in the Appendix, Table 3.A.2. We observed a negative relationship between N_e and F_{IS} (Figure 3.4, $R^2 = 0.71$), which may indicate some inbreeding in populations with smaller effective population sizes. Wilcoxon tests for bottlenecks found strong support for a bottleneck among individuals at Site 7 and modest support for a bottleneck in populations 6, 9, and 10, and mode-shift tests found no evidence of bottlenecks (Table 3.4).

Global genetic differentiation measures provided evidence for genetic structure among populations with values of $F_{ST} = 0.04$ and $G'_{ST} = 0.19$. Pairwise F_{ST} values were highly correlated with D_{ps} ($R^2 > 0.9$) and revealed significant different among populations, where 25 of 28 pairwise comparisons were significantly different from zero (F_{ST}, Bonferroni correction applied, Table 3.5). The three non-significant pairwise comparisons all involved Site 6, one of the most central sampling sites (Figure 3.1). Site 6 was not significantly different from Sites 1, 7 or 8.

Despite significant genetic differentiation between populations, the individual assignment test assigned 40% of individuals to populations other than their sampling location (Table 3.6). Exchange of individuals and some gene flow between populations was also evident in the Structure analyses which provided support for an isolation-by-distance pattern with hierarchical clustering for *H. wrightorum* (Figure 3.3). Support for $K = 2$ and $K = 3$ clusters across all individuals was very similar (Chapter 3 Appendix, Table 3.A.4). For both $K = 2$ and $K = 3$, we found support for a general shift from one group (blue, the dominant group for Sites 1, 2, 3, and 4) to a second group (orange, dominant for Sites 9 and 10). This pattern followed a north to south trend, with individuals from centrally located sites assigned to both clusters (Figure 3.3). In the $K = 3$ scenario, we identified a third genetic group within Site 10. Figure 3.3 shows both $K = 2$ and $K = 3$ for all individuals, and hierarchical results are shown for the $K = 3$ scenario. Hierarchical results for the alternate $K = 2$ scenario are included in the Chapter 3 Appendix (Table 3.A.4). At the secondary level (within major clusters identified across all individuals), we found support for separate genetic clusters in Sites 3 and 9. Sites 5, 6, 7 and 8 were ultimately grouped together with strongest support for K = 1. We found support for $K = 3$ clusters for the group encompassing Sites 1, 2, and 4; however, visual inspection of structure within this group does not support strong differentiation between populations but rather a possible isolation-by-distance pattern. Delta-*K* tables for all species and genetic clusters are included in the appendix (Table 3.A.4).

We found multiple lines of evidence that both distance and topography (slope) affect population structure. Of the four Mantel tests examining hypothesized relationships between spatial processes (Distance, Slope, Canopy, and Stream) and genetic distance (D_{ps}), only Distance was significantly related to D_{ps} (Mantel r = 0.50, p-value = 0.015) (Table 3.7). Distance

remained significantly related to D_{ps} in three partial Mantel tests controlling for Slope, Canopy, and Stream. Isolation-by-slope also had marginal support as a driver of genetic structure. Although the Mantel test did not find a significant relationship between D_{ps} and isolation-by-slope distances (Mantel r = 0.34, p-value = 0.123), partial Mantel tests reveal a significant relationship between Slope and D_{ps} when controlling for Distance and Canopy. Mantel tests provided little support for a relationship between either Canopy or Stream and D_{ps}. The only significant partial Mantel test for either of these processes was between Canopy and D_{ps} when controlling for Slope. However, we suspect this result could be due to collinearity between Canopy and Distance (Table 3.A.6).

Multiple regression with distance matrices provided the greatest support for a combined isolation-by-distance and isolation-by-slope model or, alternatively, a connectivity-by-canopy and isolation-by-slope model (Table 3.8). The variance inflation factors of the "global" model (Model 1) evaluated with all spatial distance matrices highlights the problematic collinearity between Distance and Canopy, where variance inflation factors were > 10 for Distance, Slope, and Canopy when Distance and Canopy were included in the same model. To address this, we evaluated two alternative models: one with Distance but not Canopy (Model 5), and with Canopy but not Distance (Model 8). In both of these scenarios, Stream was non-significant, and the models with the best support included Distance + Slope (Model 6) or Slope + Canopy (Model 9).

Finally, mixed-effects models provided the greatest support for the collective influence of Distance + Slope + Stream, or alternatively, Canopy + Slope + Stream (Table 3.9). Due to the correlation between Distance and Canopy and the high variance inflation factors associated with any MRDM models including both spatial factors, we did not include these two factors together in the same mixed-effects model. Among models with a single spatial factor, Distance had the

highest R^2_β value (0.278), followed by Canopy (0.220). In agreement with both the partial Mantel tests and multiple regression with distance matrices models, we also found support for a combined effect of Slope with other spatial factors, with a near two-fold increase in R^2_β values when Slope was combined with each of the other three spatial factors. R^2_β was the highest for the two "global" model alternatives incorporating Distance + Slope + Stream (R^2_β = 0.595), or Canopy + Slope + Stream (R^2_β = 0.631). In general, models that included Canopy outperformed those with Distance for mixed-effects models.

3E. Discussion

We found significant genetic structure and differentiation among populations of *H. wrightorum* in the Huachuca and Canelo Hills region of southeastern Arizona. Estimates of N_e were higher than expected, with some populations estimated to have effective population sizes well over 100. Despite significant genetic differentiation between most populations, we also found clear evidence of gene flow between sampling locations from individual-based approaches. Additionally, the influence of spatial processes on population structure was evident, with significant support for isolation-by-distance and some evidence of isolation-by-slope and possibly connectivity-by-canopy. Taken together, these results suggest that populations of *H. wrightorum* in the Huachuca Mountains may constitute a metapopulation in which the spatial and temporal variability of available breeding habitat may contribute to local extinctions, colonizations, and exchange of individuals (as is the case for many pond breeding amphibians; Marsh and Trenham 2001).

Our results suggest that previous assumptions of consistently small population sizes, with estimates near or below 30 individuals (U.S. Fish and Wildlife Service 2013), likely

underestimate the population sizes of this species. We found that N_e for *H. wrightorum*, which averaged 116.7 individuals across populations, is larger than two sympatric anurans, *H. arenicolor* (average N_e = 30.7) and *Anaxyrus punctatus* (average N_e = 83.0), reported in Mims et al. (2015). N_e estimates the size of an idealized population that would lose heterozygosity at the same rate of the observed population, and N_e is typically smaller than a population's census size, or N_c. In the case of our study in which samples are collected for one year, our N_e estimates more closely approximate the number of breeding adults (N_b) in 2014. N_b may fluctuate internannually due to natural population dynamics or environmental factors, and the N_e values reported here should be considered in the context of this uncertainty. Future analyses of N_b or N_e for this species may be useful in monitoring the stability of this species over time (Whitley et al. 2015).

For highly fecund species or r-selected species, such as amphibians, "sweepstakes" recruiting may result in a N_e / N_c ratio that is quite low (Hedrick 2005). Thus, it is likely that N_c of *H. wrightorum* populations in the study region are larger than the estimated N_e values reported here. Still, concern regarding the size of *H. wrightorum* populations in the region may be warranted. N_e was less than 100 for half the populations we sampled, and the 95% confidence interval of N_e included values < 100 for all populations, as is typical for many pond breeding amphibians (Beebee and Griffiths 2005). N_e < 100 may indicate these populations are at risk of genetic depletion due to genetic drift and/or inbreeding (Beebee 2005), particularly if gene flow is sufficiently low. The negative relationship between N_e and F_{IS} indicates that inbreeding may indeed be occurring in the smallest populations.

Significant pairwise F_{ST} comparisons as well as evidence of hierarchical structure among populations indicate considerable, but not complete, genetic differentiation between populations, with a significant influence of spatial processes. Individual-based cluster analyses of *H.*

wrightorum most strongly supported a predominant pattern of isolation-by-distance. Additional hierarchical analyses reveal some genetic clusters having strong associations with a certain locality (Sites 3, 9, and 10), but in two of these three cases a high degree of heterogeneity in assignment of individuals to clusters were observed (Sites 9 and 10). Gene flow between sites was also supported with the assignment test results. In cases of more complete genetic isolation, we might expect to see near-perfect correlation of cluster assignments with sampling location, as observed in the one of the region's macroinvertebrates, the perennial specialist *Abedus herberti* (Phillipsen and Lytle 2013).

Our findings suggest limited but not completely restricted gene flow between populations of *H. wrightorum*. This is in contrast to some other sympatric pond-breeding anurans found to have panmictic population structure across similar spatial scales (Mims et al. 2015, Chan and Zamudio 2009). However, the pond-breeding anurans in those studies are likely more desiccation tolerant, more mobile, have higher fecundity, and are able to better utilize more ephemeral breeding ponds due to short larval periods (i.e., one- to three-week larval periods for species with the lowest larval requirements versus one to a few months for hylids in the region) (Zweifel 1961, Stebbins 2003). These life history differences may explain the greater genetic differentiation observed for *H. wrightorum* in this study. In contrast, Storfer et al. (2014) report much greater genetic differentiation among populations of an endangered pond breeding salamander, *Ambystoma mavortium stebbinsi*, in the San Rafael Valley and foothills of the Huachuca Mountains and Canelo Hills. They found no support for isolation-by-distance among populations and instead found evidence that genetic drift and small population sizes are responsible for high levels of genetic differentiation among populations. We found that *H. wrightorum* population structure was most similar to *H. arenicolor* in the Huachuca Mountains

(Mims et al. 2015), a predominantly stream-dwelling amphibian and *H. wrightorum*'s only congener in the region.

Finally, our analyses comparing the relationship between genetic distance and spatial factors of distance, slope, canopy, and stream provide additional support for the role of spatial processes in the genetic structure we observed. Our goal with these simple landscape genetic analyses was to test for the presence of spatial processes, which we confirmed. Taken together, we found strong support for physical distance as a driver of genetic structure as well as topography, indicating that populations closer together have greater gene flow, and those separated larger distance and/or higher slope areas are likely to be more isolated. Though we found little evidence for gene flow along stream corridors, our analyses provide marginal support for the role of canopy cover as a corridor for gene flow. Correlation between canopy cover and distance highlights the difficulty of interpreting collinear landscape distances and raises concerns about spurious correlations (Cushman and Landguth 2010); however, our use of Mantel and partial Mantel tests in a causal framework (Cushman et al. 2006) provides strong support for distance as the most likely factor affecting gene flow. Another important note is that although we did not detect an influence of streams or a strong influence of canopy cover in this study, the study region receives considerable precipitation during most summers and has reasonable canopy cover throughout this portion of the species range. If favorable landscapes (i.e., those that promote gene flow) occur at a high density on the landscape, detecting their influence can be difficult using genetic approaches (Cushman et al. 2013). Thus, these findings do not rule out the possible important role of these corridors in connecting populations.

The discovery of previously unknown breeding sites for this species as part of this research effort supports two alternative hypotheses for why this species has not been observed at

historical sites over the last few decades. First, previous survey efforts may simply have missed active breeding sites due to spatial or temporal mismatches between survey efforts and breeding activity. Alternatively, natural population fluctuations or metapopulation dynamics may account for the absence of this species at historical breeding sites and the discovery of the species at new sites over the last two decades. Over the course of an intensive 3-week field season in 2014, we found *H. wrightorum* in 4 new locations (Sites 2, 4, 5, and 10). Site 4 is a confirmed breeding site (larvae present), and Site 10 is a presumed breeding site (> 20 adults sampled in a breeding chorus). Site 10 extends the known range of contiguous breeding sites in the Huachuca Mountains southeast by roughly 7km. Additionally, limited observations of *H. wrightorum* have been reported at a small number of wetland habitats at Rancho Los Fresnos, Sonora, Mexico, south of the Huachuca Mountains (U.S. Fish and Wildlife Service 2013). The Los Fresnos population is presumed to be small and is typically described as an "outlier" from the Huachuca and Canelo Hills populations due to its isolation and distance from other known breeding sites in the Huachuca Mountains. However, the newly discovered Site 10 is approximately intermediate in distance between Los Fresnos and previously described breeding sites, representing a significant reduction in the spatial gap between these sites. In general, the discovery of new sites during this study supports the hypotheses that these populations exist within a metapopulation in the region, or alternatively that more intensive survey efforts are required for detection of this species. In either case, continued survey efforts exploring additional plausible breeding sites within the region are recommended. For example, within a 7km buffered area encompassing all sites in this study, > 90 ponds with intermediate hydroperiods were identified using satellite imagery (M. C. Mims, *unpublished data*). Many of these ponds were not visited in 2014 due to logistical and time constraints and have not been surveyed for this species. *Hyla wrightorum* are

thought to prefer or require emergent vegetation in breeding habitat (Gergus 2000), and they likely avoid ponds with predatory or competitive species present (Collins 1994). These two criteria alone may exclude many of the intermittent ponds within 7 km of known breeding sites; however, specific habitat associations and requirements of *H. wrightorum* remain uncertain. Additional survey efforts aimed at detecting this species and refining knowledge of suitable breeding habitat will be critical in identifying other potential breeding sites for this Distinct Population Segment and for optimal management of known breeding sites (Rosen and Schwalbe 1998).

In conclusion, we found evidence of larger than expected effective population sizes, significant genetic differentiation but not complete genetic isolation between populations, and evidence of spatial processes contributing to the genetic structure of *H. wrightorum* in the Huachuca Mountains and Canelo Hills region. Despite higher than expected N_e and genetic connectivity, concern for this species within the DPS is warranted. Predation by the invasive American bullfrog (*Lithobates catesbeianus*) could significantly reduce the number of adults at breeding ponds – particularly if choruses of *H. wrightorum* are small (Jones and Timmons 2010). Chytridiomycosis, a disease associated with the decline and/or extinction of many amphibians worldwide (Berger et al. 1998), is documented in the region (Arizona Game and Fish Department 2006) and is known to infect *H. wrightorum* (Sredl et al. 2003), although the effects on this species are not currently known. On a regional scale, climate change will likely bring drier conditions to the southwestern United States (Seager et al. 2007) with the possibility of spatial and temporal reduction in aquatic breeding habitat as well as changes in disease dynamics (Pounds et al. 2006). Shifts in climate along with other human modifications to the landscape will also likely result in larger and more intense wildfires in the region (Westerling et al. 2006).

Such fires are often accompanied by major flooding and erosion events that can scour or fill breeding sites with sediment. We suggest continued survey efforts to determine occupancy of breeding habitats by *H. wrightorum*, and we suggest additional research aimed at quantifying both the habitat requirements of and threats to this species to characterize suitable breeding habitat. Such efforts will help inform efficient and effective management of intermittent ponds within the Huachuca Mountains and Canelo hills to promote the persistence and continued connectivity of *H. wrightorum* populations within the region.

3F. Acknowledgements

We would like to extend our sincerest gratitude to the following funding sources and people for making this work possible. Funding for this research was provided by the Hall Conservation Genetics Graduate Research Award at the University of Washington's College of the Environment and through the U.S. Army Award Number W9214A-14-P-0048. Debbie Brewer (US Army, Fort Huachuca), Sheridan Stone (US Army, Fort Huachuca), John Kraft (US Forest Service), and Tom Jones (Arizona Game and Fish Department) all provided logistical and planning support for this work. Caren Goldberg, Katherine Strickler, Kody Cochrell, Trevor Eakes, and Jessica Hale assisted in fieldwork and sampling.

3G. References

Allendorf F, Luikart G (2007) Conservation and the genetics of populations. Blackwell Publishing, Malden MA

Arizona Game and Fish Department (2006) *Rana subaquavocalis*. Unpublished abstract compiled and edited by the Heritage Data Management System. Phoenix, AZ

Balkenhol N, Waits LP, Dezzani RJ (2009) Statistical approaches in landscape genetics: an evaluation of methods for linking landscape and genetic data. Ecography 32:818–830

Bates D, Maechler M, Bolker B, Walker S (2012) lme4: Linear mixed-effects models using Eigen and S4. R package version 1.1-7. http://CRAN.R-project.org/package=lme4

Beebee TJC (2005) Conservation genetics of amphibians. Heredity 95:423–427

Beebee TJC, Griffiths RA (2005) The amphibian decline crisis: a watershed for conservation biology? Biol Conserv 125:271–285

Berger L, Speare R, Daszak P, et al (1998) Chytridiomycosis causes amphibian mortality associated with population declines in the rain forests of Australia and Central America. Proc Natl Acad Sci 95:9031–9036

Bowcock AM, Ruiz-Linares A, Tomfohrde J, et al (1994) High resolution human evolutionary trees with polymorphic microsatellites. Nature 368:455–457

Bradley GA, Rosen PC, Sredl MJ, et al (2002) Chytridiomycosis in native Arizona frogs. J Wildl Dis 38:206–212

Brennan TC, Holycross AT (2006) A field guide to amphibians and reptiles in Arizona. Arizona Game and Fish Department, Phoenix, Arizona

Chadès I, McDonald-Madden E, McCarthy MA, et al (2008) When to stop managing or surveying cryptic threatened species. Proc Natl Acad Sci 105:13936–13940

Chan LM, Zamudio KR (2009) Population differentiation of temperate amphibians in unpredictable environments. Mol Ecol 18:3185–3200

Collins JP (1994) Final report: a status of three species of endangered/sensitive amphibians in Arizona. Report to the Arizona Game and Fish Department, Heritage Fund IIPAM #I92014. Phoenix, Arizona

Cushman SA, McKelvey KS, Hayden J, Schwartz MK (2006) Gene flow in complex landscapes: testing multiple hypotheses with causal modeling. Am Nat 168:486–499

Cushman SA, Landguth EL (2010) Spurious correlations and inference in landscape genetics. Mol Ecol 19:3592–3602

Cushman SA, Shirk AJ, Landguth EL (2013) Landscape genetics and limiting factors. Conserv Genet 14:263–274

Dieringer D, Schlötterer C (2003) Microsatellite analyser (MSA): a platform independent analysis tool for large microsatellite data sets. Mol Ecol Notes 3:167–169

Do C, Waples RS, Peel D, et al (2014) NeEstimator v2: re-implementation of software for the estimation of contemporary effective population size (N_e) from genetic data. Mol Ecol Resour 14:209–214

Duellman WE (2001) The Hylid frogs of Middle America. Society for the Study of Amphibians and Reptiles, St. Louis, MO

Edwards LJ, Muller KE, Wolfinger RD, et al (2008) An R^2 statistic for fixed effects in the linear mixed model. Stat Med 27:6137–6157

Evanno G, Regnaut S, Goudet J (2005) Detecting the number of clusters of individuals using the software STRUCTURE: a simulation study. Mol Ecol 14:2611–20

Fox J, Weisberg S (2011) An R companion to applied regression, second edition. Thousand Oaks CA: Sage. URL: http://socserv.socsci.mcmaster.ca/jfox/Books/Companion
Gergus EWA (2000) Demography, population genetics, and systematics of Huachuca tree frogs (*Hyla wrightorum*): taxonomic and conservation implications. Arizona Game and Fish Department Heritage Grant Project #I96047, IIPAM Project Report. Tempe, AZ
Gergus EWA, Reeder TW, Sullivan BK (2004) Geographic variation in *Hyla wrightorum*: advertisement calls, allozymes, mtDNA, and morphology. Copeia 2004:758–769
Goldberg CS, Kaplan ME, Schwalbe CR (2003) From the frog's mouth: buccal swabs for collection of DNA from amphibians. Herpetol Rev 34:220–221
Goldberg CS, Waits LP (2010) Quantification and reduction of bias from sampling larvae to infer population and landscape genetic structure. Mol Ecol Resour 10:304–313
Goslee SC, Urban DL (2007) The ecodist package for dissimilarity-based analysis of ecological data. J Stat Software 22:1–19
Halekoh U, Højsgaard S (2012) PBKRTEST: parametric bootstrap and Kenward Roger based methods for mixed model comparison. R package version 0.3-2. http://CRAN.R-project.org/package=pbkrtest
Hedrick PW (2005) A standardized genetic differentiation measure. Evolution 59:1633–1638
Hedrick PW (2005b) Large variance in reproductive success and the N_e/N ratio. Evolution 59 1596–1599
Holzhauer SIJ, Ekschmitt K, Sander A, et al (2006) Effect of historic landscape change on the genetic structure of the bush-cricket Metrioptera roeseli. Landsc Ecol 21:891–899
Jones O, Wang J (2009) COLONY: a program for parentage and sibling inference from multilocus genotype data. Mol Ecol Resour 10:551–555
Jones TR, Timmons RJ (2010) *Hyla wrightorum* (Arizona treefrog): predation. Herpetol Rev 41:473–474
Kutner M, Nachsheim C, Netter J (2004) Applied linear regression models. McGraw-Hill, New York, NY
Luikart G, Allendorf FW, Cornuet JM, Sherwin WB (1998) Distortion of allele frequency distributions provides a test for recent population bottlenecks. J Hered 89:238–247
Mantel N (1967) The detection of disease clustering and a generalized regression approach. Cancer Research 27:209–220
Marsh DM, Trenham PC (2001) Metapopulation dynamics and amphibian conservation. Cons Bio 15:40–49
Matschiner M, Salzburger W (2009) TANDEM: integrating automated allele binning into genetics and genomics workflows. Bioinformatics 25:1982–3
McRae BH (2006) Isolation by resistance. Evolution 60:1551–1561
Mims MC, Phillipsen IC, Lytle DA, et al (2015) Ecological strategies predict associations between aquatic and genetic connectivity for dryland amphibians. 96:1371–1382
Phillipsen IC, Lytle DA (2013) Aquatic insects in a sea of desert: population genetic structure is shaped by limited dispersal in a naturally fragmented landscape. Ecography 36:731–743
Piry S, Alapetite A, Corneut JM, Paetkau D, Baudouin L, Estoup A (2004) GENECLASS2: A software for genetic assignment and first-generation migrant detection. J Hered 95:536–539
Piry S, Luikart G, Cornuet JM (1999) BOTTLENECK: a computer program for detecting recent reductions in the effective population size using allele frequency data. J Hered 90:502–503
Pounds JA, Bustamante MR, Coloma LA, et al (2006) Widespread amphibian extinctions from epidemic disease driven by global warming. Nature 439:161–167

Pritchard JK, Stephens M, Donnelly P (2000) Inference of population structure using multilocus genotype data. Genetics 155:945–59
Rannala B, Mountain JL (1997) Detecting immigration by using multilocus genotypes. Proc Natl Acad Sci USA 94:9197–9201
Raymond M, Rousset F (1995) GENEPOP (version 1.2): population genetics software for exact tests and ecumenicism. J Hered 86:248–249
Rosen PC, Schwalbe CR (1998) Using managed waters for conservation of threatened frogs *in* Environmental, economic, and legal issues related to rangeland water developments. Arizona State University, College of Law, Tempe, AZ, pp 180–202
Rosenberg NA (2004) Distruct: a program for the graphical display of population structure. Mol Ecol Notes 4:137–138
Seager R, Ting M, Held I, et al (2007) Model projections of an imminent transition to a more arid climate in southwestern North America. Science 316:1181–1184
Seager R, Ting M, Li C, et al (2012) Projections of declining surface-water availability for the southwestern United States. Nat Clim Chang 3:482–486
Sodhi NS, Bickford D, Diesmos AC, et al (2009) Measuring the meltdown: drivers of global amphibian extinction and decline. PLoS one 3:e1636
Spear SF, Crisafulli CM, Storfer A (2012) Genetic structure among coastal tailed frog populations at Mount St. Helens is moderated by post-disturbance management. Ecol Appl 22:856–869
Sredl MJ, Field KJ, Peterson AM (2003) Understanding and mitigating effects of Chytrid fungus to amphibian populations in Arizona. Phoenix, AZ
Sredl MJ, Wallace JE, Miera V (2000) Aquatic herpetofauna inventory of Fort Huachuca and vicinity. Phoenix, Arizona
Stebbins, R (2003) Western reptiles and amphibians. Houghton Mifflin. Singapore
Storfer A, Mech SG, Reudink MW, Lew K (2014) Inbreeding and strong population subdivision in an endangered salamander. Conserv Genet 15:137–151
Stuart SN, Chanson JS, Cox NA, et al (2004) Status and trends of amphibian declines and extinctions worldwide. Science 306:1783–1736
U.S. Fish and Wildlife (2013) U.S. Fish and Wildlife Service species assessment and listing assignment form: *Hyla wrightorum*. 36 pp
Van Oosterhout C, Hutchinson WF, Wills DPM, Shipley P (2004) MICRO-CHECKER: software for identifying and correcting genotyping errors in microsatellite data. Mol Ecol Notes 4:535–538
Van Strien MJ, Keller D, Holderegger R (2012) A new analytical approach to landscape genetic modelling: least-cost transect analysis and linear mixed models. Mol Ecol 21:4010–4023
Waples R, Do C (2008) LDNE: a program for estimating effective population size from data on linkage disequilibrium. Mol Ecol 8:753–756
Weir BS, Cockerham CC (1984) Estimating F-statistics for the analysis of population structure. Evolution 38:1358–1370
Westerling AL, Hidalgo HG, Cayan DR, Swetnam TW (2006) Warming and earlier spring increase western U.S. forest wildfire activity. Science 313:940–943
Whiteley AR, Coombs JA, Cembrola M, et al (2015) Effective number of breeders provides a link between interannual variation in stream flow and individual reproductive contribution in a stream salmonid. Mol Ecol, in press

Williams SE, Shoo LP, Isaac JL, Hoffmann AA, Langham G (2008) Towards an integrated framework for assessing the vulnerability of species to climate change. PloS Biology 6:e325
Wright, S (1943) Isolation by distance. Genetics 28:114–138
Yang RC (2004) A likelihood-based approach to estimating and testing for isolation by distance. Evolution 58:1839–1845
Zweifel R (1961) Larval development of the treefrogs *Hyla arenicolor* and *Hyla wrightorum*. American Museum Novitates 2056:1–20

3H. Tables

Table 3.1. Population number (Pop), population sampling size as total number of individuals samples (N_{total} = all individuals; N_{adults} = adults sampled; N_{larvae} = larvae sampled), and as corrected for family structure with full siblings removed (N_{larvae} = number larval samples retained after removing all but one full sibling from family groups; N_{total} = total sample size after removing all but one full sibling from family groups), and genetic diversity metrics including observed heterozygosity (H_o) expected heterozygosity (H_e), allelic richness (AR) corrected for smallest sample size, effective population size estimate (N_e) and a 95% confidence interval of N_e ($N_{e, low}$ and $N_{e, high}$) as estimated using a jackknifing approach. "*Inf.*" indicates infinite upper confidence intervals for N_e. Note that Populations 2 and 5 were not included in population genetic analyses due to small sample sizes.

Pop	Sample size			Sample size, siblings removed		Genetic diversity					
	N_{total}	N_{adults}	N_{larvae}	N_{larvae}	N_{total}	H_o	H_e	AR	N_e	$N_{e, low}$	$N_{e, high}$
1	19	19	0	0	19	0.69	0.73	6.1	140.5	54.6	*Inf.*
3	43	0	43	30	30	0.67	0.69	5.8	277.9	88.0	*Inf.*
4	48	0	48	23	23	0.65	0.67	5.5	79.0	36.5	7999.7
6	34	6	28	14	20	0.69	0.73	6.0	51.7	31.4	120.0
7	50	0	50	37	37	0.70	0.74	5.7	109.1	56.8	526.0
8	28	0	28	24	24	0.66	0.71	6.2	43.3	29.4	74.9
9	49	29	20	11	40	0.69	0.68	5.5	199.2	65.8	415.3
10	22	22	0	0	22	0.67	0.74	6.2	32.5	23.1	50.4
2	5	5	0	0	5	-	-	-	-	-	-
5	1	1	0	0	1	-	-	-	-	-	-

Table 3.2. Summary of COLONY results for family structure identification. Sampling location number (Pop) for sites at which larvae were sampled, number of families identified, mean family size, and maximum number of siblings within a family are shown.

Pop	$N_{families}$	Mean family size	Max N_{sibs}
3	30	1.43	7
4	23	2.09	5
6	20	1.70	6
7	37	1.35	3
8	24	1.17	2
9	40	1.23	3

Table 3.3. Attributes of each of 17 microsatellite loci. Allelic richness was computed using the minimum sample number (smallest population minus missing data) for each locus. Additional information, including attributes by population and results of Hardy-Weinberg equilibrium testing, linkage equilibrium, and null allele screening are included in the Appendix.

Locus	H_e	H_o	Allelic attributes			
			Min	Mean	Max	Richness
Hwri1316	0.742	0.744	157	214.93	237	5.99
Hwri1422	0.762	0.656	188	200.06	212	5.66
Hwri2688	0.677	0.646	236	262.07	272	5.54
Hwri2932	0.627	0.637	200	209.00	224	5.53
Hwri3318	0.783	0.802	250	259.77	274	6.72
Hwri4093	0.634	0.570	145	160.17	169	5.10
Hwri4269	0.452	0.429	152	154.64	172	3.70
Hwri4370	0.829	0.798	177	244.82	269	10.14
Hwri10374	0.722	0.637	321	328.64	341	5.14
Hwri12115	0.860	0.843	186	227.02	270	10.89
Hwri16672	0.719	0.764	177	195.06	265	6.91
Hwri20812	0.818	0.816	296	340.12	376	8.40
Hwri23452	0.620	0.591	155	169.05	175	4.24
Hwri29495	0.778	0.754	257	280.89	305	6.61
Hwri30215	0.695	0.634	303	311.02	327	5.55
Hwri30594	0.719	0.548	233	245.13	265	6.02
Hwri34484	0.650	0.636	135	142.00	163	4.88

Table 3.4. Results (P-values) of the five bottleneck tests. The first four columns show results of a Wilcoxon sign rank tests (10,000 iterations) following four different mutation models: the infinite allele model (IAM), the strict one-step stepwise mutation model (SSM), and the two-phase model with 70% single step mutations and a variance among multiple steps of 30 (TPM_{70}, program default) and with 95% single step mutations with a variance among multiple steps of 12 (TPM_{95}, as recommended by Piry et al. (1999) for microsatellite loci). Mode-shift test results with a dash (-) indicate a normal L-shaped mode. Results are based on 17 microsatellites and 8 populations of *H. wrightorum*.

Pop	IAM	SSM	TPM_{70}	TPM_{95}	Mode-shift
1	**<0.001**	0.661	0.087	0.537	-
3	**0.001**	0.960	0.122	0.878	-
4	**<0.001**	0.888	0.066	0.627	-
6	**<0.001**	0.555	**0.005**	0.229	-
7	**<0.001**	0.322	**<0.001**	**0.036**	-
8	**0.008**	0.951	0.259	0.934	-
9	**<0.001**	0.798	**0.032**	0.555	-
10	**<0.001**	0.678	**0.008**	0.322	-

Table 3.5. GeneClass2 results for individual genetic assignment of *H. wrightorum.* Table includes sample location (Pop), sample size (*N*), assigned population number, and total individuals assigned to locations other than their sampling location (Total). Underlined values represent individuals assigned to their sampling location. Empty cells indicate value of zero.

		Assigned population								
Pop	*N*	1	3	4	6	7	8	9	10	Total
1	19	9	1	3	1	2		1	2	10
3	30	2	21	3	1	2	1			9
4	23	2	2	16	1	1		1		7
6	20	2		4	7	3	1	3		13
7	37	1		1	4	18	4	8	1	19
8	24	1	3		3	1	12	4		12
9	40	1	1		2	2		32	2	8
10	22	2		1	1		1	3	14	8

Table 3.6. Results for Mantel and partial Mantel tests in a causal modeling framework to examine relationships between the distance matrices of D_{ps} (proportion shared alleles) with four spatial distance matrices derived from the resistance surfaces representing isolation-by-distance, isolation-by-slope, connectivity-by-canopy, and connectivity-by-stream for *H. wrightorum*. Mantel r and associated p-values are shown for each analysis.

	Distance		Slope		Canopy		Stream	
	r	p-value	r	p-value	r	p-value	r	p-value
Mantel	0.50	0.015	0.34	0.123	0.21	0.249	0.17	0.291
partial Mantel, controlled for:								
Distance	-	-	0.42	0.082	-0.30	0.836	0.15	0.312
Slope	0.55	0.012	-	-	0.62	0.008	0.17	0.327
Canopy	0.53	0.005	0.65	0.003	-	-	0.17	0.295
Stream	0.50	0.034	0.38	0.140	0.21	0.263	-	-

Table 3.7. Pairwise F_{ST} values (top, upper diagonal) with p-values (lower diagonal) obtained after 10,000 permutations. Population numbers are included at top of columns and left of rows, and F_{ST} values found non-significant after a Bonferroni correction are shown in bold. Proportion of shared alleles, D_{ps}, is also shown (bottom, lower diagonal).

F_{ST}	1	3	4	6	7	8	9	10
1		0.0342	0.0245	**0.0136**	0.0247	0.0396	0.0621	0.0382
3	0.0001		0.0348	0.0357	0.0464	0.0585	0.0891	0.0883
4	0.0007	0.0001		0.0218	0.0362	0.0527	0.0670	0.0749
6	**0.0112**	0.0001	0.0003		**0.0086**	**0.0151**	0.0345	0.0292
7	0.0001	0.0001	0.0001	**0.0297**		0.0212	0.0291	0.0382
8	0.0001	0.0001	0.0001	**0.0051**	0.0001		0.0301	0.0390
9	0.0001	0.0001	0.0001	0.0001	0.0001	0.0001		0.0444
10	0.0001	0.0001	0.0001	0.0001	0.0001	0.0001	0.0001	

D_{ps}	1	3	4	6	7	8	9	10
3	0.278							
4	0.256	0.275						
6	0.237	0.286	0.249					
7	0.249	0.293	0.277	0.212				
8	0.302	0.315	0.311	0.244	0.240			
9	0.333	0.380	0.330	0.269	0.246	0.253		
10	0.309	0.392	0.370	0.277	0.303	0.307	0.283	

Table 3.8. Results of mixed-effects models (MEM) for evaluating relationships between genetic distance (D_{ps}) and landscape resistances. Spatial data are described in full in the Appendix. Canopy and Distance were not included in the same models due to high collinearity (see Appendix for correlations between distance matrices). All R^2_β correlation coefficients are positive.

Landscape resistance model	R^2_β
Isolation-by-distance (Distance)	0.278
Isolation-by-slope (Slope)	0.220
Connectivity-by-canopy (Canopy)	0.182
Connectivity-by-stream (Stream)	0.167
Distance + Slope	0.506
Canopy + Slope	0.552
Stream + Slope	0.469
Distance + Slope + Stream	0.595
Canopy + Slope + Stream	0.631

Table 3.9. Results for multiple regression with distance matrices for *H. wrightorum*. Genetic distance matrix included pairwise D_{ps} values. R^2 and p-values generated from permutation tests are shown for the overall model, and p-values (p-val), correlations (cor), and variance inflation factors (vif) are shown for each factor in a given model. Due to high collinearity between Distance and Canopy (as evidenced by high vif values), models were also compared for all except Canopy or all except Distance. Models for which all factors are significant and with the highest total R^2 were selected as the best model for a group (in bold).

	Distance			Slope			Canopy			Stream			Total	
	p-val	cor	vif	p-val	cor	vif	p-val	cor	vif	p-val	cor	vif	R^2	p-val
1	0.401	-	16.3	0.120	+	12.3	0.195	+	28.7	0.567	0.57	1.0	0.51	0.124
2	0.429	-	16.1	0.112	+	12.2	0.206	+	28.5				0.49	0.044
3				**0.002**	**+**	**1.7**	**0.022**	**+**	**1.7**				**0.45**	**0.021**
4				0.272	+								0.12	0.272
	Distance			Slope						Stream			Total	
	p-val	cor	vif	p-val	cor	vif				p-val	cor	vif	R^2	p-val
5	0.035	+	1.0	0.203	+	1.0				0.664	+	1.0	0.40	0.17
6	**0.018**	**+**	**1.0**	**0.170**	**+**	**1.0**							**0.38**	**0.05**
7	**0.034**	**+**											**0.25**	**0.03**
				Slope			Canopy			Stream			Total	
				p-val	cor	vif	p-val	cor	vif	p-val	cor	vif	R^2	p-val
8				0.002	+	1.8	0.020	+	1.8	0.645	+	1.0	0.47	0.084
9				**0.006**	**+**	**1.8**	**0.020**	**+**	**1.8**				**0.45**	**0.018**
10				0.278	+								0.12	0.278

3I. Figures

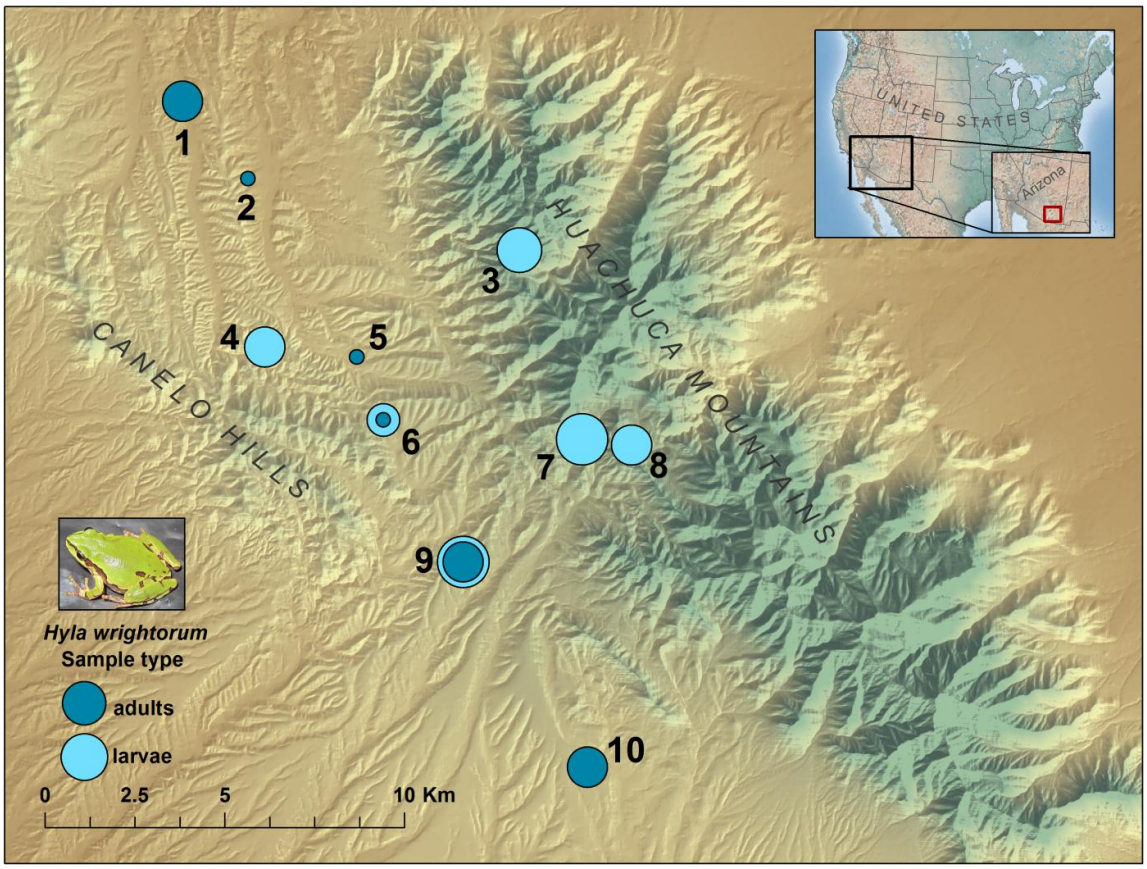

Figure 3.1. Sampling locations for *H. wrightorum* in the Huachuca Mountains and Canelo Hills region of southeastern Arizona, USA (inset). Population numbers are shown in black font, and information for each sampling location included in Table 1. Symbols for each population are proportional to sample size, and color indicates life stage of sampled individuals (dark blue = adults; light blue = larvae).

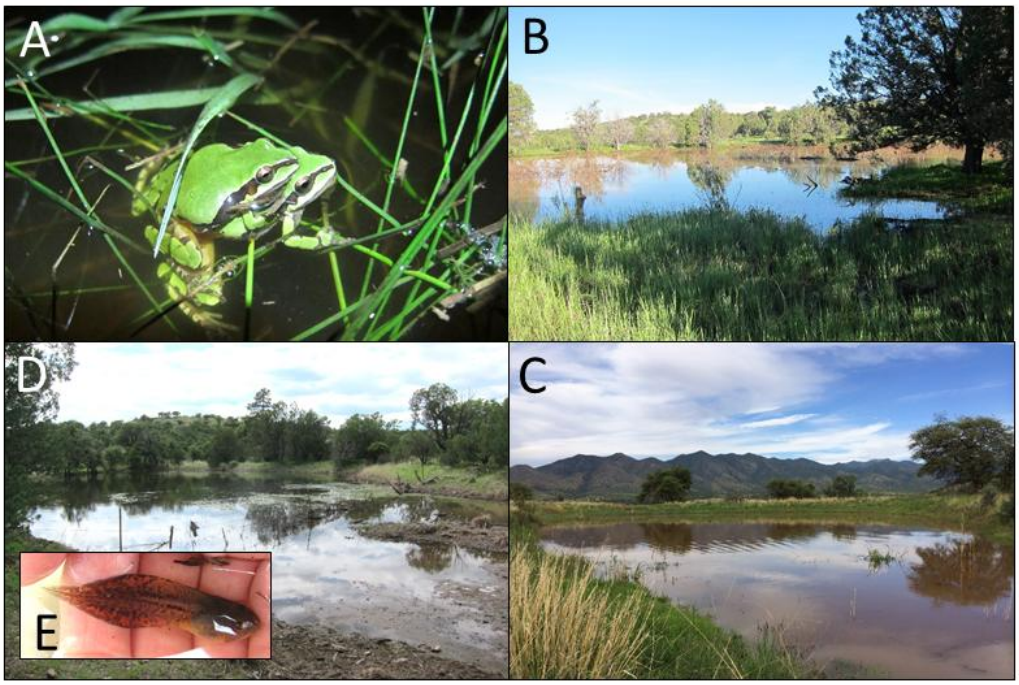

Figure 3.2. A) *H. wrightorum* breeding pair at Site 1; B) Site 10; C) Site 2; D) Site 4; and E) *H. wrightorum* larvae sampled at Site 4. Sites in B, C, and D are all new localities for this species.

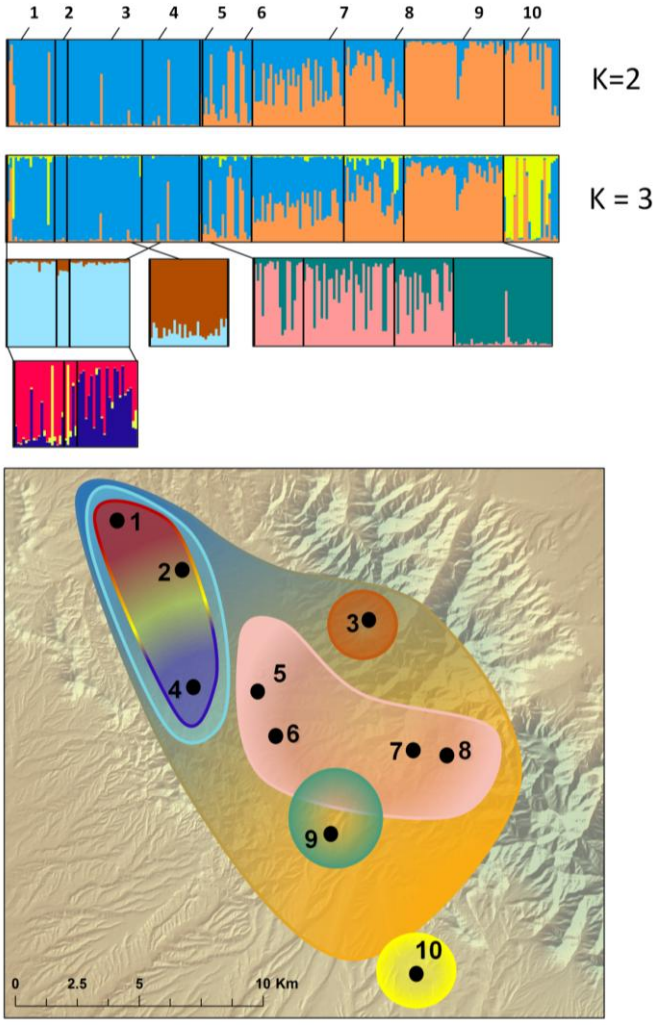

Figure 3.3. Structure results for *H. wrightorum*. Numbers correspond to sampling locations (Table 1, Figure 1). Each vertical bar represents one individual. Colors indicate the most likely genetic cluster assignments. Black vertical bars denote individuals from the same sampling locations. Each cluster was hierarchically analyzed for nested structure; nested structure results are shown directly below the original cluster. Hierarchical analyses were repeated until terminal clusters (K = 1) were reached. Note that results for K = 2 and K = 3 clusters are shown for all individuals, because both had similar support (Appendix, Table A4). Hierarchical analyses are shown following K = 3 for all individuals. Nested, colored outlines on the map correspond to population clusters.

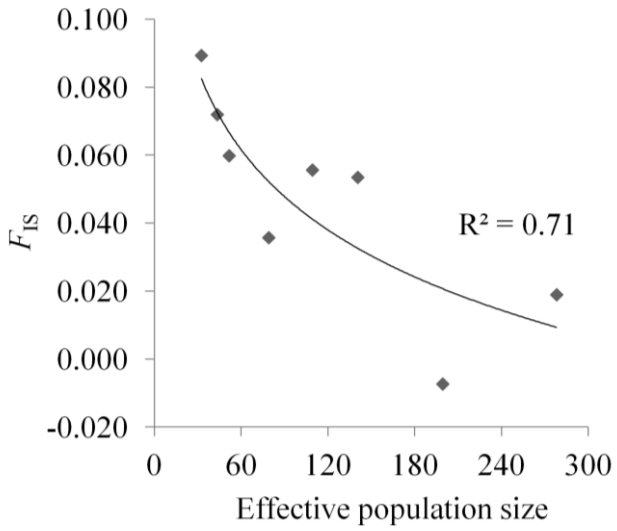

Figure 3.4. Relationship between effective population size (N_e, x-axis) and F_{IS}.

3J. Chapter 3 Appendix

Table 3.A.1. Locus, repeat length (tet = tetranucleotide), and primer sequences for all 17 polymorphic microsatellite loci for *Hyla wrightorum.*

Locus	Repeat	Forward primer (5' - 3')	Reverse primer (5' - 3')
Hwri1316	tet	GTACGTGTGACCCTACCCTC	*GTTTCTT*ACCTATAGCTTGCACCACCG
Hwri1422	tet	TGTTATGGGCCTCTGACCAG	*GTTTCTT*ACATGTGAAGTGTGCTGCTG
Hwri2688	tet	GATGTTTGCACGCTTGTCAC	*GTTTCTT*TTGTGCAATTGTTGGCTGAC
Hwri2932	tet	*ACCAAGTGCATTTCCAGGGA*GACTGGCTTCCGTGGATTTC	*GTTTCTT*CTGTAAACTCCTGTGCTAGCC
Hwri3318	tet	AAGATAGGGCCATTCGACCG	*GTTTCTT*ATGGTGCTGTGGAGAGATCC
Hwri4093	tet	CCAGACAAACCTCAGCCAAC	*GTTTCTT*TGCTTCACATATACTGGAGTGC
Hwri4269	tet	AGCGTGTGGGATTGAATGAC	*GTTTCTT*CTCAAAGACCAGGGAGTGTC
Hwri4370	tet	TCCCTCACCCTGGATTGTG	*GTTTCTT*GGGAGGAAACCATGCTTGTG
Hwri10374	tet	GGAGGGTGCAAACGAGAAATG	*GTTTCTT*GCGAGGGATTTGTTGGTTGG
Hwri12115	tet	GAACTACTCAACTCCAGCAGC	*GTTTCTT*TACTGTGTCAAGTCCTGCCC
Hwri16672	tet	ACCTGCTGCTTGGATATTTGC	*GTTTCTT*AGTGTGCTGCTGTATCCTTC
Hwri20812	tet	TGTTCTGCTAATGTCCTTCTGC	*GTTTCTT*GCGGCCCTGGATAGACATG
Hwri23452	tet	AGCACTGCAGAATATGTTGGTG	*GTTTCTT*GTGCCATACTCTCATTTGTGTG
Hwri29495	tet	AGTGCTAAGAGGCCTGACAG	*GTTTCTT*TGGAGTGCTGCAGTTCAC
Hwri30215	tet	TTTGGGTTTCACTTTGCTTGG	*GTTTCTT*ATGAGGGCATCTTGTGTTGG
Hwri30594	tet	*GTTCGTACCGCTCATTCACT*GATGTGTGCAGCAGGTCAC	*GTTTCTT*CTGCACACTTGTCTGTTCCC
Hwri34484	tet	TGAGGGAACGAATTAAAGGGAC	*GTTTCTT*TGTACTGAAGGCTGGAAGGG

Table 3.A.2. *H. wrightorum* microsatellite loci information by population. Sample size (N) by locus and population (Pop), observed heterozygosity (H_o), expected heterozygosity (H_e), minimum allele size (Min A), mean allele size (Mean A), maximum allele size (Max A), number of alleles (A Count), allelic richness (A Rich), F_{IS}, and p-values of Hardy Weinberg tests (HWE, p-val), where significant HWE tests after a Bonferroni correction are shown in bold.

Locus	Pop	N	*Ho*	*He*	Min A	Mean A	Max A	A Count	A Rich	F_{IS}	HWE, p-val
1316	1	19	0.895	0.812	201	219.53	233	5	5.00	-0.12	0.394
1316	3	29	0.931	0.815	157	220.52	237	8	7.19	-0.15	0.251
1316	4	23	0.696	0.724	201	210.57	233	5	5.00	0.03	0.658
1316	6	20	0.650	0.722	201	214.60	233	4	4.00	0.09	0.711
1316	7	37	0.649	0.703	201	214.73	233	5	4.89	0.07	0.385
1316	8	24	0.708	0.716	169	211.42	237	8	7.70	0.00	0.020
1316	9	40	0.650	0.637	201	213.20	233	5	4.91	-0.03	0.533
1316	10	22	0.773	0.804	201	214.91	233	6	5.86	0.03	0.157
1422	1	19	0.632	0.745	188	200.42	212	6	6.00	0.14	0.209
1422	3	30	0.667	0.762	188	201.80	208	5	4.95	0.12	0.224
1422	4	23	0.609	0.702	188	198.78	212	6	5.95	0.13	0.438
1422	6	20	0.550	0.787	188	198.00	212	6	5.95	0.29	0.016
1422	7	37	0.649	0.780	188	200.76	212	6	5.40	0.16	**0.003**
1422	8	24	0.708	0.740	188	201.33	212	6	5.75	0.03	0.821
1422	9	40	0.750	0.742	188	198.65	208	5	4.86	-0.02	0.816
1422	10	22	0.682	0.837	188	200.73	212	6	6.00	0.18	0.472
2688	1	19	0.632	0.714	244	261.58	268	5	5.00	0.10	0.458
2688	3	30	0.767	0.678	248	262.47	268	6	5.14	-0.14	0.037
2688	4	23	0.739	0.660	244	262.87	268	5	4.82	-0.13	0.786
2688	6	20	0.600	0.708	244	260.50	268	5	5.00	0.14	0.010
2688	7	37	0.595	0.662	252	263.57	272	6	5.05	0.10	0.076
2688	8	24	0.667	0.770	236	261.08	268	7	6.87	0.13	**0.001**
2688	9	40	0.625	0.661	252	262.60	268	5	4.72	0.05	0.307
2688	10	22	0.545	0.564	244	261.91	268	4	4.00	0.02	0.848
2932	1	18	0.667	0.716	200	210.22	224	7	7.00	0.06	0.391
2932	3	30	0.667	0.710	204	210.60	224	6	5.68	0.05	0.761
2932	4	23	0.609	0.521	204	207.22	220	4	4.00	-0.18	1.000
2932	6	20	0.850	0.688	200	209.50	224	7	6.80	-0.25	0.901
2932	7	37	0.595	0.702	204	210.70	224	6	5.22	0.15	0.114
2932	8	23	0.565	0.546	204	208.17	224	6	5.52	-0.05	0.673
2932	9	39	0.462	0.467	204	206.62	224	6	5.05	0.00	0.176
2932	10	22	0.682	0.663	204	209.00	224	6	5.79	-0.04	0.707
3318	1	19	0.737	0.777	250	260.32	274	6	6.00	0.04	0.469
3318	3	30	0.833	0.802	250	258.80	274	7	6.85	-0.05	0.869
3318	4	23	0.870	0.810	250	258.26	274	7	6.94	-0.09	0.990
3318	6	20	0.950	0.808	250	259.60	274	6	6.00	-0.19	0.168
3318	7	37	0.757	0.811	250	258.00	274	7	6.53	0.06	0.071
3318	8	23	0.739	0.796	250	258.61	274	6	5.95	0.06	0.385
3318	9	40	0.800	0.726	250	260.05	274	7	6.68	-0.11	0.037

Table3.A.2, Continued.

Locus	Pop	N	*Ho*	*He*	Min A	Mean A	Max A	A Count	A Rich	F_{IS}	HWE, p-val
3318	10	22	0.727	0.737	250	264.55	274	7	6.97	0.00	0.497
4093	1	19	0.684	0.784	145	158.58	165	5	5.00	0.12	0.160
4093	3	29	0.379	0.416	145	162.79	165	5	4.83	0.08	0.346
4093	4	23	0.522	0.584	145	161.35	169	6	5.94	0.10	0.147
4093	6	20	0.500	0.699	145	160.20	165	5	5.00	0.28	0.193
4093	7	36	0.694	0.689	145	159.89	165	5	4.98	-0.02	0.072
4093	8	22	0.682	0.678	145	160.82	165	5	4.98	-0.02	0.375
4093	9	40	0.525	0.551	145	161.30	165	5	4.91	0.04	0.488
4093	10	21	0.571	0.674	145	156.43	165	5	4.90	0.14	0.568
4269	1	19	0.421	0.408	152	154.42	172	4	4.00	-0.05	0.717
4269	3	30	0.433	0.437	152	155.00	164	3	2.95	0.00	0.841
4269	4	23	0.130	0.204	152	152.78	164	3	2.97	0.36	0.093
4269	6	20	0.550	0.613	152	156.70	172	4	4.00	0.09	0.424
4269	7	37	0.622	0.619	152	156.43	172	4	4.00	-0.01	0.031
4269	8	24	0.417	0.451	152	153.67	164	3	2.99	0.07	0.253
4269	9	40	0.450	0.466	152	154.00	164	3	3.00	0.03	0.282
4269	10	22	0.409	0.415	152	154.09	164	3	3.00	0.00	0.269
4370	1	19	0.895	0.862	189	245.84	269	9	9.00	-0.05	0.633
4370	3	30	0.833	0.856	177	243.27	265	11	9.86	0.02	0.123
4370	4	23	0.783	0.826	201	249.26	269	9	8.60	0.04	0.754
4370	6	19	0.789	0.836	201	248.79	269	9	9.00	0.04	0.482
4370	7	37	0.730	0.849	201	245.27	269	10	8.49	0.13	0.282
4370	8	24	0.750	0.763	201	247.58	269	9	8.33	0.01	0.386
4370	9	40	0.875	0.842	185	240.95	265	10	8.88	-0.05	0.201
4370	10	22	0.727	0.796	185	237.64	265	9	8.69	0.08	0.037
10374	1	19	0.684	0.801	321	329.74	341	5	5.00	0.14	0.585
10374	3	27	0.704	0.758	321	330.70	341	5	4.70	0.06	0.019
10374	4	23	0.783	0.753	321	329.09	341	5	5.00	-0.05	0.648
10374	6	20	0.650	0.791	321	330.50	341	5	5.00	0.17	0.041
10374	7	37	0.568	0.650	321	328.08	341	5	4.76	0.12	0.653
10374	8	22	0.545	0.682	321	327.73	341	5	4.98	0.19	0.073
10374	9	40	0.525	0.546	321	324.85	341	5	4.79	0.03	0.322
10374	10	22	0.636	0.799	321	328.45	341	6	5.98	0.20	0.401
12115	1	19	0.789	0.868	186	228.95	250	11	11.00	0.08	0.494
12115	3	30	0.900	0.877	186	232.20	270	13	11.29	-0.04	0.337
12115	4	23	0.826	0.844	186	222.96	250	10	9.74	0.01	0.239
12115	6	20	0.900	0.892	186	219.80	250	11	10.94	-0.02	0.892
12115	7	36	0.861	0.874	194	230.78	250	11	9.55	0.01	0.228
12115	8	24	0.875	0.849	186	223.25	250	10	9.53	-0.04	0.168
12115	9	40	0.775	0.798	186	228.40	254	11	8.28	0.02	0.345
12115	10	22	0.818	0.881	186	229.82	254	10	9.71	0.06	0.267
16672	1	19	0.737	0.762	177	194.47	217	6	6.00	0.02	0.044
16672	3	29	0.552	0.583	177	186.52	265	6	5.31	0.05	0.159

Table3.A.2, Continued.

Locus	Pop	N	*Ho*	*He*	Min A	Mean A	Max A	A Count	A Rich	F_{IS}	HWE, p-val
16672	4	23	0.826	0.668	177	193.96	217	4	3.97	-0.25	0.288
16672	6	20	0.850	0.721	177	193.60	217	6	5.90	-0.20	0.751
16672	7	37	0.865	0.703	177	191.43	217	7	6.02	-0.24	0.116
16672	8	24	0.708	0.790	177	198.67	265	9	8.32	0.09	0.619
16672	9	40	0.850	0.756	177	198.85	217	6	5.20	-0.13	0.577
16672	10	22	0.727	0.765	177	203.00	217	7	6.85	0.04	0.106
20812	1	19	0.842	0.788	296	344.53	372	9	9.00	-0.08	0.940
20812	3	29	0.759	0.736	296	343.59	376	8	6.92	-0.04	0.620
20812	4	23	0.826	0.836	296	340.35	368	8	7.65	0.00	0.770
20812	6	20	0.900	0.842	296	336.10	376	8	7.90	-0.08	0.743
20812	7	37	0.784	0.805	296	342.81	376	9	7.79	0.02	0.539
20812	8	23	0.870	0.853	296	340.96	372	7	6.97	-0.03	0.971
20812	9	40	0.775	0.828	296	336.05	372	7	6.90	0.06	0.263
20812	10	22	0.773	0.857	296	336.55	376	9	8.73	0.09	0.766
23452	1	19	0.474	0.542	155	169.21	175	3	3.00	0.12	0.446
23452	3	27	0.769	0.668	155	169.46	175	5	4.97	-0.16	0.016
23452	4	23	0.348	0.590	155	169.43	175	4	4.00	0.41	**0.004**
23452	6	20	0.650	0.606	155	169.80	175	4	4.00	-0.09	0.392
23452	7	37	0.622	0.631	155	168.62	175	3	3.00	0.01	0.791
23452	8	24	0.500	0.568	155	170.58	175	4	3.95	0.11	0.832
23452	9	40	0.775	0.638	155	168.55	175	4	3.73	-0.22	0.322
23452	10	22	0.591	0.719	155	166.73	175	5	4.85	0.17	0.027
29495	1	19	0.737	0.797	257	279.00	301	6	6.00	0.06	0.644
29495	3	30	0.700	0.797	257	281.87	301	5	5.00	0.11	0.184
29495	4	23	0.696	0.719	257	277.52	301	5	5.00	0.02	0.722
29495	6	20	0.650	0.718	257	275.60	305	6	5.95	0.08	0.245
29495	7	37	0.784	0.755	257	278.30	305	7	6.22	-0.05	0.218
29495	8	24	0.750	0.837	257	286.75	305	7	6.95	0.10	0.237
29495	9	40	0.900	0.783	257	281.25	305	7	6.40	-0.16	0.867
29495	10	22	0.818	0.815	257	286.82	305	7	6.73	-0.02	0.114
30215	1	19	0.632	0.653	303	310.79	327	5	5.00	0.02	0.713
30215	3	29	0.414	0.561	303	307.48	323	4	3.88	0.26	0.195
30215	4	23	0.565	0.574	303	307.43	323	5	4.48	0.00	0.711
30215	6	20	0.650	0.683	303	308.60	327	6	5.90	0.04	0.022
30215	7	37	0.649	0.714	303	310.78	327	5	4.90	0.09	0.395
30215	8	24	0.708	0.779	303	312.25	327	6	5.95	0.08	0.640
30215	9	40	0.725	0.770	303	315.20	327	6	5.47	0.05	0.472
30215	10	22	0.727	0.822	303	315.64	327	6	5.86	0.11	0.232
30594	1	17	0.529	0.656	233	245.47	265	7	7.00	0.18	0.383
30594	3	30	0.367	0.527	233	238.80	261	5	4.82	0.30	0.035
30594	4	23	0.348	0.672	233	242.04	261	5	4.93	0.48	**0.004**
30594	6	20	0.500	0.777	233	245.20	261	5	5.00	0.35	0.038
30594	7	36	0.611	0.804	233	246.39	265	6	5.95	0.24	0.046

Table3.A.2, Continued.

Locus	Pop	N	*Ho*	*He*	Min A	Mean A	Max A	A Count	A Rich	F_{IS}	HWE, p-val
30594	8	24	0.708	0.764	233	248.00	265	7	6.55	0.06	0.406
30594	9	40	0.700	0.810	233	244.40	261	6	5.42	0.13	0.394
30594	10	21	0.619	0.744	233	250.71	265	7	6.40	0.16	0.151
34484	1	19	0.737	0.704	135	142.37	163	5	5.00	-0.06	0.365
34484	3	28	0.750	0.666	135	146.07	163	5	4.58	-0.14	0.304
34484	4	23	0.826	0.729	135	144.30	163	4	4.00	-0.15	0.756
34484	6	20	0.550	0.601	135	139.50	163	5	5.00	0.07	0.368
34484	7	37	0.784	0.760	135	143.81	163	5	5.00	-0.04	0.928
34484	8	22	0.273	0.458	135	138.64	163	5	4.85	0.40	**0.001**
34484	9	40	0.575	0.620	135	139.75	163	5	4.85	0.07	0.200
34484	10	22	0.591	0.661	135	141.55	163	5	5.00	0.10	0.397

Table 3.A.3. Results of test for linkage disequilibrium using the log likelihood ratio statistic as implemented in GenePop. Each pairwise test between markers had 16 degrees of freedom. P-values significant with a Bonferroni correction applied are shown in bold. Note that the only two significant tests were driven by an estimated p-value of zero in one of 8 populations (population-specific results shown for those two marker pairs following overall pairwise comparisons).

Locus 1	Locus 2	Chi^2	p-value
1316	2688	9.46	0.893
1316	4093	7.07	0.972
1316	4370	16.02	0.452
1316	10374	16.98	0.387
1316	12115	15.43	0.494
1316	16672	5.26	0.994
1316	20812	15.21	0.509
1316	23452	6.85	0.976
1316	30594	14.13	0.589
1316	34484	8.99	0.914
1422	1316	14.97	0.526
1422	2688	26.43	0.048
1422	2932	14.47	0.564
1422	3318	19.21	0.258
1422	4093	17.30	0.367
1422	4269	12.67	0.697
1422	4370	16.02	0.452
1422	10374	13.14	0.662
1422	12115	15.28	0.505
1422	16672	9.34	0.899
1422	20812	15.09	0.518
1422	23452	18.91	0.274
1422	29495	15.49	0.489
1422	30215	21.50	0.160
1422	30594	6.07	0.987
1422	34484	10.94	0.813
2688	4093	16.69	0.406
2688	4370	27.08	0.041
2688	10374	13.64	0.626
2688	12115	13.37	0.645
2688	20812	16.90	0.392
2688	23452	21.06	0.176
2688	30594	17.67	0.344
2688	34484	8.30	0.940
2932	1316	15.28	0.504
2932	2688	7.91	0.951
2932	3318	9.56	0.888
2932	4093	13.43	0.641
2932	4269	11.57	0.773

Table 3.A.3, continued.

Locus 1	Locus 2	Chi^2	p-value
2932	10374	11.55	0.774
2932	12115	9.33	0.899
2932	16672	11.09	0.804
2932	20812	13.33	0.648
2932	23452	24.23	0.085
2932	29495	14.16	0.587
2932	30215	8.08	0.946
2932	30594	15.56	0.484
2932	34484	9.38	0.897
3318	1316	7.18	0.970
3318	2688	26.03	0.054
3318	4093	23.17	0.109
3318	4269	12.48	0.710
3318	4370	13.70	0.621
3318	10374	18.29	0.307
3318	12115	14.55	0.558
3318	16672	11.88	0.753
3318	20812	10.62	0.832
3318	23452	15.35	0.499
3318	30594	10.02	0.866
3318	34484	11.49	0.778
4093	4370	20.98	0.179
4093	10374	4.60	0.997
4093	12115	10.63	0.832
4093	20812	8.36	0.937
4093	23452	11.46	0.780
4093	30594	11.38	0.786
4269	1316	20.59	0.195
4269	2688	19.59	0.239
4269	4093	13.82	0.612
4269	4370	14.95	0.528
4269	10374	11.54	0.775
4269	12115	12.27	0.725
4269	16672	12.72	0.693
4269	20812	17.44	0.358
4269	23452	17.04	0.383
4269	30594	9.85	0.874
4269	34484	13.61	0.628
10374	4370	14.14	0.589
10374	12115	5.54	0.992
10374	20812	6.22	0.986
10374	23452	5.54	0.992
10374	30594	17.57	0.350
12115	4370	10.42	0.844
12115	20812	12.19	0.731

Table 3.A.3, continued.

Locus 1	Locus 2	Chi^2	p-value
16672	4093	13.32	0.649
16672	4370	17.78	0.337
16672	10374	8.68	0.926
16672	12115	7.40	0.965
16672	20812	11.13	0.802
16672	23452	23.44	0.102
16672	30594	13.57	0.631
16672	34484	8.67	0.926
20812	4370	8.24	0.941
20812	23452	16.88	0.393
20812	**30594**	**Infinity**	**Highly**
23452	4370	12.05	0.741
23452	30594	15.30	0.503
29495	1316	9.90	0.872
29495	2688	15.80	0.467
29495	3318	13.46	0.639
29495	4093	19.49	0.244
29495	4269	16.46	0.421
29495	4370	15.61	0.481
29495	10374	23.62	0.098
29495	12115	6.60	0.980
29495	16672	19.70	0.234
29495	20812	16.57	0.414
29495	23452	14.04	0.596
29495	30215	11.23	0.795
29495	30594	10.27	0.852
29495	**34484**	**Infinity**	**Highly**
30215	1316	20.49	0.199
30215	2688	14.69	0.548
30215	3318	12.31	0.722
30215	4093	19.27	0.255
30215	4269	19.81	0.229
30215	4370	8.07	0.947
30215	10374	11.80	0.758
30215	12115	12.34	0.720
30215	16672	25.34	0.064
30215	20812	13.05	0.669
30215	23452	16.03	0.451
30215	30594	26.25	0.051
30215	34484	14.17	0.586
30594	4370	8.80	0.922
34484	4093	13.15	0.662
34484	4370	15.90	0.460
34484	10374	6.52	0.981
34484	12115	13.51	0.635

Table 3.A.3, continued.

Locus 1	Locus 2	Chi^2	p-value
Comparison of Loci 20812 and 30594 by population:			
Pop	Locus 1	Locus 2	P-Value
1	20812	30594	0.643
3	20812	30594	0.015
4	20812	30594	0.114
6	20812	30594	0.338
7	20812	30594	0.014
8	20812	30594	0.036
9	**20812**	**30594**	**0.000**
10	20812	30594	1.000
Comparison of loci 29495 and 34484 by population:			
Pop	Locus 1	Locus 2	P-Value
1	29495	34484	1.000
3	29495	34484	0.121
4	29495	34484	0.357
6	29495	34484	0.190
7	29495	34484	0.082
8	29495	34484	0.794
9	**29495**	**34484**	**0.000**
10	29495	34484	0.325

Table 3.A.4. Delta K calculations and log likelihoods for Structure output.

HYWR: all individuals:

# K	Reps	Mean LnP(K)	Stdev LnP(K)	Ln'(K)	|Ln"(K)|	Delta K
1	10	-11959.15	0.40	NA	NA	NA
2	**10**	**-11576.89**	**9.01**	**382.26**	**180.20**	**20.01**
3	**10**	**-11374.83**	**5.21**	**202.06**	**99.93**	**19.19**
4	10	-11272.70	24.36	102.13	57.39	2.36
5	10	-11227.96	13.40	44.74	17.58	1.31
6	10	-11200.80	15.73	27.16	55.88	3.55
7	10	-11229.52	51.43	-28.72	5.40	0.11
8	9	-11263.64	60.67	-34.12	NA	NA

Following K = 3 for all individuals (results visualized in Figure 3)

HYWR 1: Populations 1, 2, 3, and 4:

# K	Reps	Mean LnP(K)	Stdev LnP(K)	Ln'(K)	|Ln"(K)|	Delta K
1	10	-3973.01	0.64	NA	NA	NA
2	**10**	**-3928.04**	**5.29**	**44.97**	**61.43**	**11.60**
3	10	-3944.50	28.02	-16.46	1.22	0.04
4	10	-3959.74	71.62	-15.24	47.82	0.67
5	10	-4022.80	50.85	-63.06	NA	NA

HYWR 1.1: Populations 1, 2, and 4:

# K	Reps	Mean LnP(K)	Stdev LnP(K)	Ln'(K)	|Ln"(K)|	Delta K
1	10	-2413.62	0.68	NA	NA	NA
2	10	-2398.15	16.78	15.47	6.33	0.38
3	**10**	**-2376.35**	**20.11**	**21.80**	**118.76**	**5.90**
4	10	-2473.31	74.17	-96.96	NA	NA

HYWR 2: Populations 6, 7, 8, and 9:

# K	Reps	Mean LnP(K)	Stdev LnP(K)	Ln'(K)	|Ln"(K)|	Delta K
1	10	-6377.88	0.41	NA	NA	NA
2	**10**	**-6251.28**	**2.36**	**126.60**	**128.97**	**54.59**
3	10	-6253.65	8.42	-2.37	31.64	3.76
4	10	-6287.66	28.90	-34.01	155.91	5.39
5	10	-6477.58	231.96	-189.92	NA	NA

HYWR 2.2: Populations 6, 7, and 8:

# K	Reps	Mean LnP(K)	Stdev LnP(K)	Ln'(K)	|Ln"(K)|	Delta K
1	**10**	**-4315.63**	**0.54**	**NA**	**NA**	**NA**
2	10	-4348.21	40.25	-32.58	5.43	0.13
3	10	-4375.36	51.64	-27.15	86.83	1.68
4	10	-4489.34	160.65	-113.98	NA	NA

Table 3.A.4, continued.

Following K = 2 for all individuals

HYWR (B) 1: Populations 1, 2, 3, and 4:

# K	Reps	Mean LnP(K)	Stdev LnP(K)	Ln'(K)	|Ln''(K)|	Delta K
1	10	-3973.01	0.64	NA	NA	NA
2	**10**	**-3928.04**	**5.29**	**44.97**	**61.43**	**11.60**
3	10	-3944.50	28.02	-16.46	1.22	0.04
4	10	-3959.74	71.62	-15.24	47.82	0.67
5	10	-4022.80	50.85	-63.06	NA	NA

HYWR (B) 1.1: Populations 1, 2, and 4:

# K	Reps	Mean LnP(K)	Stdev LnP(K)	Ln'(K)	|Ln''(K)|	Delta K
1	10	-2413.62	0.68	NA	NA	NA
2	10	-2398.15	16.78	15.47	6.33	0.38
3	**10**	**-2376.35**	**20.11**	**21.80**	**118.76**	**5.90**
4	10	-2473.31	74.17	-96.96	NA	NA

HYWR (B) 2: Populations 6, 7, 8, and 9:

# K	Reps	Mean LnP(K)	Stdev LnP(K)	Ln'(K)	|Ln''(K)|	Delta K
1	10	-6377.88	0.41	NA	NA	NA
2	**10**	**-6251.28**	**2.36**	**126.60**	**128.97**	**54.59**
3	10	-6253.65	8.42	-2.37	31.64	3.76
4	10	-6287.66	28.90	-34.01	155.91	5.39
5	10	-6477.58	231.96	-189.92	NA	NA

HYWR (B) 2.1: Populations 6, 7, and 8:

# K	Reps	Mean LnP(K)	Stdev LnP(K)	Ln'(K)	|Ln''(K)|	Delta K
1	**10**	**-4315.63**	**0.54**	**NA**	**NA**	**NA**
2	10	-4348.21	40.25	-32.58	5.43	0.13
3	10	-4375.36	51.64	-27.15	86.83	1.68
4	10	-4489.34	160.65	-113.98	NA	NA

HYWR (B) 2.2: Populations 9 and 10:

# K	Reps	Mean LnP(K)	Stdev LnP(K)	Ln'(K)	|Ln''(K)|	Delta K
1	10	-3250.09	0.36	NA	NA	NA
2	10	-3109.40	0.63	140.69	141.61	226.44
3	10	-3110.32	30.41	-0.92	37.82	1.24
4	10	-3149.06	27.72	-38.74	NA	NA

Table 3.A.5. Landscape data - sources, description, and details.

	Canopy	Streams	Slope	Distance
Details	2001 NLCD canopy density dataset.	NHDPlus Version 2, downloaded from National Map Viewer (USGS).	Calculated with 9-m Digital Elevation Model from National Elevation Dataset.	Uniform resistance layer.
Resolution	30 m	100 m shapefile buffer around streams, converted to raster with resolution of 30 m	9 m, resampled to 30 m	30 m
Resistance scale	1 - 100: inversely scaled to % canopy cover (0-100%)	1 or 100: binary - 1 (low resistance) for riparian buffer area, 100 for non-riparian area	1 - 100: inversely related to % slope	1: uniform throughout
Source	http://www.mrlc.gov/nlcd01_data.php	http://viewer.nationalmap.gov/viewer/	http://ned.usgs.gov/downloads.asp	

Table 3.A.6. Pearson correlation coefficients between all distance matrices (genetic and spatial).

	D_{ps}	Canopy	Stream	Slope
Canopy	0.212			
Stream	0.171	0.005		
Slope	0.340	-0.660	0.050	
Null	0.502	0.756	0.075	-0.045

Chapter 4: Reduced population size and increased population isolation and synchrony in response to simulated reductions in breeding habitat in a dryland amphibian

Authors: M.C. Mims, J.L. Lawler, J.D. Olden

4A. Abstract

Amphibians are declining worldwide due to a collection of threats including disease, invasive species, and habitat loss. Climate change may exacerbate habitat loss by altering the availability or suitability of aquatic breeding habitat through changes in precipitation (e.g., altering the timing and duration of hydroperiod) and temperature (evaporation rates). Simulation-based approaches offer a promising way to evaluate the possible responses of amphibians to these changes. In this study, we constructed a spatially-explicit individual based model (SIBM) to simulate the response of the Arizona Treefrog (*Hyla wrightorum*) to reductions in breeding habitat availability in an isolated portion of its range. The populations of *Hyla wrightorum* in the Huachuca Mountains and Canelo Hills of Arizona are considered a Distinct Population Segment (DPS) that is currently a candidate for federal protection under the Endangered Species Act. The *H. wrightorum* DPS is known to occur in < 15 breeding ponds that may become unsuitable due to climate-induced changes in hydroperiod, increased rates of invasion by non-native predator, or filling by sedimentation. We simulated *H. wrightorum* response to a range of breeding habitat reduction scenarios. We found that reductions in breeding habitat resulted in population declines, with the greatest population declines for *H. wrightorum* associated with both a reduction in breeding habitat availability and recruitment failure. Reduced breeding habitat also resulted in

increased synchrony and decreased variability through time, which likely indicates a transition from a metapopulation to isolated populations.

4B. Key words: spatially explicit individual-based models, dryland ecology, hydroperiod, *Hyla wrightorum*

4C. Introduction

Declines and extinctions of many amphibian species worldwide have been well-documented over the last decade (Stuart *et al.* 2004). Habitat loss, invasive species, and disease are among the primary threats to many amphibians (Sodhi *et al.* 2008), and climate change may exacerbate many of these threats into the future (e.g. disease, Pounds *et al.* 2006). In the arid southwestern US, much of the historical aquatic breeding habitats used by the region's amphibians have been heavily modified to meet a range of human water requirements. Continued urban and agricultural development in the region has resulted in increasing water needs, with demand projected to be greater than supply in many regions (Marshall *et al.* 2010). In addition, climate change is poised to further reduce aquatic habitat in the region (Jaeger *et al.*; Seager *et al.* 2012), which may lead to additional loss of breeding habitat.

Many amphibians in the region now rely on artificial habitat such as ponds built to retain water runoff and create reservoirs for livestock. These "stock tanks" (hereafter referred to as stock ponds) are now a dominant form of aquatic habitat throughout most of the region and are increasingly recognized as important surrogate habitat for the region's native aquatic fauna (Rosen and Schwalbe 1998; Hale *et al.* 2015). For example, in the Huachuca Mountains and San Rafael Valley of southeastern Arizona, the endangered Sonoran tiger salamander (*Ambystoma*

tigrinum stebbinsi) now breeds almost exclusively in stock ponds throughout its small range (Storfer *et al.* 2014), and stock ponds are important breeding habitat for the threatened Chiricahua leopard frog (*Lithobates chiricahuensis*) (Rosen and Schwalbe 1998). Stock ponds span a range of hydroperiods (length of time the ponds are full) from perennially to intermittently wetted.

Management of stock ponds is complex and involves consideration of livestock use, protection for native aquatic species occupying ponds, and control of invasive species such as the American bullfrog (*Lithobates catesbeianus*) (Hale *et al.* 2015). Furthermore, projected changes in precipitation, temperature, and surface water availability (Seager *et al.* 2012) may alter both the number of wetted ponds and their hydroperiods in the future. The frequency and intensity of wildfires in the region are also anticipated to increase (Westerling *et al.* 2006; Dennison *et al.* 2014), and monsoon rains that follow fire season can produce intense floods and erosion in recently burned areas. Floods result in scouring and sedimentation events that may severely alter or destroy aquatic habitat and may fill stock ponds with sediment.

Appropriate management and availability of stock ponds in the future will likely be critical to the persistence of many of the region's amphibians, including the Arizona treefrog (*Hyla wrightorum*) in the Huachuca Mountains of southeastern Arizona. *Hyla wrightorum* populations within the Huachuca Mountains and Canelo Hills region are considered a Distinct Population Segment and are a candidate for federal protection under the Endangered Species Act (U.S. Fish and Wildlife Service 2013). *Hyla wrightorum* breed only in intermittent aquatic habitat (i.e., dry for at least some part of the year). The geographic range occupied by *H. wrightorum* in the Huachuca Mountains and Canelo Hills is small compared to the larger two portions of its distribution, with known breeding sites occurring within an area no larger than 85 km^2. Effective

population size estimates range from tens to many thousands, and population genetic structure suggests significantly differentiated populations that likely exist within a metapopulation framework (Mims, Dissertation, Chapter 3). Potential threats to local persistence of this species include disease (Bradley *et al.* 2002) and predation by invasive American bullfrogs (*Lithobates catesbeianus*, Jones and Timmons 2010). The number of verified breeding sites is currently < 15 (Mims, Dissertation, Chapter 3), and all are human modified environments (stock ponds and one wetland resulting from a road crossing of a stream). Reduced precipitation, sedimentation of ponds, or increased evaporation rates (due to higher temperatures) may eliminate breeding habitat or reduce hydroperiods such that *H. wrightorum* larvae are not allowed sufficient time to metamorphose (failed recruitment). However, the question of how *H. wrightorum* would respond to and cope with reductions in available breeding habitat remains unanswered.

To address this question, we used a simulation-based approach to evaluate the response of *H. wrightorum* to different scenarios of breeding habitat reduction through its range in the Huachuca Mountains. Simulations provide an opportunity to test a range of possible responses of a species to environmental change, and simulations are particularly useful in cases where experimental or observational approaches in the field would be extremely resource-intensive and would present a number of logistical and practical challenges. Because the degree and nature of change in pond hydroperiods resulting from climate change is unknown, we used tested a range of possible reductions in breeding habitat (Wenger *et al.* 2013). Our objectives included: 1) create a spatially-explicit individual based model (SIBM) of the population dynamics and demographics of *H. wrightorum* in the Huachuca Mountains of southeastern Arizona, and 2) examine response of *H. wrightorum* to a range of breeding habitat loss scenarios.

4D. Methods

To simulate the response of *H. wrightorum* to changes in breeding habitat availability, we constructed a spatially explicit individual-based model using the software HexSim (Schumaker 2015). The model was informed using empirical spatial and ecological information for each species and simulates population dynamics in the Huachuca Mountains of Southeastern Arizona. Detailed descriptions of spatial, demographic, and dispersal parameters follow.

Spatial data

We used empirical spatial data describing the Huachuca Mountains to build all simulated landscapes for our SIBM. Available spatial databases describing water bodies in the region fail to capture small or intermittent ponds. Because such ponds constitute most of the breeding sites we wished to simulate, we required a comprehensive spatial database of all ponds and small basins in the region. To achieve this, we coupled a US Forest Service Ranger District Map, which reliably reports stock pond locations, with Google Earth (2014) to manually create a digital pond database for the Huachuca Mountains and its drainages (Figure 4.1). We used Google Earth to create polygons representing pond basins. We then used historical satellite imagery available via the Google Earth Historical Imagery tab to construct a time series of when ponds contained water. The wet/dry historical records for ponds were then used to determine whether ponds and lakes were intermittent (dry in at least one historical image). All perennial ponds (those always observed with water) and dry basins (those never observed to hold water) were excluded from the candidate set of breeding ponds for the simulations. All intermittent ponds were considered candidate ponds for use in the SIBM. We defined the study's spatial focal area as all intermittent ponds within a 7km buffer of all known breeding sites for *H. wrightorum*

in the Huachuca Mountains. 7km was selected because it represents the longest distance between known breeding sites in the range (Mims, Dissertation, Chapter 3). To avoid ponds close to the edge of the simulated landscape, we included a rectangular area that extended a minimum of 1.5 km beyond all ponds. The final extent of all spatial data spanned the following dimensions in NAD83/UTM Zone 12: top: 3497710; left: 534353; right: 570017; and bottom: 3463428.

Summer precipitation events in the form of sporadic, isolated, and intense thunderstorms are responsible for filling these intermittent ponds. Therefore, not all ponds fill every summer. To simulate this temporal and spatial heterogeneity, we constructed 10 variable pond surfaces informed by historical imagery. The month and year of all historical images were recorded as well as whether each pond was dry or wetted. The image time series was also used to construct hydroperiod indices for each pond. In order to determine how many ponds to include as available breeding habitat each year, we calculated the annual percent of ponds containing water during the wet season. A "wet season" index was calculated as the % of images from the months of July through November (the primary breeding and larval development season for *H. wrightorum*), across all observed years, for which a pond was observed to have water. A "dry season" index (April – June) was also calculated for each pond. For each of the 10 variable pond surfaces, the annual percent of ponds wetted during the wet season was used to determine how many ponds should be available. Ponds were then selected using a random draw weighted by the wet season index. Three pond map series were constructed: 1) Base: the "baseline" breeding habitat availability (e.g., that informed by available satellite imagery); 2) Dry 1: a 30% reduction in breeding habitat availability; and 3) Dry 2: a 60% reduction in breeding habitat availability. For Dry 1 and Dry 2, 30% or 60% of ponds (respectively) were removed from the Base pond series

by inverse ranking of their wet season index. In the case of ties, ponds with lower dry season index values were removed first.

To simulate non-breeding habitat requirements, we also characterized percent canopy cover (from 0-100) (Table 4.1), which may be important for *H. wrightorum* for shelter (e.g., desiccation avoidance, overwintering, or to avoid predation). Forested areas may also provide important food resources for *H. wrightorum* (Chapel 1939, Degenhardt 2005). Hexagons were considered eligible for the overwintering or "non-breeding" range of *H. wrightorum* if canopy cover was 15% or greater, and total canopy in an individual's non-breeding range must sum to at least 30 (2 hexagons with at least 15% canopy cover). We quantified the inverse of slope using a digital elevation model and scaled from 1-100 (Table 4.1), and hexagons with an average slope < 45 degrees was considered suitable for overwintering. Finally, we estimated that movement likely occurs along corridors with low slope corridors (Murphy *et al.* 2010; Mims *et al.* 2015) and/or along streams (Mims *et al.* 2015). To simulate these hypothesized corridors, we created a dispersal surface in which low slope (flat land) and riparian areas were given a high "attraction" score to promote the movement of individuals through these areas rather than steep, dry regions. Slope was characterized in the same manner described above, and riparian habitat was constructed using a 100m buffer around streams as defined in the National Hydrography Dataset (NHD Plus, USGS). The composite raster summed the inverse of slope scaled from 1-100 (such that flat land = 100, the highest value) with the riparian habitat data (riparian corridor = 100, non-corridor = 1).

To import all spatial data into HexSim, we used the HexMap Builder to convert bitmap rasters (all 1m cell size) into a landscape of hexagonal cells, each 30-m in width. Hexagon values were determined using a 120-point sampling scheme where 120 points within each hexagon were

"sampled" from each input raster. For the slope, canopy, and dispersal surfaces, the final hexagon value was determined by averaging across all 120 sampling points. To construct HexMaps for breeding ponds, hexagons were scored with a value of 1 if a pond was detected within the hexagon and 0 if no pond was detected.

Demographic parameters

In general, we aimed to examine the effect of changes in breeding pond availability on population persistence over time. Thus, we attempted to set demographic parameters that allowed for stable populations over time such that differences between scenarios could be attributed to the primary factor of interest (breeding pond availability). A short description of parameters by category follows, and all demographic parameters are outlined in detail in Table 4.2. Demographic parameters were informed by literature-derived values, and citations are included in Table 4.2. If parameter values were not available for *H. wrightorum*, values for congeners or ecologically similar species were consulted.

Population attributes for breeding events: Individuals were assigned three simple traits: sex (female or male), age (class 0 = larvae, 1 = 1 year old, 2 = 2 years old, 3 = 3+ years old; accumulated once per time step), and group status (group member or transient). 100 individuals of age class 2 and 3 were initiated at known *H. wrightorum* breeding sites. Range data was used to control group membership (defined as being at a breeding pond), and only group members were allowed to breed during the reproduction events. Range area and span were set to encompass the largest pond in the dataset to ensure that male and female individuals at the same pond were able to pair for reproduction. Hexagons were range-eligible if the value was equal to 1 (pond present). Group membership was limited to 25 individuals.

Reproduction: Females required males to reproduce, and both must be members of the same group. Average body size for females was derived from snout-to-vent lengths (SVL) for adults sampled in the Huachuca Mountains (M. Mims, unpublished but on file with AZ Game and Fish Department) and was used to calculate fecundity following relationships between fecundity and body size for Hylidae (Table 4.2, Wells 2007). Reproductive maturity in 2-year-old females is not common but is possible; thus, we allowed reproduction for 2-year-olds but with ½ the fecundity of age class 3 (3-year-olds and older) females. Fecundity was adjusted for larval mortality. Average larval mortality for *H. wrightorum* was estimated from values reported for tadpoles of a a sympatric congener (*H. arenicolor*) in temporary ponds (Sredl and Collins 1992) (Table 4.2).

Population attributes, non-breeding events: Range sizes are poorly known for many amphibian species, and estimates are not available for *H. wrightorum*. We set range size according to published values for a surrogate species (Table 4.2). No data are available for non-breeding range size; instead, we set range size to ensure that non-breeding range size was sufficiently large to allow stable simulation runs (rather than range sizes being a limiting factor). Range eligibility of hexagons for canopy surface (*H. wrightorum*) reflected eligibility rules described in spatial inputs (Table 4.2). Finally, maximum group size was set to no more than 5 group members per hexagon.

Mortality: Mortality was implemented following non-breeding group membership assignment. Because non-breeding range parameters allow high densities of individuals and set relatively low requirements for hexagon range eligibility, we set mortality for any remaining transients (e.g., those not assigned to a group) to 100%. This implemented a conservative density-dependence catch in the model that prevented exponential growth while still allowing for high population

numbers. Mortality is likely higher for recently metamorphosed individuals, thus Age Class 1 group member mortality was set to 70%. Finally, mortality for Age Class 2 and 3 group members was set to 40%. A review by Wells (2007) found mortality rates for adult anurans to average roughly 60% in mark-recapture studies; thus, we consider our mortality rates of 40% for adult group members to be conservative.

Dispersal parameters

Movement to breeding ponds: A spatial affinity parameter was used to attract individuals to the closest pond, and the dispersal surface was used to provide more favorable routes along streams and flat ground. Individual movements were set to a maximum of 35 hexagons (maximum 1050m straightline distance). Autocorrelation of dispersal paths was set to 90%, allowing relatively straight paths with only occasional lateral movement. Upon reaching the breeding pond, the dispersal event terminated; thus, in most instances dispersal events were much shorter than the maximums reported. Dispersal distances > 700m have been recorded for another sympatric dryland anuran (*Anaxyrus punctatus*, Tevis 1966), and high mobility of dryland-adapted anurans is thought to contribute to high genetic connectivity of some desert anurans (Chan and Zamudio 2009; Mims *et al.* 2015); thus, this maximum distance was set to allow for even the most extreme movement events.

Movement away from breeding ponds: Non-breeding dispersal in anurans is likely more random than directional movement to breeding ponds (Coster *et al.* 2014). Distances traveled also likely follow the more traditional leptokurtic distribution as individuals forage and seek appropriate cover rather than move toward a breeding site. To simulate movement to non-breeding or "overwintering" locations, dispersal paths for individuals were drawn from a log normal

distribution of with a mean of 10 hexagons (300m) and a standard deviation of 2 (60m). Paths were not allowed to exceed 35 hexagons (1050m). These values were selected to incorporate the maximum observed dispersal distances for other sympatric anurans (Tevis 1966). Autocorrelation of movements were informed from spatial data over a trend period of five hexagons, and no stopping criteria were used. Individuals were then permitted to explore the occupied hexagon and 6 neighboring hexagons before initiating an optional second dispersal event. If suitable habitat was not found after two dispersal and exploration events, individuals remained transients and were assigned mortality rate of 100%.

Spatially explicit individual-based model scenarios

The event sequence for the SIBM is shown in Figure 4.2. Briefly, the suites of demographic, dispersal, and non-breeding habitat use parameters described above were assembled to simulate *H. wrightorum* based on the best available biological and ecological knowledge. Demographic parameters were then paired with 5 breeding habitat map series to simulate population response to different breeding habitat availability over 100 generations (20 generations burn-in). All simulations were run with the Base map series for 20 generations burn-in and for an additional 20 generations to allow populations to reach the Base equilibrium, at which point the Dry map series were used to simulated reduced breeding habitat scenarios.

4E. Results

Comprehensive pond map and hydroperiod time series for the Huachuca Mountains

We generated a spatial database of ponds and lakes within the Huachuca Mountain Range, Canelo Hills, and their drainages (N_{ponds}=380) (Map 1). Through analysis of > 20 years of

historical imagery, we identified 92 intermittent ponds within the 7km buffer area surrounding all known *H. wrightorum* breeding sites. On average, 70% of intermittent ponds within the buffer area were filled during the wet season (N=65). For each of the pond map series, this resulted in: 65 recruiting ponds for Base, 45 recruiting ponds for Dry 1, and 26 recruiting ponds for Dry 2. For the scenarios with reproductive traps, Dry 3 included 65 ponds capable of attracting individuals (the same as Base) but only 45 with successful reproduction (the same as Dry 1). Dry 4 included 45 ponds capable of attracting individuals (the same as Dry 1) but only 26 ponds with successful reproduction (the same as Dry 2).

SIBM results

Overall, population size declined in response to all breeding habitat reduction scenarios (Figure 4.7, Table 4.3). Mean *H. wrightorum* population was 2259.2 for time steps 61-100 for the Base scenario, and percent difference between the Base Scenario and Dry Scenarios ranged from 4.5% (Dry 1) to 72.8% (Dry 4) (Table 4.3). Scenarios Dry 1 and Dry 2 simply reduced breeding ponds on the landscape by 30% and 60% respectively with no attraction to dry ponds. In both scenarios, we saw a reduction in population size, although the reduction in populating size was not proportional to the loss of breeding habitat. Rather, reductions in population size were most dramatic for Dry 2 with modest reductions between Base and Dry 1 (Figures 4.7 and 4.8). In addition, Dry 1, Dry 2, and Dry 4 produced a high degree of synchrony between replicates and a reduction in variability of population size within simulations (Figure 4.7, Table 4.3).

Scenarios Dry 3 and Dry 4 allowed attraction to breeding ponds that were then simulated to have failed recruitment (no reproduction). Population numbers declined in both scenarios, but variability across replicates and across time was highest among Dry 3 replicates (Figure 4.7,

Table 4.3). In fact, standard deviation across Dry 3 replicates only marginally reduced from the Base scenario (Table 4.3). Scenarios Dry 1 and Dry 3 produced the same number of successful breeding ponds (a 30% reduction from base), but Dry 3 allowed attraction to ponds where breeding ultimately did not occur. The smallest final population sizes were produced by scenario Dry 4, which simulated a 30% reduction in available ponds and a 30% failure of recruitment (leaving 40% of ponds available). Mean population size over the second half of the simulation period decreased from 2259.2 to 1035.1 in Dry 4. In Dry 1, 2, and 4, *H. wrightorum* quickly (< 5 generations after initiation of Dry pond map series) reached equilibriums in which little variability across generations was observed. In these cases, individuals were isolated at a few breeding ponds that never dried during the pond map series.

4F. Discussion

We found that population sizes of *H. wrightorum* decreased in response to reduced pond availability on the landscape, regardless of whether ponds acted as reproductive traps or not. We also found that absolute loss of habitat (e.g., ponds did not fill) resulted in populations quickly becoming isolated at ponds that reliably filled, as evidenced by smaller population sizes with very little variation between years and across simulation replicates. Alternatively, a conversion of 30% of ponds to reproductive traps maintained greater variability over time, possibly maintaining a metapopulation dynamic within the study area. Finally, we found evidence that the overall population size was likely strongly influenced by non-breeding habitat requirements.

Variability over time and between replicates indicates natural population fluctuations, and the loss of variability was driven by the isolation of individuals at “reliable” ponds – those that never dried, even in the driest scenarios. A low variability equilibrium was observed in 3

scenarios, two of which also had substantial population size reductions. In these scenarios, loss of these few remaining "reliable" ponds to habitat change (e.g., sedimentation over time or following erosion after a fire) may represent a significant decrease in overall population size, and recolonization by individuals from other ponds is unlikely. Such scenarios have already been observed for the threatened Chiricahua leopard frog in Miller Canyon of the Huachuca Mountains. An artificial pond home to one of the only populations of the amphibian in the Huachuca Mountains was destroyed by floods and sedimentation following the 2011 Monument Fire (S. Stone, US Army, Fort Huachuca, AZ, *pers. comm.*). Populations may also be vulnerable to predation or competition from other anurans similarly restricted to fewer ponds (e.g., the invasive bullfrog, a predator of *H. wrightorum* (Jones and Timmons 2010) and may face increased exposure to disease (Bradley *et al.* 2002). Finally, isolation in small pockets of breeding habitat can result in reductions of the genetic health of populations due to inbreeding and the accumulation of deleterious alleles, as observed in other native amphibians in the region that are currently restricted to isolated breeding ponds (Storfer *et al.* 2014).

A loss of 30% of the driest ponds on the landscape (Dry 1) did not result in large declines in population size, but the loss of an additional 30% of ponds (Dry 2) did cause large declines. This may indicate some threshold effect and suggests that ponds that fill rarely provide important stepping stones of connectivity between ponds that fill most years. Dry 4 resulted in the smallest populations for both species across all scenarios. This may be driven by a tendency to become attracted to "poor" ponds that fill only occasionally rather than being dispersal limited and staying in the vicinity of a "good" pond. This suggests that in a variable landscape, dispersal ability may not be related linearly to probability of persistence. When considering the conservation implications of this research, it is clear that both species may see population

declines in response to breeding habitat reductions – even the loss of 30% of the most ephemeral ponds.

Canopy cover is heterogeneous throughout the landscape, particularly near lower elevation breeding ponds. Future analyses will examine a range of non-breeding habitat requirements to determine how sensitive the SIBM is to these parameters. However, even with little knowledge about the exact non-breeding habitat requirements of *H. wrightorum*, this result demonstrates the importance of considering functional connectivity in simulating amphibian responses to changing habitat availability (Fordham *et al.* 2014). Canopy cover is patchy and heterogeneous on the landscape and may promote longer straightline travel from ponds to patches of canopy (Figure 4.6B).

The SIBM approach used in this research allows for coupling of demographic processes with functional connectivity between populations, which is an important process for aquatic organisms and may have profound influence on the projections of population viability and persistence (Fordham *et al.* 2014). Future applications for this SIBM include evaluating hypotheses of landscape connectivity between ponds as well as changes to the landscape over time, such as canopy cover change, increased aridity, and reductions in aquatic habitat for corridors (Jaeger *et al.* 2014) as well as breeding. In addition, we present a novel method for estimating hydroperiod of small ponds via historical satellite imagery. The value of remotely sensed data in conservation continues to gain recognition (Rose *et al.* 2015). This method could be used to formally examine changes in aquatic habitat availability over time and examine regional and climate drivers of hydroperiod, particularly for stock ponds in arid regions which are 1) conspicuous in satellite imagery, and 2) the dominant aquatic habitat.

In conclusion, we found that reductions in breeding habitat resulted in reduced population numbers for *H. wrightorum* in a subset of its range. Loss of 60% of breeding ponds resulted in > 30% population declines for *H. wrightorum*. Reduced breeding habitat can also result in increased synchrony and decreased variability through time, which may indicate a loss of function in metapopulations and a transition to isolated populations. Future research will consider the important role of non-breeding habitat in population persistence and connectivity and will evaluate the effects of local stressors such as predators, disease, or other factors that may interact with hydroperiod to decrease breeding habitat suitability.

4G. Acknowledgements

Funding for this research was provided by the Hall Conservation Genetics Graduate Research Award at the University of Washington's College of the Environment and through the U.S. Army Award Number W9214A-14-P-0048. Adam Leaché and Lorenz Hauser provided helpful comments and feedback on this manuscript.

4H. References

Bradley GA, Rosen PC, Sredl MJ, *et al.* 2002. Chytridiomycosis in native Arizona frogs. *J Wildl Dis* 38: 206–12.

Chan LM and Zamudio KR. 2009. Population differentiation of temperate amphibians in unpredictable environments. *Mol Ecol* 18: 3185–200.

Chapel WL. 1939. Field notes on *Hyla wrightorum* (Taylor). *Copeia* 1939: 225–7.

Coster SS, Veysey Powell JS, and Babbitt KJ. 2014. Characterizing the width of amphibian movements during postbreeding migration. *Conserv Biol* 28: 756–62.

Degenhardt WG, Painter CW, and Price AH. 2005. Amphibians and reptiles of New Mexico. University of New Mexico Press, Albuquerque.

Dennison PE, Brewer SC, Arnold JD, and Moritz MA. 2014. Large wildfire trends in the western United States, 1984-2011. *Geophys Res Lett* 41: 2928–33.

Fordham DA, Shoemaker KT, Schumaker NH, *et al.* 2014. How interactions between animal movement and landscape processes modify local range dynamics and extinction risk. *Biol Lett* 10: 1–5.

Hale J, Mims MC, Bogan MT, and Olden JD. 2015. Links between two interacting factors – novel habitats and non-native predators – and aquatic invertebrate communities in a dryland environment. *Hydrobiologia* 746: 313–326.
Jaeger KL, Olden JD, and Pelland NA. 2014. Climate change poised to threaten hydrologic connectivity in dryland streams. *Proc Natl Acad Sci* 111: 13894–13899.
Johnson JR, Knouft JH, Semlitsch RD. 2007. Sex and seasonal differences in the spatial terrestrial distribution of gray treefrog (*Hyla versicolor*) populations. *Biological Conservation* 140: 250–258.
Jones TR and Timmons RJ. 2010. *Hyla wrightorum* (Arizona treefrog): predation. *Herpetol Rev* 41: 473–4.
Kramer DC. 1973. Movements of western chorus frogs, *Pseudacris triseriata triseriata* tagged with CO^{60}. *Journal of Herpetology* 7: 231–235.
Marshall RM, Robles MD, Majka DR, and Haney JA. 2010. Sustainable water management in the southwestern United States: reality or rhetoric? *PLoS One* 5: e11687.
Mims MC, Phillipsen IC, Lytle DA, *et al.* 2015. Ecological strategies predict associations between aquatic and genetic connectivity for dryland amphibians. *Ecology* 96: 1371–1382.
Murphy MA, Evans JS, and Storfer A. 2010. Quantifying *Bufo boreas* connectivity in Yellowstone National Park with landscape genetics. *Ecology* 91: 252–61.
Pounds JA, Bustamante MR, Coloma LA, *et al.* 2006. Widespread amphibian extinctions from epidemic disease driven by global warming. *Nature* 439: 161–7.
Rose RA, Byler D, Eastman JR, *et al.* 2015. Ten ways remote sensing can contribute to conservation. *Conserv Biol* 29: 350–9.
Rosen PC and Schwalbe CR. 1998. Using managed waters for conservation of threatened frogs. In: Environmental, economic, and legal issues related to rangeland water developments. Tempe, AZ: Arizona State University, College of Law.
Schumaker NH. 2015. Version 3.2.2. U.S. Environmental Protection Agency, Environmental Research Laboratory, Corvallis, Oregon, USA. www.hexsim.net
Seager R, Ting M, Li C, *et al.* 2012. Projections of declining surface-water availability for the southwestern United States. *Nat Clim Chang* 3: 482–6.
Sodhi NS, Bickford D, Diesmos AC, *et al.* 2008. Measuring the meltdown: drivers of global amphibian extinction and decline. *PLoS One* 3: e1636.
Sredl MJ, Collins JP. 1992. The interaction of predation, competition, and habitat complexity in structuring an amphibian community. *Copeia* 1992: 607–614.
Stebbins RC. 2003. Western reptiles and amphibians. Singapore: Houghton Mifflin.
Storfer A, Mech SG, Reudink MW, and Lew K. 2014. Inbreeding and strong population subdivision in an endangered salamander. *Conserv Genet* 15: 137–51.
Stuart SN, Chanson JS, Cox NA, *et al.* 2004. Status and trends of amphibian declines and extinctions worldwide. *Science* 306: 1783–6.
Tevis L. 1966. Unsuccessful breeding by desert toads (*Bufo punctatus*) at the limit of their ecological tolerance. *Ecology* 47: 766–75.
Turner FB. 1959. Some features of the ecology of *Bufo punctatus* in Death Valley, California. *Ecology* 40: 175–81.
US Fish and Wildlife Service. 2013. Species assessment and listing priority assignment form: *Hyla wrightorum*. 36pp.
Wells KD. 2007. The ecology and behavior of amphibians. The University of Chicago Press, London.

Wenger SJ, Som NA, Dauwalter DC, *et al.* 2013. Probabilistic accounting of uncertainty in forecasts of species distributions under climate change. *Glob Chang Biol* 19: 3343–54.
Westerling AL, Hidalgo HG, Cayan DR, and Swetnam TW. 2006. Warming and earlier spring increase western U.S. forest wildfire activity. *Science* 13: 940–3.

4I. Tables

Table 4.1. Spatial data and HexMaps used in simulations.

Spatial inputs				
	Details	Resolution	Scale for HexMap conversion	Source
Canopy	2001 NLCD canopy density dataset	30m, resampled to 1m grid cell	Canopy cover (0 - 100%), imported with true values.	http://www.mrlc.gov/nlcd01_data.php
Streams	NHDPlus Version 2, downloaded from National Map Viewer (USGS)	100m stream buffer constructed as shapefile; converted to 1m grid cell	1 or 100: 100 for riparian buffer area, 1 for non-riparian area	http://viewer.nationalmap.gov/viewer/
Slope	9-m Digital Elevation Model from National Elevation Dataset	9m, resampled to 1m grid cell	Inverse-scaled to 1-100	http://ned.usgs.gov/downloads.asp
HexMaps	Description			
Initial Ponds	Pond map with known breeding sites for *H. wrightorum* (N=12). Hexagon in which a pond occurs were assigned a score of 1; all others received a score of 0. More details are included in the methods.			
Breeding Ponds	10 landscapes with 65 ponds each were generated using a random weighted draw to select 65 ponds for each (described in methods). Pond maps were then drawn at random from the 10 landscapes to construct a randomized series of 100 maps (to avoid artificial cyclic patterns from repetitive cycles through 10 landscapes). Hexagon in which a pond occurs were assigned a score of 1; all others received a score of 0.			
Dry1	The BreedingPonds map series with a 30% reduction of ponds. Ponds were discarded according to wet season hydroperiod index (lowest index discarded first), and ties were settled by evaluating the dry season hydroperiod index. More details are included in the methods.			
Dry2	The BreedingPonds map series with a 60% reduction of ponds. Ponds were discarded according to wet season hydroperiod index (lowest index discarded first), and ties were settled by evaluating the dry season hydroperiod index.			
Canopy	Hexagons were scored according to average canopy cover (0-100).			
Slope	Hexagons scored according to average inverse slope, scaled from 1-100.			
StreamSlope	Streams and Slope data (described above) were averaged to produce a combined input layer in which the highest values were assigned to cells with low slope (flat land) and riparian buffers, and the lowest scores were assigned to steep terrain outside riparian buffers. Hexagons scored according average (1-100).			

Table 4.2. HexSim event parameters, organized by tab in each HexSim event sequence. Spatial inputs are underlined and described in the paper and in Table 4.1. Additional notes are available in the Methods.

Parameter	Value	Notes	Multiple inputs?
Populations Tab			
Properties			
Initial Population Size	100	Because initiation places adults at breeding ponds, the initial value does not need to be large. Initial N of 100 allows simulations to reach equilibrium at ~10-15 generations.	No.
Initial Population Placement	InitialPonds	Initial individuals located at known breeding ponds for *H. wrightorum*.	No.
Range Data			
Range Spatial Data - breeding	Breeding Ponds	Breeding ponds for various simulation scenarios used in range spatial data; see Table 4.1 for spatial data details.	Yes.
Max Range Area - hexagons	1	Maximum range area was set to the largest pond in the dataset.	No.
Max Range Span - hexagons	1	Maximum range span set to encompass the span of the largest pond in the dataset.	No.
Maximum Group Members	25	Set to conservatively allow a maximum of 200 group members per 30m hexagon. **Note: initial sensitivity analyses indicate group membership has little impact on simulation results (results not yet shown).	No.
Hexagons Range-Eligible if Value is at least	1	Allows all ponds to be counted as "range" for breeding.	No.
Minimum Range Resource	1	Insures individuals are at a pond (group members) to breed.	No.
Traits			
Group Status	Floater or Group Member	Uses group size as accumulator to set individual status to floater or group member.	No.
Stages (age)	0-3	Individual ages. 0 = egg/larvae, 1 = juveniles (non-reproducing), 2 = young adults (reduced fecundity), 3 = mature adults.	No.
Sex	Female and Male	50/50 for both initializations and birth. Non-50/50 ratios do occur in nature, but without specific ratios for this species, 50/50 is used.	No.

Affinities			
Pond Spatial Affinity	Breeding Ponds	Orients individuals toward the closest pond.	Base, Dry1, or Dry 2.
Floater Creation - Initiate movement			
Global			
Resource threshold	100%	All groups processed.	No.
Enforce maximum group size	Yes	This refers to maximum group size for pond-defined ranges (above).	No.
Traits	All	All individuals become floaters at start of breeding season to allow movement to breeding pond.	No.
Set Pond Spatial Affinity - Orient to nearest pond			
Global			
Spatial Series	BreedingPonds	Sets pond map series for individual orientation for movement to pond.	Base, Dry1, or Dry 2.
Strategy	Closest Hexagon	Selects closest pond hexagon for movement.	No.
Movement - Move to breeding pond			
Strategy	Disperse then exploration	Individuals disperse first then explore a given area.	No.
Maximum number of explorations	1	The single exploration is designed to capture the singularity and synchrony of breeding events for both target species.	No.
Traits - Stages (age)	1, 2, and 3	All individuals move; there are no eggs/larvae at this stage (stage 0).	No.
Dispersal			
Dispersal spatial data	StreamSlope	Resistance surface used to prioritize movement through flat landscape and riparian corridors.	No.
Distribution of path lengths	Uniform	Spatial affinity for ponds was used to determine dispersal targets, and dispersal events were terminated upon reaching a pond or upon reaching the maximum path length.	No.

Path length bounds	35	Allows movements up to ~1050m (35 hexagons) to reach breeding sites.	Yes – sensitivity analyses performed (but not shown).
Stopping criteria?	No	Individuals stop upon reaching a pond, thus no stopping criteria were required.	No.
% Auto-correlation	90%	Creates direct movement to ponds while allowing for minor lateral movements along the way.	No.
Use Affinity?	Pond Spatial Affinity	Directs movements toward ponds.	No.
Exploration			
Maximum explored area - hexagons	5	Upon terminating a dispersal event, individuals are allowed to explore a maximum of 5 hexagons for suitable habitat or to explore other hexagons if a group has reached its maximum group number.	No.
Resource threshold	100	Individuals must find a pond in order to become a group member (and to reproduce).	No.
Exploration goal	Join Existing else start New	Individuals can join groups that have not yet reached the maximum group member, or they can start a new group.	No.
Exploration algorithm	Adaptive	Adaptive algorithm in which pond hexagons would be preferentially explored rather than non-pond hexagons.	No.
Accumulate - Set Individual Status			
Update "Group Size"	Accumulate	Updater and target accumulator for group size - sets status of individuals at ponds as "group member" (can reproduce) or "floater" (not allowed to reproduce).	No.
***For scenarios with reproductive traps only; other scenarios did not use steps marked with asterisk (*).**			
*Adjust Range Parameters - Adjust group membership to recruiting ponds only			
Properties and inputs all the same as initial Range Parameters, but new pond map series supplied to indicate which ponds have successful recruitment. Group members assigned to ponds not included in the new pond map series are reassigned as transients and not able to reproduce.			
*Floater Creation - Pond dries, initiate movement			

Global			
Resource threshold	100	All individuals move.	No.
Enforce maximum group size?	Yes		No.
*Movement - Exploration-only event to reassign group status to individuals at ponds with successful recruitment			
Exploration			
Maximum explored area - hexagons	1	Individuals do not move, but the resource score of the hexagon they occupy is evaluated.	No.
Resource threshold	100	Individuals must occupy a pond in order to become a group member (and to breed).	No.
Exploration goal	Start New else Join Existing	Ensures creation of new groups at ponds.	No.
Exploration algorithm	Adaptive	Strategy does not matter because individuals do not move.	No.
*Accumulate - Set Individual Status			
Update "Group Size"	Accumulate	Create groups at ponds with successful recruitment.	No.
Reproduction - Rates reflect fecundity adjusted for expected larval mortality.			
Properties			
Maximum number of births	145	Maximum recorded body sizes (SVL) within the Huachuca Mountains (Mims, unpublished: *H. wrightorum* = 37mm) was first used to estimate fecundity following the body size and fecundity relationships reported in Wells (2007) for Hylidae (*H. wrightorum*: ln(clutch size) = 1.44(ln(SVL in mm)+1.16) Values were then adjusted for larval mortality 75% in temporary pools for surrogate species *H. eximia* (Sredl and Collins 1992).	No.
Use mate selection?	Yes	Requires male-female pairs for breeding to occur.	No.
Rates			
Stage 3, group member, female	Mean = 120, SD = 24	Mean recorded body size (SVL) within the Huachuca Mountains (Mims, unpublished: *H. wrightorum* = 32mm) were used to estimate mean fecundity and adjusted for larval mortality following the same methods as maximum births. Means and 20% standard deviation (SD) were used to draw clutch size from a normal distribution.	No.

Stage 2, group member, female	Mean = 60, SD = 12	Mean recorded body size (SVL) within the Huachuca Mountains (Mims, unpublished: *H. wrightorum* = 32mm) were used to estimate mean fecundity and adjusted for larval mortality following the same methods as maximum births. Means and 20% standard deviation (SD) were used to draw clutch size from a normal distribution. Fecundity for Stage 2 (one-year-old) group members was estimated at 1/2 the rates of mature adults (Stage 3).	No.
Choose mate with replacement?	No	Females and males can mate with only one partner.	No.
Mate selection traits	Stage 2 and 3, male, group member	Requires that male mates be stage 2 or 3 and be a group member (established at pond).	No.
Census - Census after reproduction for counts of all age classes			
Accumulate - Age all individuals by one			
Adjust Range Parameters - Non-breeding range adjustments			
Properties			
Range spatial data - non-breeding	Canopy	We hypothesized canopy to be important for *H. wrightorum*. *H. eximia* (congener in the region) diet and observations suggest associations with forested areas (Chapel 1939, Degenhardt *et al.*1996); *H. wrightorum* associated with pine-oak and pine-fir forests (Duellman 1970, Stebbins 1985, Holm and Lowe 1995).	No.
Maximum range area - hexagons	7 hexagons	Allows individuals a maximum range size of 75 hexagons in order to achieve resource requirements (below). Range size estimates were set to roughly half the size of two surrogate species (*Pseudacris triseriata*= 2117 m^2 (Kramer 1974) and *Bufo bufo*= 1900m^2 (Sinsch 1987)). This was set to allow individuals sufficient range size for resource acquisition while adjusting for the assumption that amphibians in xeric environments may have reduced range sizes compared to those in more mesic environments (Wells 2007).	No.

Maximum range span - hexagons	7 hexagons	Maximum range span selected to create a compact range size and to reflect maximum observed movement events for sympatric amphibians (excluding migration to breeding sites) (Turner 1959).	No.
Maximum group members	5	Non-breeding amphibian density or relative abundance for this species and surrogates are not well studied. We set maximum group membership to 5 individuals per 30m hexagon.	No.
Hexagons range-eligibility	15 % canopy cover	The non-breeding habitat requirements of these species are not known, and we selected conservatively low canopy cover requirements for nonbreeding range criteria.	No.
Minimum range resource	30 % canopy cover	Requires at least two hexagons of at least 15% canopy cover for *H. wrightorum*, or one hexagon of a value > or = 30%.	No.
Floater Creation - *Pond dries, initiate movement*			
Global			
Resource threshold	100	All individuals move.	No.
Enforce maximum group size	Yes	This parameter does not ultimately matter because all individuals move.	No.
Movement - Move from dried ponds to overwintering/non-breeding habitat			
Global			
Strategy	Disperse then exploration	Individuals disperse first then explore a given area (additional parameters below).	No.
Maximum number explorations	2	Allows individuals to move twice if a given area is not suitable or already has too many individuals (max group size reached).	No.
Dispersal			
Dispersal spatial data	Canopy	Individuals move according to resource surface for each species.	No.
Distribution of path lengths	LogNormal	To capture leptokurtic distribution of animal movement.	No.
Path mean (hexagons)	10	Equates to 300m movement mean. 100m is mean dispersal distance reported for surrogate species *Hyla versicolor* with range of 0-330m (Johnson et al. 2007). 300m used here as conservative estimate for this xeric-adapted species.	No.

Path SD (hexagons)	2	60m (20%) standard deviation.	No.
Path length bounds	35	Allows extreme movements up to ~1050m.	No.
Use quality stopping criteria	Yes	Allows individuals to terminate dispersal upon reaching suitable habitat.	No.
Quality stopping - mean	15	Individuals stop after encountering an average of 15% canopy cover over 3 hexagons. Example: moving from 0 to 15 to 30 would allow a stop.	No.
Quality stopping - path length	3	Path length over which quality stopping mean is reached.	No.
Quality stopping - beginning with dispersal step	1	Ponds may be encountered immediately after dispersal; this allows individuals to stop.	No.
Auto-correlation from spatial data	Yes	Derives auto-correlation of movement from spatial data and allows individuals in low-quality habitat to move in a straight line trajectory through it until reaching higher quality habitat (Figure 4.6B).	No.
Trend Period	5	Auto-correlation trend period of 5 hexagons.	No.
Exploration			
Maximum explored area - hexagons	7	Upon terminating a dispersal event, individuals are allowed to explore a maximum of 7 hexagons for suitable habitat or to explore other hexagons if a group has reached its maximum group number.	No.
Resource Threshold	100	Individuals must achieve resource minimums in order to join or start a group.	No.
Exploration Goal	Join Existing else start New	Allows individuals to join a group (if the group has not yet reached the maximum size) or start a new group.	No.
Accumulate - Update Group Sizes			
Census - Census after reproduction for counts of all age classes			
Survival - Foraging and overwintering			
Survival Rates			
All transients	0%	If individuals were not able to join or create a group after two dispersal and exploration attempts, they remained transients with a 100% chance of mortality.	No.

Stage 1, group members	30%	Juveniles are likely more vulnerable to predation, and their survival rates were set to 1/2 those of age 2 and 3 individuals. Slightly lower value than average survival reported across pond breeding anurans in Wells 2007 (39%).	No.
Stages 2 and 3, group members	60%	We assumed highest survival for individuals able to establish themselves as group members in higher quality habitat (as determined by canopy cover or slope). Survival rates set higher than reported average for pond breeding anurans in Wells 2007 (39%).	No.

Census - *Census after overwintering/non-breeding season.* This census was used for all simulation summary graphs and tables.

Table 4.3. Population means, standard deviations (SD), and percent difference from the Base Scenario (for Scenarios Dry 1 - Dry 4) are shown for 50 replicates of 5 scenarios. Means and SD are reported from timesteps T 61-100 from the final census of each time step. Additional information on input parameters is available in Table 4.2.

	Base	Dry 1		Dry 2		Dry 3		Dry 4	
		Avg	%Dif	Avg	%Dif	Avg	%Dif	Avg	%Dif
Mean, T_{61}-T_{100}	2259.2	2160.2	4.5	1641.3	31.7	1677.9	29.5	1053.1	72.8
SD, T_{61}-T_{100}	435.8	198.9	74.6	163.4	90.9	482.9	10.3	96.9	127.2

4J. Figures

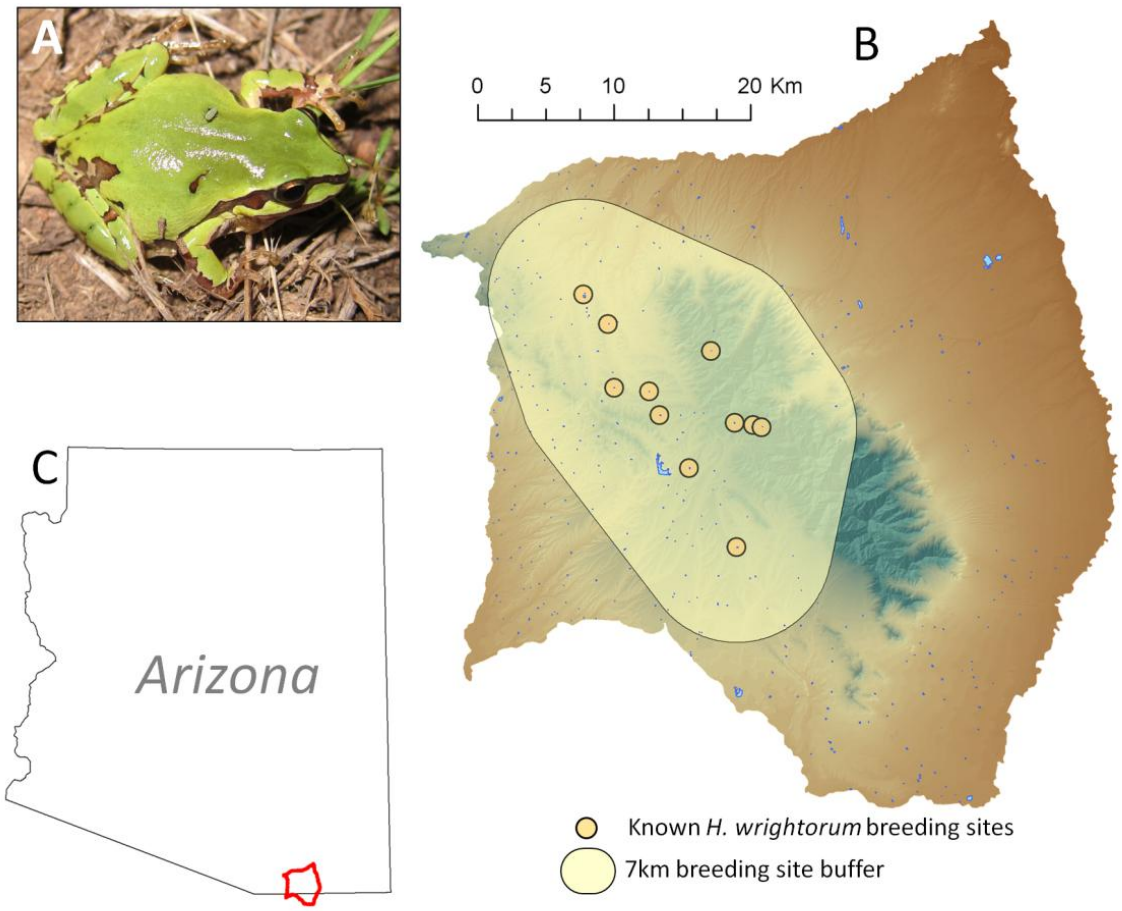

Figure 4.1. A. Adult *Hyla wrightorum* in the Huachuca Mountains (photo by M.C. Mims). B. Map of the Huachuca Mountains and their drainages; ponds and lakes display the pond database created for this project. *H. wrightorum* breeding sites are shown by orange circles, and 7km buffer area is denoted by yellow shaded area. C. Location of map B in the state of Arizona.

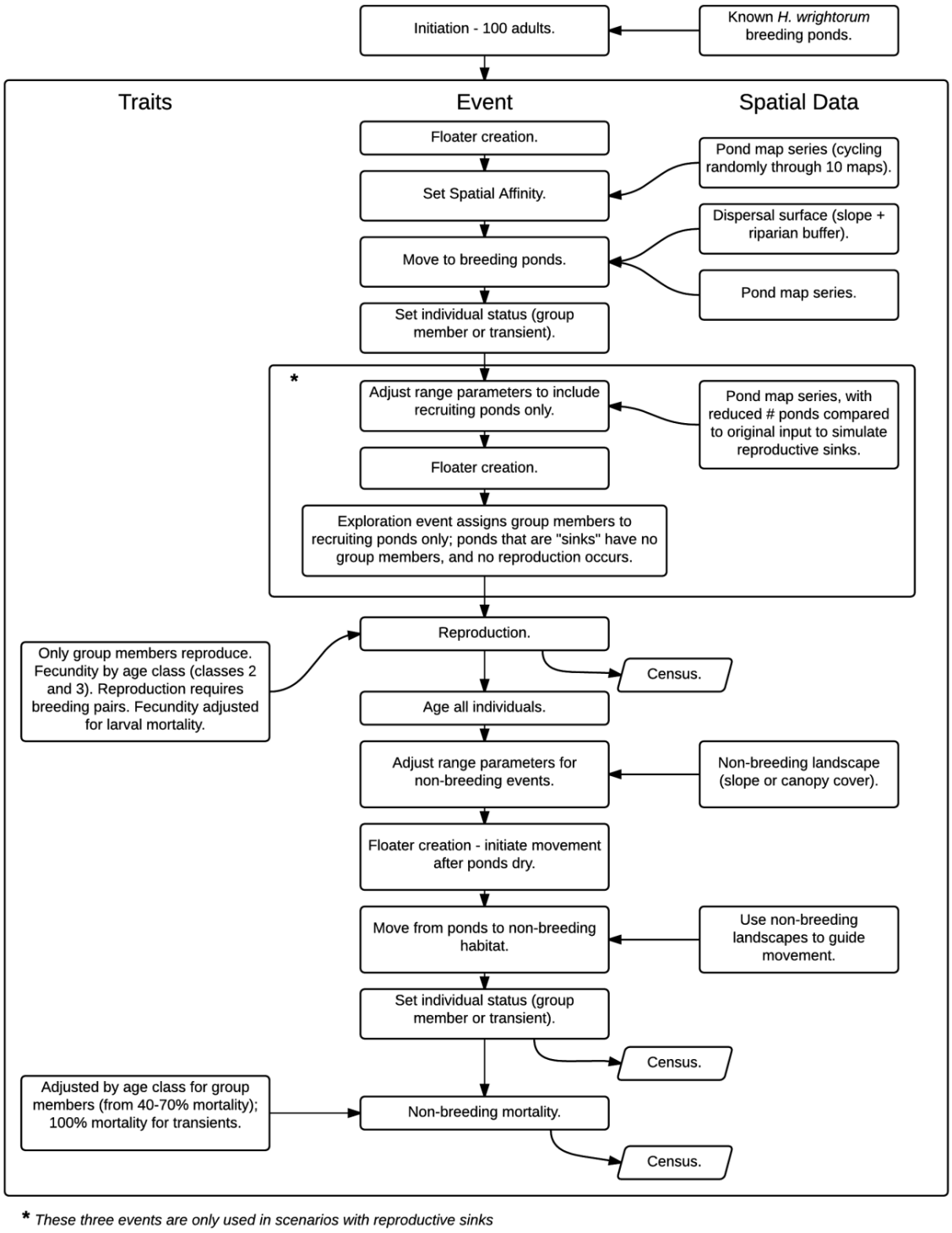

Figure 4.2. HexSim SIBM flow chart.

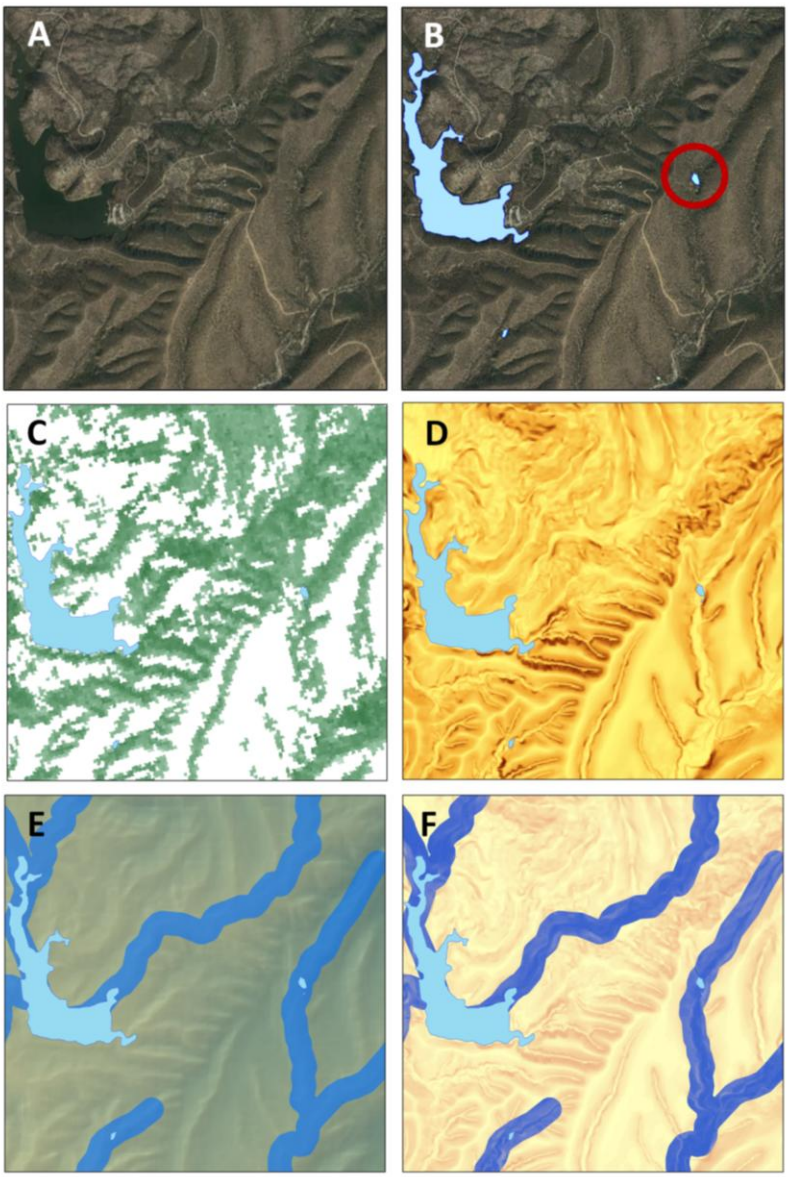

Figure 4.3. Examples of spatial data used to create HexMaps. A. Satellite imagery from Google Earth. B. Examples of constructed pond and lake polygons using a combination of spatial resources. Large water body on left is Parker Canyon Reservoir; small pond in red circle is a known *H. wrightorum* breeding site (Scotia Tank from Chapter 3), and historical imagery for that pond is shown in Figure 4.4 and HexMaps in Figure 4.5. C. Canopy cover. D. Slope. E. Riparian corridors shown in blue. F. Combination of slope and stream corridors used for the dispersal surface in HexSim models.

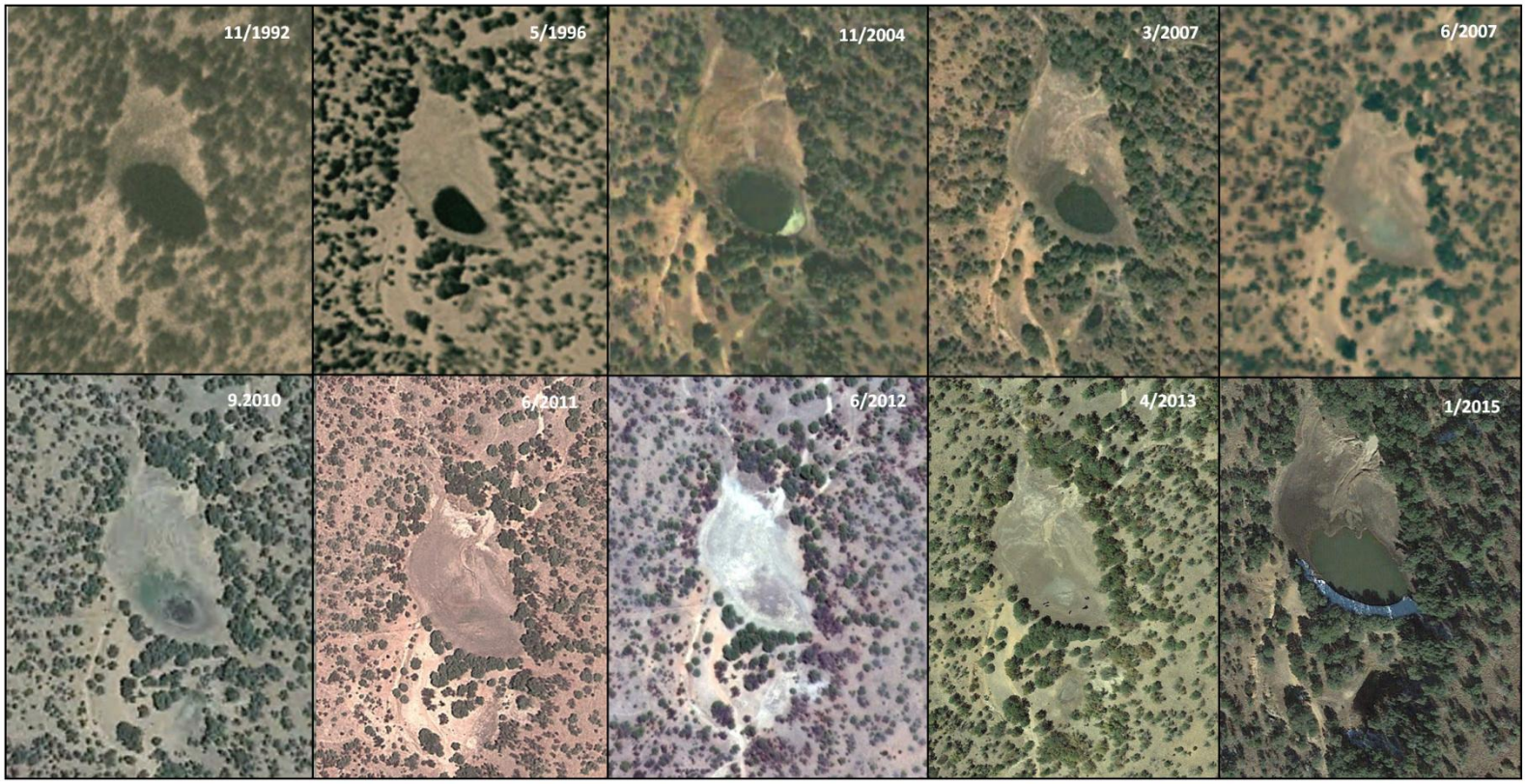

Figure 4.4. Historical satellite imagery for Scotia Tank (shown in the red circle in Figure 4.3).

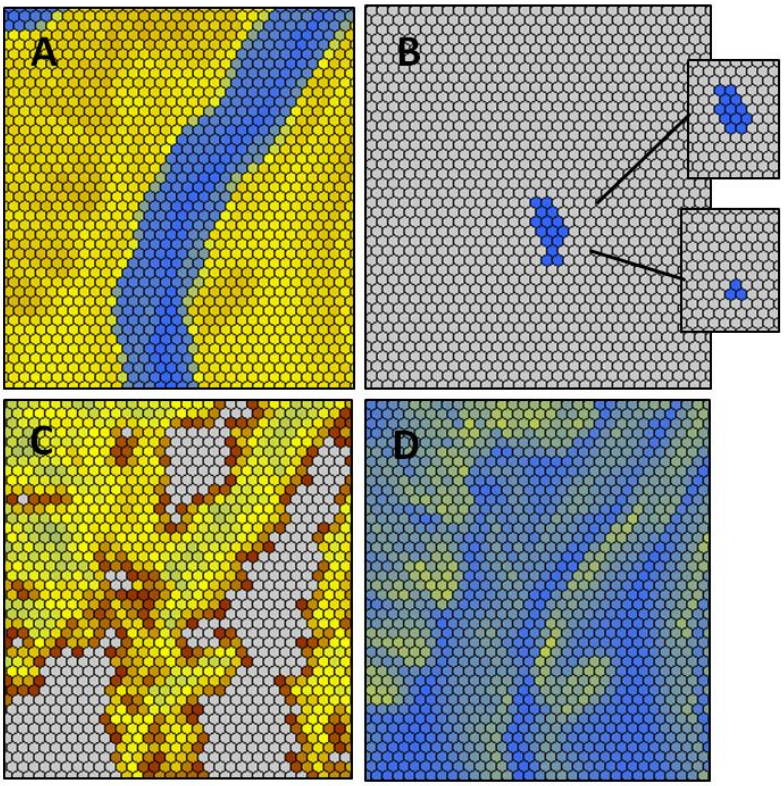

Figure 4.5. HexMaps for Scotia Tank (Figures 4.3 and 4.4). A. Stream and slope dispersal surface. B. Scotia Tank and a small pond just to the south; inset images show two different versions of the stochastic map series in which only Scotia Tank fills or only the small pond fills. C. Canopy cover. D. Slope.

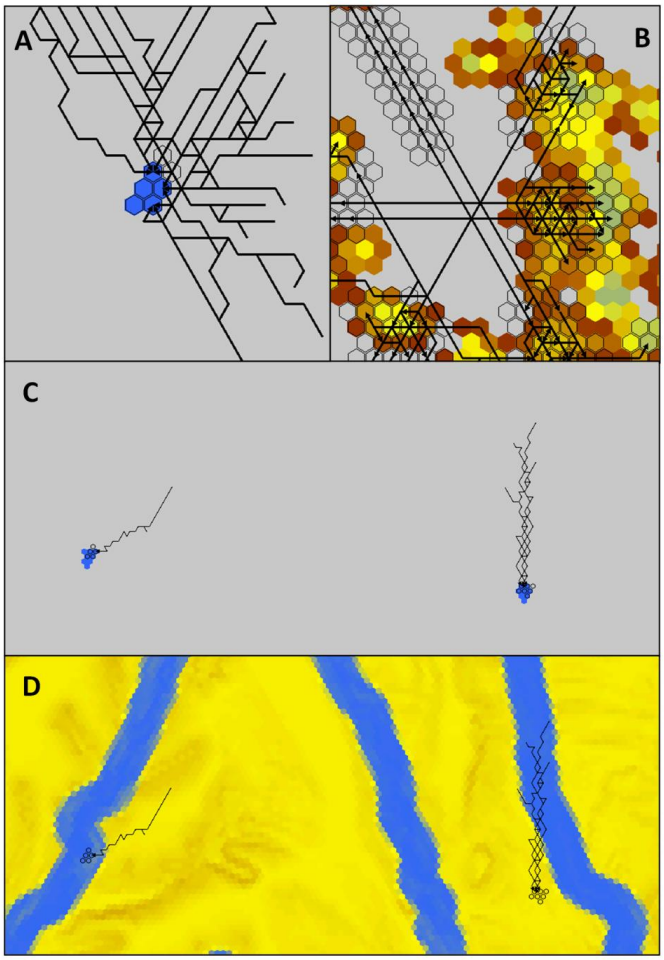

Figure 4.6. Movement events shown for individuals on HexMaps. A. Individuals move to a pond. B. Individuals move away from a pond to canopy cover. C and D. Examples individuals moving from a pond that did not fill during a time step to two new ponds. C shows the dispersal target ponds, and D shows the dispersal surface.

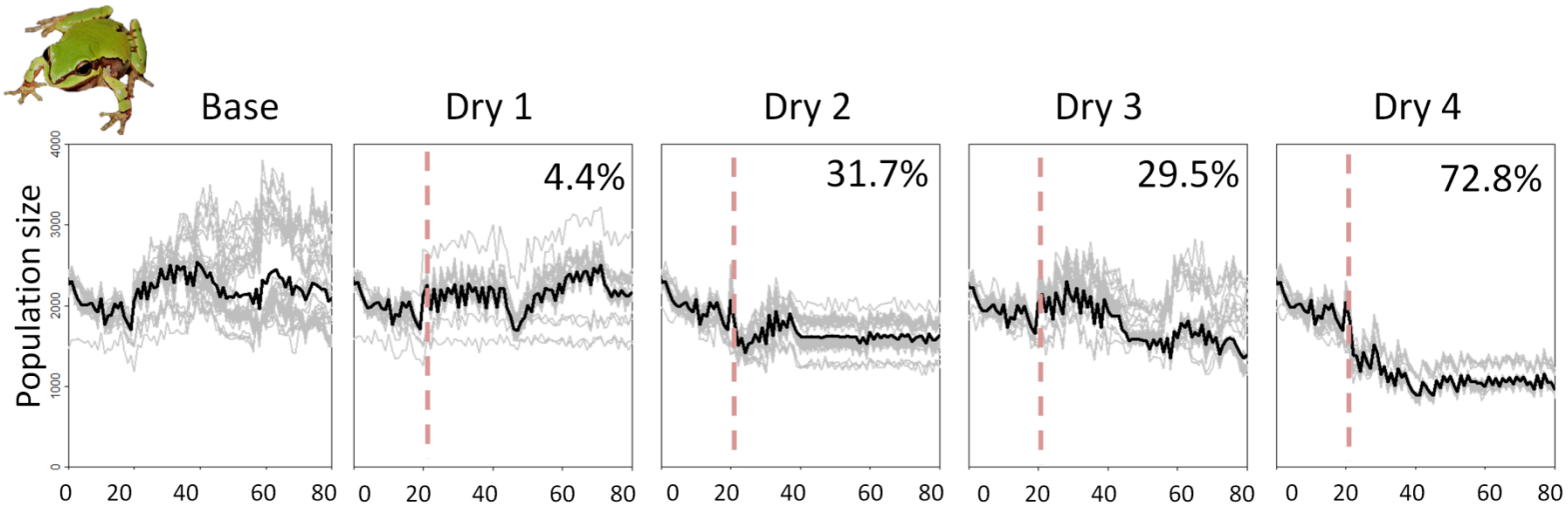

Figure 4.7. Results of initial simulations of *H. wrightorum* shown by pond availability scenario. Each of 50 replicates is plotted as a grey line, and the average of all runs is plotted as a black line. Summary statistics are summarized in Table 4.2.

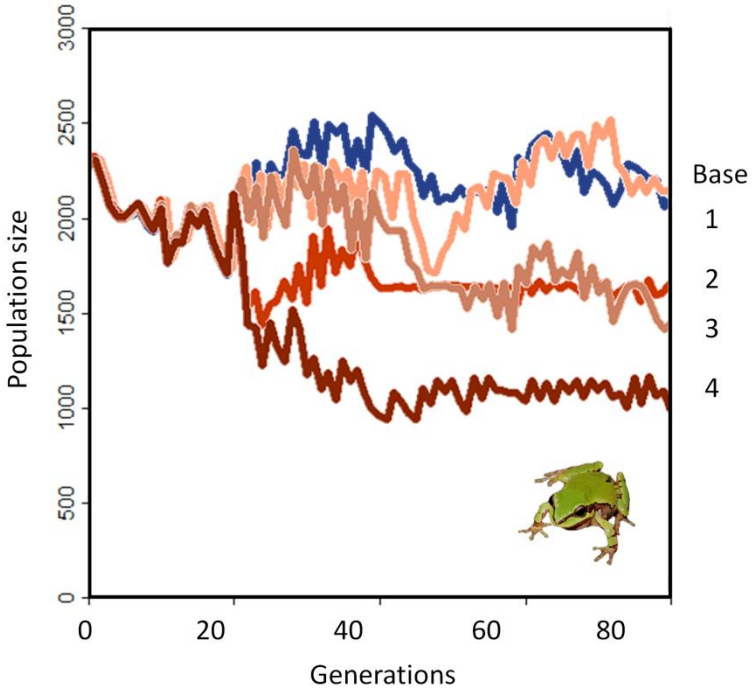

Figure 4.8. Results of changes to fecundity and dispersal parameters for *H. wrightorum*, shown as different colored lines that represent the average of 50 simulation replicates per scenario. Results are summarized in Table 4.3.